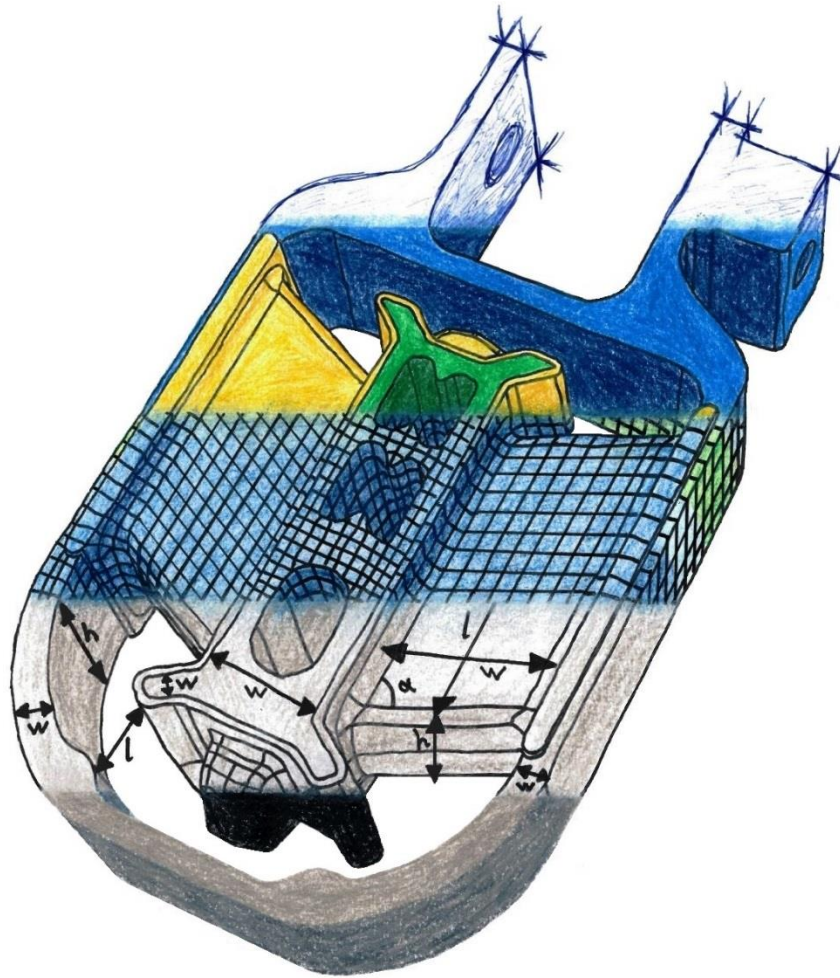




CHALMERS
UNIVERSITY OF TECHNOLOGY



Method for structural optimization of powertrain mounts

Shape optimization of torque rods to meet static stiffness requirement

Master's thesis in Master's programme Product Development

JENS MEDBO

MASTER'S THESIS IN PRODUCT DEVELOPMENT

Method for structural optimization of powertrain mounts

Shape optimization of torque rods to meet static stiffness requirement

JENS MEDBO

Department of Applied Mechanics
Division of Dynamics
CHALMERS UNIVERSITY OF TECHNOLOGY
Gothenburg, Sweden 2016

Method for structural optimization of powertrain mounts
Shape optimization of torque rods to meet static stiffness requirement
JENS MEDBO

© JENS MEDBO, 2016

Master's thesis 2016:44
ISSN 1652-8557
Department of Applied Mechanics
Division of Dynamics
Chalmers University of Technology
SE-412 96 Gothenburg
Sweden
Telephone: + 46 (0)31-772 10 00

Cover:

The cover picture illustrates the Volvo V40 LLTB studied in this project and the different phases a torque rod would go through during a development process using the proposed optimization method: From an initial concept to a CAD geometry and an FE model, which is then morphed to enable shape optimization of the geometry, which should then be manufactured to a finished product. The optimization method proposed in this report covers the FE modelling and optimization phases. For more details on the optimization method, see Subsection 4.3.

Chalmers Reproservice / Department of Applied Mechanics
Gothenburg, Sweden 2016

Method for structural optimization of powertrain mounts
Shape optimization of torque rods to meet static stiffness requirement
Master's thesis in Master's programme Product Development
JENS MEDBO
Department of Applied Mechanics
Division of Dynamics
Chalmers University of Technology

Abstract

Volvo Cars is in need of a development method to be used for in-house new product development of powertrain mounts. The current development process includes development of requirements in-house and component design by an external supplier. To reduce the development lead-time and cost Volvo Cars is investigating the possibilities to do component design of powertrain mounts in-house. It is suggested to use structural optimization as a tool in the design work. A method for using structural optimization to design the geometry of powertrain mounts to meet stiffness specifications has been developed in this project. The project focused on shape optimization of torque rods to meet static stiffness requirement.

An iterative approach was used, where the optimization method was developed using a simplified torque rod to facilitate the development. It was also studied if it is possible to obtain material parameters to sufficiently accurate model rubber materials by doing tensile tests on rubber from existing components. Finally, the optimization method was applied to a real Volvo torque rod for validation and adjustment.

The proposed optimization method is based on finite element (FE) modelling of the mount. A concept geometry and a requirement stiffness curve are needed as input to the method. An FE model of the concept geometry is created and then morphed, creating shapes that are used as design variables. The morphing enables controlled geometry changes that are used in the optimization. An objective function, that represents the sum of the squared distances that a certain design's displacement values for certain force levels deviates from the required displacement values, is used to determine the goodness of the design. The shape of the FE model is then optimized by changing the shapes to minimizing the value of the objective function. The output from the optimization method is an optimized mount geometry that can be used as basis in final design work.

The proposed method is performing well; it is able to optimize a concept geometry far from the final geometry into a shape that has a static stiffness close to the required. It is also able to fine-tune the shape of a full-feature geometry to a static stiffness very close to the requirement. The method is very flexible, and additional optimization constraints can easily be added.

The proposed optimization method has potential of being an important tool in new product development of powertrain mounts or other rubber components. A modified version of the method was also shown to be useful for optimizing hyperelastic material parameters to model a certain rubber compound more accurately.

Key words: Structural optimization, shape optimization, rubber, powertrain mounts, torque rods, hyperelasticity, Yeoh hyperelastic model, morphing, finite element analysis

Metod för strukturoptimering av motorupphängningskomponenter
Formoptimering av momentstag för att möta krav på statisk styvhet
Examensarbete inom Produktutveckling
JENS MEDBO
Institutionen för tillämpad mekanik
Avdelningen för dynamik
Chalmers tekniska högskola

Sammanfattning

Volvo Cars är i behov av en utvecklingsmetod för intern nyproduktutveckling av motorupphängningskomponenter. Den nuvarande utvecklingsprocessen innefattar utveckling av krav internt och komponentkonstruktion av en extern leverantör. För att reducera utvecklingstid och kostnad undersöker Volvo Cars möjligheterna att göra komponentkonstruktion av motorupphängningskomponenter internt. Strukturoptimering är föreslaget att användas som ett verktyg i konstruktionsarbetet. En metod för att använda strukturoptimering för utformning av motorupphängningskomponenters geometri för att möta styvhetskrav har utvecklats i detta projekt. Projektet fokuserade på formoptimering av momentstag för att möta krav på statisk styvhet.

Ett iterativt tillvägagångssätt användes, där optimeringsmetoden utvecklades med hjälp av ett förenklat momentstag för att förenkla utvecklingen. Möjligheten att erhålla materialparametrar för att tillräckligt noggrant modellera gummimaterial genom att utföra dragprov på gummi från existerande komponenter studerades också. Optimeringsmetoden tillämpades slutligen på ett verkligt Volvo-momentstag för validering och justering.

Den föreslagna optimeringsmetoden är baserad på finit element (FE) modellering av komponenten. En konceptgeometri och en kravstyvhetskurva behövs som indata till metoden. En FE modell av konceptgeometrin skapas och morfas (manipuleras), vilket skapar former som används som designvariabler. Morfningen möjliggör kontrollerade geometriändringar som används i optimeringen. En målfunktion, som representerar summan av de kvadrerade avstånden som en viss konstruktions förskjutningsvärden för vissa kraftnivåer avviker med från kravvärdena på förskjutning, används för att bedöma hur bra en konstruktion är. Formen på FE modellen optimeras sedan genom att ändra på formerna för att minimera värdet på målfunktionen. Utdata från optimeringsmetoden är en optimerad komponentgeometri som kan användas som underlag för slutgiltig konstruktion.

Den föreslagna metoden presterar väl; den kan optimera en konceptgeometri långt från den slutgiltiga geometrin till en form som har en statisk styvhet nära krävda. Den kan också finjustera formen av en komplett geometri till en statisk styvhet väldigt nära den krävda. Metoden är väldigt flexibel och ytterligare optimeringstväng kan lätt läggas till.

Den föreslagna metoden har potential till att vara ett viktigt verktyg i nyproduktutveckling av motorupphängningskomponenter eller andra gummikomponenter. En modifierad version av metoden visades också vara användbar för optimering av hyperelastiska materialparametrar för att modellera en viss gummiblandning mer exakt.

Nyckelord: Strukturoptimering, formoptimering, gummi, motorupphängningskomponenter, momentstag, hyperelasticitet, Yeoh hyperelastisk modell, morfning, finit elementanalys

Acknowledgements

This Master's thesis project has been carried out at the Powertrain Mounts group at Volvo Car Corporation (Volvo Cars) and in cooperation with the Department of Applied Mechanics at Chalmers University of Technology (Chalmers). The project was carried out mainly on site at Volvo Cars Research and Development in Torslanda, Sweden.

First, I would like to thank my supervisor at Volvo Cars, CAE Structure Analyst Daniel Högberg, who has been supporting me during the whole project. He had answers to almost all my questions and for those he had not he always had time for fruitful discussions. Thank you Daniel for motivating me and making this Master's thesis project a fun and interesting time, giving me a lot of knowledge and experience. I am also grateful to have had Mikael Enelund, Professor at the Department of Applied Mechanics at Chalmers, as my academic supervisor and examiner. He has been supportive and helpful with useful knowledge in rubber modelling. I am especially thankful for the time he spent giving me very useful feedback on my report, and for the help he gave me to perform tensile tests on Chalmers.

I would also like to thank all employees at the Powertrain Mounts group at Volvo Cars. You have all been very kind and helpful during the project. I would especially like to thank Stefan Nilsson, Manager at the Powertrain Mounts group, for giving me the possibility of carrying out this project, and to the Powertrain Mounts CAE team: Magnus Wickström, Jesper Larsson and Henrik Åkesson, for support on powertrain mounting system theory and calculations. Thanks also to Martin Gillenäng, Technical Expert at the Powertrain Mounts group for sharing your knowledge on powertrain mounting systems.

Further, I would like to thank Britta Käck, Application Specialist at Altair, for her support and enthusiasm on the HyperWorks software used in this project. I am very grateful for the time she spent demonstrating the software and answering my questions. Thanks also to Joakim Lindholm, Area Sales Manager at Altair, who has also been helpful by answering my questions about the HyperWorks software. Moreover, thanks to Reine Nohlborg, Research Engineer at Chalmers, for help with water jet cutting rubber test specimens.

Finally, thanks to my family and friends, your support means a lot!

Gothenburg, July 2016

JENS MEDBO

Contents

1	Introduction.....	1
1.1	Background	1
1.1.1	Powertrain mounts	1
1.1.2	Development process.....	4
1.1.3	Previous work	5
1.2	Purpose	6
1.3	Problem analysis.....	6
1.4	Scope and delimitations.....	8
1.5	Report outline	8
2	Theory	9
2.1	Rubber	9
2.1.1	Material properties.....	9
2.1.2	Modelling rubber elasticity.....	12
2.1.3	Modelling dynamic behaviour.....	16
2.2	Finite element analysis of torque rods.....	17
2.3	Structural optimization	17
2.4	Theory summary.....	19
3	Project methodology	20
3.1	Phase 1: Pre-study	20
3.2	Phase 2: Method development – simplified torque rod.....	21
3.3	Phase 3: Obtaining hyperelastic material parameters.....	22
3.4	Phase 4: Method validation and adjustment – Real case.....	23
3.5	Phase 5: Planning, documentation and presentation	23
4	Results	24
4.1	Method development – simplified torque rod	24
4.1.1	Pre-processing	25
4.1.2	Initial analysis.....	26
4.1.3	Morphing	27
4.1.4	Requirement and objective function.....	29
4.1.5	Optimization set-up and system bounds check	32
4.1.6	Design of experiments	34
4.1.7	Optimization	34
4.1.8	Post-processing.....	36
4.1.9	Dynamic analysis.....	38
4.2	Obtaining hyperelastic material parameters	38
4.2.1	Tensile test result	38

4.2.2	Obtaining the material parameters.....	40
4.2.3	Model validation.....	40
4.2.4	Material parameter optimization	41
4.2.5	Summary.....	43
4.3	Presentation of the optimization method.....	44
4.3.1	Top level: Compact flowchart	44
4.3.2	Middle level: Detailed flowchart.....	45
4.3.3	Base level: Step-by-step guide	45
4.3.4	Using the optimization method.....	45
4.4	Method validation and adjustment – Real case	47
4.4.1	Pre-processing and initial analysis	47
4.4.2	Morphing	49
4.4.3	Requirement and objective function.....	50
4.4.4	Optimization set-up and system bounds check	51
4.4.5	Design of experiments	51
4.4.6	Optimization and post-processing	51
5	Discussion	54
5.1	Project discussion	54
5.2	Results discussion.....	54
5.2.1	Development phase.....	54
5.2.2	Material parameter-obtaining phase	55
5.2.3	Presentation of the optimization method	56
5.2.4	Validation and adjustment phase	56
5.3	General topics.....	57
6	Conclusion	59
6.1	Research question answers	59
6.2	General conclusions	60
7	Future work.....	61
7.1	Recommendations for next step	61
7.2	Suggestions on future research areas.....	61
	References.....	63
	Appendix.....	65
A	Design variables	65
B	Compact flowchart: Material parameter-optimization	66
C	Detailed flowchart: Optimization method.....	67
D	Detailed flowchart: Material parameter-optimization	68
E	Extract from step-by-step guide	69

1 Introduction

This report documents a Master's thesis project of 30 ECTS credits within the Master's programme Product Development at Chalmers University of Technology (Chalmers). A method for structural optimization of powertrain mounts rubber parts was developed in the project, with focus on shape optimization of torque rod geometry to meet static stiffness requirements. Volvo Car Corporation (Volvo Cars), who had done some initial investigations in the subject before this project started, initiated the project.

This section presents the background to the project, the problem statement, the purpose and an analysis of the problem, which results in a number of research questions. Last, the scope and delimitations and the report outline are presented.

1.1 Background

Volvo Cars is a Swedish automotive company aiming for the premium segment, developing and manufacturing private cars (Volvo Cars, 2016). Car engines, especially internal combustion engines (ICEs), are sources of vibration, which is something unwanted in a passenger car, both for comfort and performance reasons among others. It is therefore necessary to isolate the engine from the car body and chassis to minimize propagation of vibrations. This is done by the powertrain mounts, which suspend the engine in the car using flexible rubber mounts that allow the powertrain to move relative to the car body and chassis. In this report, the powertrain refers to the engine and gearbox assembly.

1.1.1 Powertrain mounts

The main tasks for powertrain mounts according to Volvo Cars¹ include:

1. Mount the powertrain in the car
2. Isolate the car body from powertrain excitations and road disturbances
3. Limit the powertrain movements within the allowed packaging
4. Keep function and efficiency during vehicle lifetime
5. Satisfy crash and safety requirements
6. Allow assembly and serviceability

Studying these tasks, it is obvious that the performance of the powertrain mounts will have strong influence on the complete vehicle behaviour. The complete vehicle main attribute areas dictated by Volvo Cars that are affected by the powertrain mounts in their vehicles are:¹

- Noise, Vibration & Harshness (NVH)
- Driveability
- Ride comfort
- Durability

These areas all have their own requirements, which are combined into requirements on the powertrain mounts in terms of, for example, static stiffness, dynamic stiffness and damping over an engine's operational loads and frequencies. The attribute areas listed above are some of all the complete vehicle attributes that affect the overall impression of a premium car.

¹ Martin Gillenäng (Technical Expert Powertrain Mounts, Volvo Car Corporation, Gothenburg) interviewed by the author 2016, July 1.

Performing well in these areas is important to reach the premium segment, wherefore the performance of the individual powertrain mount components plays a key role.

There are several different ways of installing a powertrain in a car. Most of the current Volvo cars are front wheel driven with transverse installed ICEs, using a pendulum type mounting system, see Figure 1.1. There are two main types of components in such systems; main mounts and torque rods (also called tie-bars), see Figure 1.2. In a pendulum mounting system, the powertrain is hanging in two weight carrying main mounts, one on each side of the engine bay fixed to the car body. The powertrain is restricted to roll due to engine torque by one or up to three torque rods that are fixed to the chassis and/or car body. This project focuses on torque rods, wherefore the main mounts will not be described in detail.

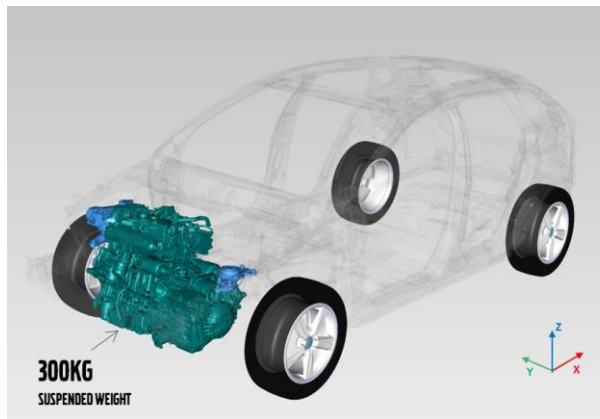


Figure 1.1: Engine position in a Volvo car with a pendulum type powertrain mounting system.

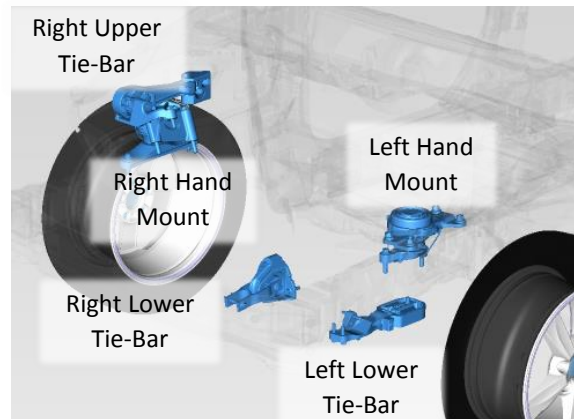


Figure 1.2: Components of the mounting system with Volvo Cars' part names.

Torque rods restrict the engine and gearbox assembly to move in the longitudinal direction of the car, that is, restricting it from rolling around the main mounts axis. They take up the reaction forces due to the engine torque in a controlled way. Volvo Cars' torque rods are in most cases composed of an extruded aluminium insert bonded inside an extruded aluminium frame by a main rubber element (MRE); see Figure 1.3.¹ One of the two rigid parts is fixed to the car body or chassis and the other is fixed to the powertrain. The flexibility of the MRE allows for relative movement between the frame and the insert, which allows the powertrain to move relative to the chassis. The MRE gives a linear component stiffness around the torque rod's unloaded position. For large displacements from the unloaded position, torque rods have rubber bump stops that will make contact with the frame. The shape of the bump stops results in a gradual increase in component stiffness, preventing the insert from a sudden impact with the frame when it approaches its end position. To protect the bump stops from too large compression and to define the mount's maximum allowed displacement, the insert has rubber-covered arms that will make contact with the frame at its end positions. From the point where the insert arms make contact with the frame, the component stiffness increases rapidly and is mostly governed by the stiffness of the aluminium frame. The overall component stiffness, which is the main attribute of torque rods, is largely defined by the geometry but also by the material of the different constituent parts. For the rubber parts of torque rods and most powertrain mounting components, natural rubber filled with carbon-black particles is used.

¹ Gillenäng 2016.

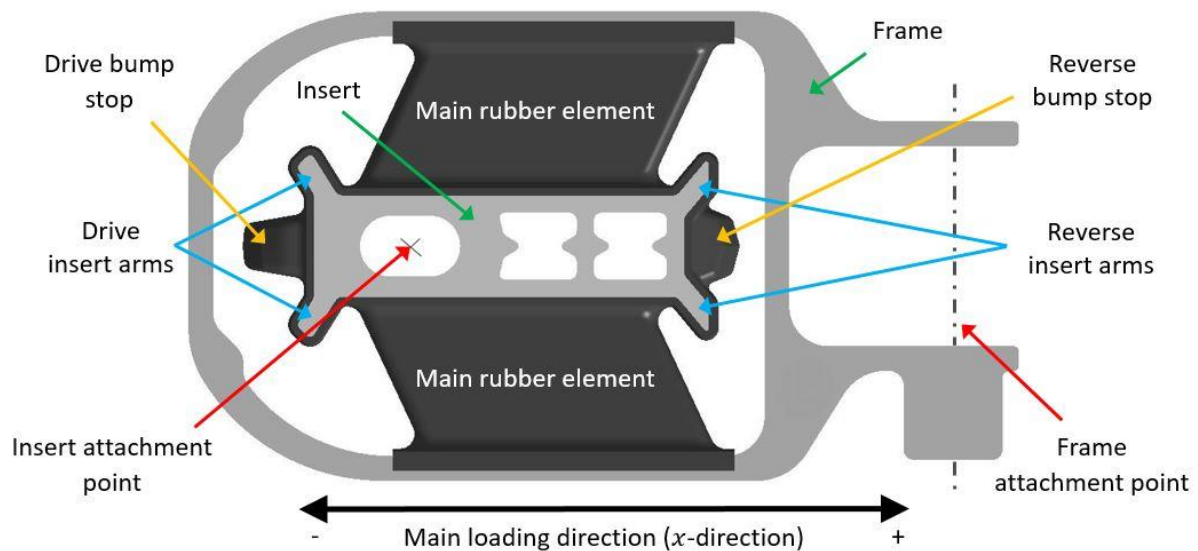


Figure 1.3: A schematic representation of the Volvo V40 LLTB torque rod with its parts named.

The requirements on the torque rods are often opposing; in an NVH perspective, soft rubber parts with good damping characteristics are preferred, but in a driveability perspective, stiff rubber parts that decrease powertrain movements are preferred. This makes it necessary to do trade-offs to find a good balance. Volvo Cars develops the requirements by doing Multi-Disciplinary Optimizations, which take into account the four different attribute areas that the powertrain mounting system affect (see the beginning of this section) and finds the best balance according to a predefined strategy.¹ The requirements are expressed in static stiffness in form of desired force-displacement curves; see Figure 1.4. Requirements on dynamic stiffness are expressed as dynamic stiffness $\leq 1.5 \times$ static stiffness in the operational frequency range and in a specified range of displacement and amplitude around the neutral position or a predefined pre-load.¹ The torque rods are then, based on Volvo Cars' requirements, designed and manufactured by an external supplier specialized on powertrain mounts.

¹ Gillenäng 2016.

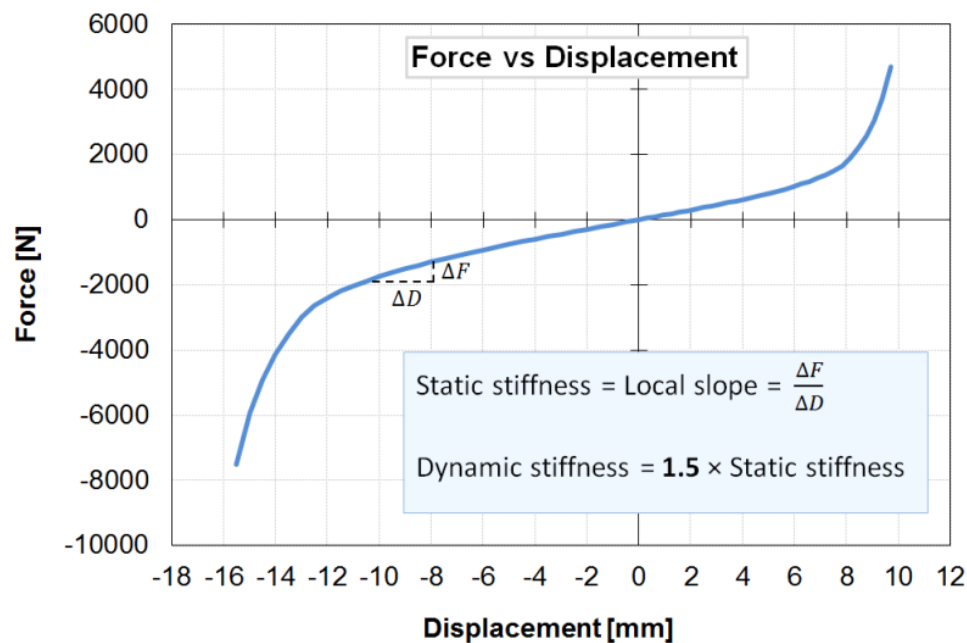


Figure 1.4: Force-displacement curve showing an example of a static stiffness requirement of a torque rod. The main rubber elements give the linear characteristics in the middle part of the curve, and the bump stops give the progressive characteristics for large displacements.

1.1.2 Development process

The current development process can be time consuming with several iterations between Volvo Cars and the supplier to achieve the desired characteristics of the components. It is also very expensive for Volvo Cars to have an external supplier doing the design work of the components.¹ Volvo Cars is currently working on decreasing their development lead-times, wherefore Volvo Cars wishes to build knowledge to do design work of powertrain mounts in-house.¹ Having that knowledge, Volvo Cars would have the possibility of producing Build-to-Print components, that is, components that are developed and designed by Volvo Cars where the supplier only stands for manufacturing of the components. In such a process Volvo Cars has complete control over the whole development chain from concept to drawing, which in turn gives the possibility of reduced lead times. Another use of such knowledge would be to verify or make suggestions on improvements of components designed by external suppliers. See Figure 1.5 for an illustration of the current development process and the proposed future development process.

¹ Gillenäng 2016.

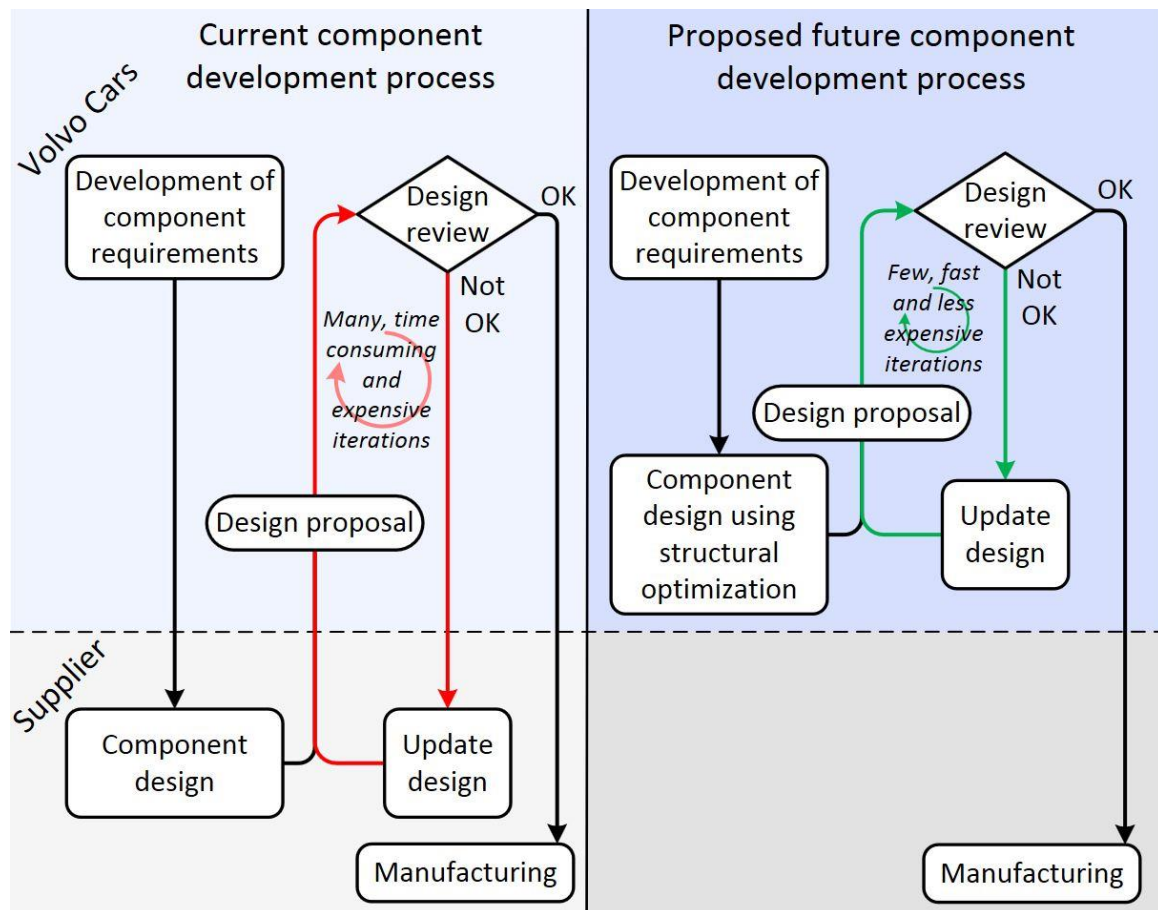


Figure 1.5: Illustration of the current powertrain mount development process at Volvo Cars (left) and the proposed future development process using structural optimization (right).

1.1.3 Previous work

As Volvo Cars currently do not design their powertrain mounts in-house, they are in need of a new development method for doing this. To design powertrain mounts in-house, without the experience of specialized suppliers but with retained (or improved) component performance, structural optimization is proposed by Volvo Cars to be used as a tool in the design work.¹ It would be used to develop a geometry numerically that meet requirements using a finite element (FE) model. Volvo Cars had recently gained knowledge in modelling and analysing rubber using FE modelling in another master's thesis project (Öhrn, 2015) and this project is the continuation of that. Volvo Cars had also before this project started, in cooperation with Computer Aided Engineering (CAE) software company *Altair*, made an initial study in how structural optimization could be used to design powertrain mounts. Volvo Cars has a number of software for structural optimization in use, but for the Powertrain Mounts group Altair gave the best opportunity for support, which was an important reason for using their software in the initial study. As torque rods are less complex than the load carrying mounts, the Powertrain Mounts group chose torque rods as the first subject for this new tool. The initial study showed that shape optimization could be a suitable type of optimization. The project objective is to develop the findings in the initial study into a complete optimization method for powertrain mounts.

¹ Gillenäng 2016.

Structural optimization for rubber structures has been proposed earlier in other studies. Kim and Kim (1997) presented a parameter optimization method for shape design of engine mounts with the objective of optimizing a single static stiffness value in three perpendicular directions. Li et al. (2009) presented a similar method with the same objective function, but with Genetic Neural Network as optimization method. Kaya (2014) presented an optimization method for a 2D model of a rubber bushing with the objective of meeting a stiffness curve with an arbitrary number of data points in contrast to the earlier two methods. Kaya used the statistical term Chi-square as an expression for the difference between the actual force and the target force for a certain displacement, which was used as objective function in the optimization. Park et al. (2012) presented a shape optimization method for rubber isolators in automotive cooling modules to maximize vibration isolation and fatigue life of the isolators. The method included parameterization of a 2D finite element model using Altair's software *HyperMesh* with its morphing tools. Topology optimization has also been suggested for optimization of rubber components; Lee and Youn (2004) presented a topology optimization method for rubber isolators considering both static and dynamic stiffness.

All of the methods presented above are applied either to simple 2D models or to 3D models with a small number of design variables. Modern powertrain mounts are more complex; they have to be modelled in 3D for accurate results and there are many geometrical features affecting the overall component stiffness. They often have non-symmetrical stiffness curves for different loading directions such as tensile and compression. There is a need for a structural optimization method for today's complex powertrain mounts.

1.2 Purpose

The purpose of this project is to develop an efficient powertrain mounts development method for Volvo Cars, which by structural optimization finds the optimal mount geometry so that the mount meets stiffness requirements. This would enable Volvo Cars to develop and design powertrain mounts in-house, which gives the potential of reduced development lead-times and cost compared to today's development process.

1.3 Problem analysis

To ensure that the project will fulfil its purpose, the basic problem described in the background is here broken down into four research questions. These questions will guide the work in the project so that no part of the problem is left unexplored.

The first question that needed to be answered in order to develop a well-functioning optimization method is the question of what the method should deliver. This is an important question since the method will not cover the whole product development process; it has both preceding and succeeding phases, which will need the correct input and output from the phase where this method is to be used. The surrounding phases will most likely include different kind of roles with different prerequisites for carrying out their tasks, which will also be important to consider.

Research question 1

Rq 1 What kind of output should the optimization method deliver? What phase and what role is the receiver of the output?

The first research question is probably not very extensive, but nevertheless important, and it leads to the perhaps most extensive research question that constitutes the core of this project. It is about the content of the optimization method, and is broken down further into three sub questions. The optimization method will include several steps and deciding which steps and in what order they should be performed is important to be considered. As mentioned earlier, the optimization method needs to be integrated with surrounding development phases, wherefore it is also important to ensure that the preceding phase can deliver what is necessary for the phase to function well.

Research question 2

How should the method be designed to deliver what is asked for in Research question 1 in an efficient way?

Rq 2.1 How should shape optimization be implemented to meet the demands of this project?

Rq 2.2 How should the method workflow look like? What steps should be included, and in what sequence?

Rq 2.3 What kind of input is needed to perform these tasks?

A model of what is going to be optimized is needed when doing structural optimization. Such a model needs material parameters to model the material behaviour properly. Currently, the Powertrain Mounts group at Volvo Cars does not have much material data on rubber to use. It would therefore be interesting to see if material parameters can be extracted from powertrain mounts already in production.

Research question 3

Rq 3 Is it possible to obtain material data from powertrain mounts rubber parts to properly model rubber material?

The last research question is of great importance if the optimization method actually is to be used in the product development process at Volvo Cars. Since structural optimization of rubber parts is something new for the Powertrain Mounts group, surrounding phases needed to utilize the method fully will have to be developed. This is an extensive question, but not the core of this project, thus, it will not be in much focus:

Research question 4

Rq 4 How and where should the optimization method be implemented in the product development process at Powertrain Mounts, Volvo Cars? Who (what role) is the end user of the optimization method?

1.4 Scope and delimitations

The method developed in this project is intended to be applicable to different types of powertrain mounts, but it will be developed by studying a specific type of powertrain mount; torque rods. For the validation and adjustment phase of this project, the Left Lower Tie-Bar (LLTB) found in Volvo Cars' V40 car model will be studied. The Volvo V40 LLTB is the torque rod studied in Öhrn's thesis (Öhrn, 2015); wherefore a large set of analysis data exists for this component, which makes it suitable also for this study.

Focus will be on optimizing torque rod geometry to meet static stiffness requirement in the main loading (x -) direction. Static stiffness requirements in other directions will not be studied, as they are not as important as the main loading direction for torque rods. Dynamic stiffness requirement will be considered, but not in focus. Other requirements such as manufacturing constraints, durability and fatigue resistance will not be studied, but the optimization method should not hinder a future complement of such requirements.

As the initial study showed promising results, the same modelling and analysis software, the *HyperWorks* platform by Altair, will be used in this project. The *Yeoh* hyperelastic model will be used for modelling rubber, as it was shown to be sufficiently accurate for torque rods (Öhrn, 2015).

As mentioned in Research questions 4, focus will not be on implementation of the method, this question will only be studied briefly. Neither will focus be on evaluation of the method; this will only be treated in the discussion section.

1.5 Report outline

This report is divided into seven sections, starting with the Introduction. The Theory section provides the essential theory of which the optimization method is built up. The Project methodology section describes the methodology used to carry out the project. The Results are then presented, followed by Discussion, Conclusion and Future work.

2 Theory

In this section, the most important theory that the optimization method is based on is presented. The section has four parts: Rubber, Finite element analysis of torque rods, Structural optimization and Theory summary. In the last part, the theories of the three first parts are summarized and linked together to show how they form the base for the optimization method. Powertrain mounts are not only made of rubber as described earlier, but modelling rubber is more complex than modelling, for example, aluminium. Furthermore, the Powertrain Mounts group at Volvo Cars already has sufficient knowledge regarding aluminium structures, wherefore the material part of this theory section only focuses on rubber materials.

2.1 Rubber

The word *rubber* is originally referring to the material obtained from the tree *Hevea Braziliensis*, and the word is derived from the ability of the material to erase (rub out) pencil-lead marks from paper (Freakley & Payne, 1978). The current use of the word rubber has though changed to include more materials than the original natural rubber, such as synthetic rubbers. A perhaps more appropriate and descriptive word for such materials is the term *elastomer*, referring to that they are polymers with highly elastic properties (Austrell, 1997).

2.1.1 Material properties

Natural rubber is obtained from latex, the sap of the rubber tree. The solid rubber material is extracted by separating the rubber molecules from the watery liquid that forms the latex, which contains about 35% rubber (Treloar, 1975). Rubber is a hydrocarbon in the form of long polymer chains, for natural rubber consisting of mainly isoprene. Natural rubber was the first material to be used in elastomeric products and still is the most common material for most purposes (Austrell, 1997). For synthetic rubbers, the most common is Styrene-butadiene rubber (SBR) (Austrell, 1997). SBR was developed as a synthetic replacement for natural rubber, and has very good abrasion and aging resistance wherefore it is mainly used in car tyres (Freakley & Payne, 1978).

The most important mechanical properties of rubber that are utilized in engineering applications are the ability to sustain large deformations that are not permanent, vibration damping abilities and resistance to lubrication (Austrell, 1997). In powertrain mounting applications, it is of course the two first properties that are of importance. Rubber has a very high extensibility and can deform elastically (that is, reversible) up to 500-1000% (Treloar, 1975). A typical force-extension curve for a vulcanized rubber is non-linear, which means that Hooke's law does not apply. It is therefore not possible to assign an accurate value of Young's modulus, but for comparison, an approximate value for small strains is in the order of 1 MPa (Treloar, 1975). The corresponding value for steel is around 200 GPa, and the maximum elastic extensibility of steel is around 1%. There is, thus, a huge difference between rubber and other common solid engineering materials. The damping property of rubber is connected to the fact that rubber can store energy when deformed, but not all energy is recoverable (Austrell, 1997). There will be a difference in the loading and unloading curve in stress-strain plot, which is called hysteresis. Energy is stored in rubber as elastic (reversible) and heat (irreversible) energy during deformation, and the hysteresis is mainly due to heat losses.

For a rubber material to have the above-described elastic properties, three main requirements must be fulfilled (Treloar, 1975):

1. The presence of long-chain flexible molecules
2. The forces between the molecules must be weak
3. The presence of crosslinks at a few places along the length of the molecules to form a network

The long polymer molecules described above satisfies the first requirement. The second requirement is needed for the molecules to move relative to each other to give the high extensibility of the material. The third requirement is needed to restrict the relative motion of the molecules; otherwise, the material would behave as a liquid.

The third requirement above is fulfilled by the molecular structure of the material, which is largely formed during the vulcanization process. Vulcanization is a chemical reaction between rubber and sulphur, discovered by Charles Goodyear in 1839 (Treloar, 1975). It is in the vulcanization process that the important crosslinks between the polymer chains are formed, thus, creating the network structure. Other additives, fillers, are also added. For rubbers in engineering applications, carbon-black is the most common, and as mentioned earlier what is used in powertrain mounts rubber parts. Carbon-black consists of very small particles of carbon, 20 nm to 50 μm , and is added to the rubber before the vulcanizing ingredients are added (Freakley & Payne, 1978). The reason for this is that the fillers are blended into the rubber using an internal mixer producing high shear forces in the rubber mixture that results in high temperatures in the rubber, up to 130°C, which is above the activation temperature for the vulcanization process (Freakley & Payne, 1978). To prevent premature vulcanization, the rubber mixture is therefore discharged from the internal mixer and further mixed on a two-roll mill with large cooling areas where the vulcanizing ingredients can be added.

The vulcanization process is in most cases combined with the shaping process in an operation called moulding. Nowadays, injection moulding is the most common moulding process, with a vulcanization temperature of about 170°C (TrellebeorgVibracoustic (Ed.), 2015). During the vulcanization reaction, which typically takes between 4 to 10 minutes for powertrain mounts, the injection pressure is kept constant at about 100 MPa (TrellebeorgVibracoustic (Ed.), 2015). Metal parts are often bonded to the rubber parts in the moulding operation, to act as attachment points or increase the stiffness of the component. As described earlier, the powertrain mounts in current Volvo cars are made of rubber and extruded aluminium parts. Rubber is bonded very well to metal parts; the bonding surface is usually stronger than the rubber itself (Austrell, 1997).

The carbon-black-filler is added to increase the stiffness of the material or the resistance to wear (Austrell, 1997). The carbon particles are only linked to the rubber network by crosslinks. For a schematic picture of a carbon-black-filled rubber, see Figure 2.1. The carbon-black particles will also make the rubber less elastic and more leathery, reducing the maximum elongation and increasing the hysteresis and heat build-up, which in most cases is unwanted (Freakley & Payne, 1978). The amount of carbon-black to be added is therefore a balance between these properties. Usually 25-50 parts of carbon-black per 100 parts of rubber are added (Freakley & Payne, 1978).

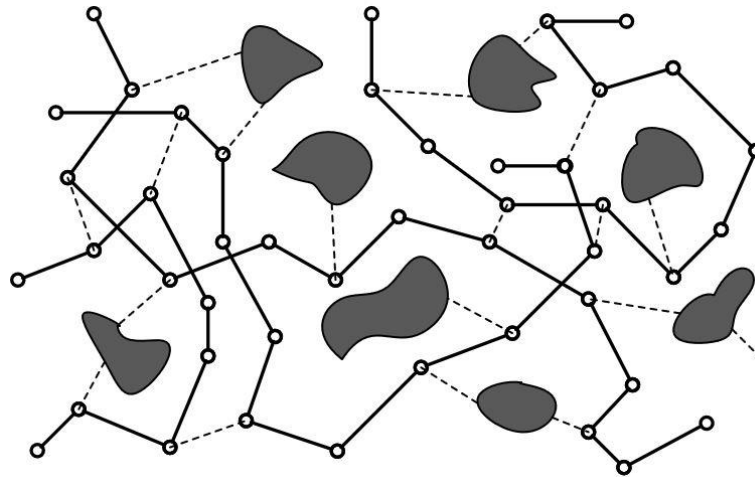


Figure 2.1 : Schematic representation of the molecular structure of carbon-black-filled rubber, showing the long rubber molecular chains, the carbon-black particles and the crosslinks.

A property widely used in engineering applications is the hardness of vulcanized rubbers. Hardness in this context means resistance to elastic deformation due to indentation by a rigid body (Freakley & Payne, 1978). The hardness of a rubber vulcanizate is determined in a hardness test, and gives an indirect measure of the elastic modulus of the rubber compound. The test procedure includes indentation of the rubber test specimen with a ball under a constant force, and then measuring the indentation depth. The indentation depth, the corresponding force and the radius of the ball is then used to calculate the hardness value. There are two common scales for hardness, the International Rubber Hardness Degrees (IRHD) and the Shore Hardness Scale. Most rubber compounds have a hardness in the range between 30-80 IRHD, where the IRHD scale and the Shore Hardness scale are almost identical. The relationship between hardness and the shear modulus G is shown in Figure 2.2. The diagram is constructed from the measurement data from Lindely (1974).

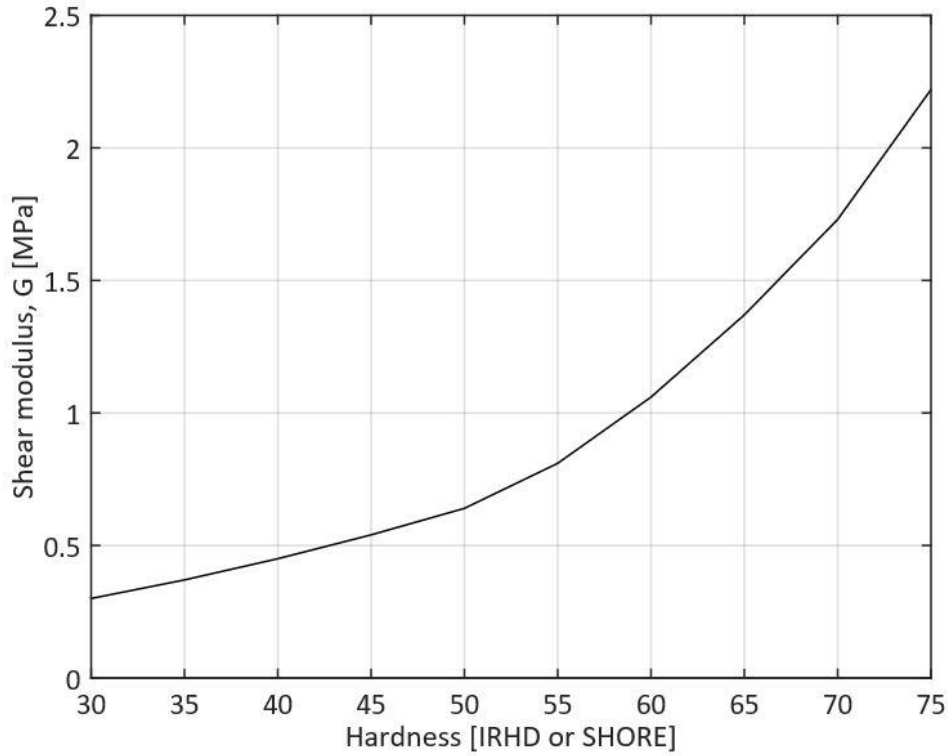


Figure 2.2: Relationship between the shear modulus G and the rubber hardness.

2.1.2 Modelling rubber elasticity

Rubber is modelled as a hyperelastic material. There are two main approaches for modelling the elastic behaviour of rubber: the statistical or kinetic theory and the phenomenological theory (Yeoh & Fleming, 1997). In this subsection three hyperelastic models from these two approaches will be presented: the *neo-Hookean*, the *Mooney-Rivlin* and the *Yeoh* models. It shall be noted that there are many other models for modelling hyperelasticity, but these are some of the most common ones. The statistical theory is based on the molecular structure of rubber and was developed by Treloar (1975) among others. Treloar (1975) showed that the elastically stored free energy per unit volume or strain-energy function, W , in a deformed rubber can be written as:

$$W = \frac{1}{2}G(\lambda_1^2 + \lambda_2^2 + \lambda_3^2) \quad (1)$$

where

$$G = NkT \quad (2)$$

where N is the number of rubber molecular chains per unit volume, k is Boltzmann's constant, T is the absolute temperature while λ_1 , λ_2 and λ_3 are the principle stretch ratios. Stretch is used in the analysis of materials subjected to large deformations, and is defined by:

$$\lambda = \frac{L_f}{L_0} \quad (3)$$

where L_0 is the initial length and L_f is the final (deformed) length. The stretch ratios are visualized in Figure 2.3. Treloar (1975) also showed that G is equal to the shear modulus. From equation (1), it is possible to derive a constitutive relation between the stress and strain in a

rubber volume. For simple extension (see Figure 2.3) or compression of a rubber specimen assumed to be incompressible, that is, $\lambda_1\lambda_2\lambda_3 = 1$, then $\lambda_1 = \lambda$ and $\lambda_2 = \lambda_3 = \lambda^{-1/2}$. The principal stress σ is then (Freakley & Payne, 1978):

$$\sigma = \frac{\partial W}{\partial \lambda} = G(\lambda - \lambda^{-2}) \quad (4)$$

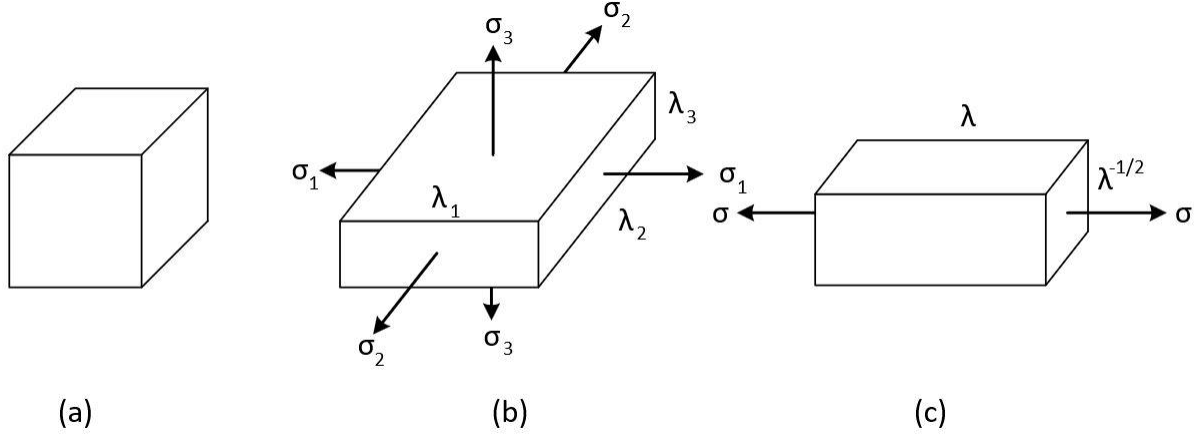


Figure 2.3: Modes of deformation: (a) undeformed unit cube, (b) general state of homogenous deformation, (c) simple extension.

The other approach of modelling rubber elasticity, the phenomenological theory, was developed in parallel with the statistical theory. This theory is more general, and is based on fitting mathematical equations to experimental data instead of trying to model the physical structure of the material. Mooney (1940) developed the first significant phenomenological theory, by showing that the strain-energy function W can be written as (Treloar, 1975):

$$W = C_1(\lambda_1^2 + \lambda_2^2 + \lambda_3^2 - 3) + C_2(1/\lambda_1^2 + 1/\lambda_2^2 + 1/\lambda_3^2 - 3) \quad (5)$$

where C_1 and C_2 are two material constants. The simple extension case described above gives the stress-strain relation (Yeoh & Fleming, 1997):

$$\sigma = \frac{\partial W}{\partial \lambda} = 2(C_1 + C_2\lambda^{-1})(\lambda - \lambda^{-2}) \quad (6)$$

Rivlin (1956) further developed the theory formulating the strain-energy function in a more general way (Treloar, 1975):

$$W = \sum_{i=0, j=0}^{\infty} C_{ij}(I_1 - 3)^i(I_2 - 3)^j \quad (7)$$

where

$$I_1 = \lambda_1^2 + \lambda_2^2 + \lambda_3^2, \quad I_2 = 1/\lambda_1^2 + 1/\lambda_2^2 + 1/\lambda_3^2 \quad (8)$$

where C_{ij} are material constants, and I_1 and I_2 are strain invariants.

Stress-strain relations can be derived in a similar way using this function, for simple extension it takes the form (Yeoh & Fleming, 1997):

$$\sigma = \frac{\partial W}{\partial \lambda} = 2 \left(\frac{\partial W}{\partial I_1} + \frac{\partial W}{\partial I_2} \lambda^{-1} \right) (\lambda - \lambda^{-2}) \quad (9)$$

Rivlin's strain-energy function is often truncated by only including the first terms of the sum. If only including the first term ($i = 1, j = 0$), equation (7) is reduced to:

$$W = C_{10}(I_1 - 3) \quad (10)$$

Materials modelled using equation (9) are called *neo-Hookean*. It can be seen that if letting $C_{10} = \frac{1}{2}G$, equations (1) and (10) are essentially identical and is, thus, forming a link between the statistical and the phenomenological theories (Yeoh & Fleming, 1997).

If the two first terms of equation (7) are included, the following equation is obtained:

$$W = C_{10}(I_1 - 3) + C_{01}(I_2 - 3) \quad (11)$$

which is called the *Mooney-Rivlin* equation, and it can be noted that for incompressible materials equation (5) and (11) are identical.

Both the neo-Hookean and the Mooney-Rivlin models are very common and useful, but for carbon-black-filled rubber vulcanizates, they are not sufficiently accurate to model the material behaviour, in particular for large deformations (Holzapfel, 2000). The statistical theory and, thus, the identical neo-Hookean model can describe the elastic behaviour of rubber accurately for small strains. In, for example, simple extension the statistical model is valid for strains up to about 30% (Yeoh & Fleming, 1997). For moderate strains (about 50-400%), the stress-strain curve falls below the theoretical curve of the statistical model, and for large strains (larger than about 300%), it rises above the theoretical curve (Yeoh & Fleming, 1997). The Mooney-Rivlin model is found to better describe the elastic behaviour, it is valid for strains up to about 100%, but is not valid for very large strains (Yeoh & Fleming, 1997).

To better model the elastic behaviour of rubber for very large strains, Yeoh (1990) proposed another phenomenological model. Yeoh made the assumption that $\partial W / \partial I_2 = 0$ based on published experimental data suggesting that $\partial W / \partial I_2$ is close to zero. It can be shown that this reduces equation (7) to (Yeoh & Fleming, 1997):

$$W = \sum_{i=0}^{\infty} C_{ij}(I_1 - 3)^i \quad (12)$$

where j is always equal to zero. Yeoh proposed a three-term version of this strain-energy function:

$$W = C_{10}(I_1 - 3) + C_{10}(I_1 - 3)^2 + C_{20}(I_1 - 3)^3 \quad (13)$$

This model can describe both the decrease in stiffness for low strains and the increase in stiffness for large strains in carbon-black-filled rubbers. The neo-Hookean and Mooney-Rivlin models are too simple to capture this behaviour (Holzapfel, 2000). Using higher order terms in I_1 as in equation (13) has also, according to Boyce and Arruda (2000), been shown to capture

the deformation state of rubber for very large deformations better. It was also shown in the Master's thesis of Öhrn (2015) that the Yeoh model modelled the V40 LLTB torque rod more accurately than the neo-Hookean and Mooney-Rivlin models. The Yeoh model is therefore used in this project.

2.1.2.1 Obtaining hyperelastic material parameters

Austrell (1997) describes a fitting procedure to calibrate the Yeoh model to test data by determining the three hyperelastic constants in equation (13). For this, the constitutive equation describing the relation between stress and strain for the Yeoh model is needed. As described above, the Yeoh model is only using the first strain invariant I_1 . For simple extension or compression of a rubber test specimen the stretch ratios are $\lambda_1 = \lambda$ and $\lambda_2 = \lambda_3 = \lambda^{-1/2}$, which means that I_1 can be written as (see equation (8)):

$$I_1 = 2\lambda^{-1} + \lambda^2 \quad (14)$$

The uniaxial stress-strain relation for the Yeoh model is (Austrell, 1997):

$$\sigma = 2(C_{10} + 2C_{20}(I_1 - 3) + 3C_{30}(I_1 - 3)^2)(\lambda - \lambda^{-2}) \quad (15)$$

Inserting equation (14) into equation (15) yields:

$$\sigma = 2(C_{10} + 2C_{20}(2\lambda^{-1} + \lambda^2 - 3) + 3C_{30}(2\lambda^{-1} + \lambda^2 - 3)^2)(\lambda - \lambda^{-2}) \quad (16)$$

Performing tensile and/or compression tests give values for the stress σ and the stretch ratio λ , making it possible to obtain the values of the three hyperelastic constant to calibrate the model to the test data by setting up the equation for each data point. For large deformations, the change in cross-sectional area is significant and the true stress need to be used. The true stress σ is defined by:

$$\sigma = \frac{F}{A} = \frac{F\lambda}{A_0} \quad (17)$$

where F is the force on the cross-section and A is the deformed cross-sectional are, while A_0 is the undeformed cross-sectional area and λ is the stretch ratio.

Normally the number of test data points and, thus, values of σ and λ , are higher than the number of coefficients in equation (16), wherefore an overdetermined linear system of equations is obtained (Austrell, 1997). To solve this system of equations, the least square fitting procedure is used. The equation system can be written as follows:

$$\mathbf{A}\mathbf{c} = \mathbf{b} \quad (18)$$

where \mathbf{A} is a matrix with three columns and equally many rows as the number of data points, containing the coefficients for each of the three material parameter in equation (16) in each column. For example, the first column in \mathbf{A} will contain the coefficient for C_{10} for each data point, with the value $2(\lambda - \lambda^{-2})/\sigma$. \mathbf{c} is a 3×1 matrix containing the three hyperelastic material parameters (the unknowns in the equation system) and \mathbf{b} is a single column matrix of ones with equally many rows as the number of data points (corresponding to the left side of equation (16) after dividing the equation by σ). Equation system (18) cannot be solved in the ordinary way because the lack of a unique solution and is therefore solved by minimizing the residual (the least square method).

By inserting a trial solution \mathbf{c}^* in equation (18), the residual \mathbf{e} can be written as (Austrell, 1997):

$$\mathbf{e} = \mathbf{A}\mathbf{c}^* - \mathbf{b} \quad (19)$$

\mathbf{e} is a vector containing difference between the left- and right-hand side of equation (18) when the trial solution \mathbf{c}^* is inserted, that is, the relative error in each data point. The objective with the least square fitting procedure is to find a \mathbf{c}^* that minimizes this residual. By using the L_2 -norm $\|\mathbf{e}\|_2^2 = \mathbf{e}^T \mathbf{e}$ an expression equal to the sum of the squares of the relative error in each data point can be written as (Austrell, 1997):

$$\Phi = \|\mathbf{e}\|_2^2 = (\mathbf{A}\mathbf{c} - \mathbf{b})^T (\mathbf{A}\mathbf{c} - \mathbf{b}) = \sum_{i=1}^n (\sigma_i^{\text{theor}} / \sigma_i^{\text{exp}} - 1)^2 \quad (20)$$

where σ_i^{theor} are the theoretical stress values from the constitutive model, and σ_i^{exp} are the experimental stress values.

Minimizing equation (20) is the same as finding the solution to the equations:

$$\frac{\partial \Phi}{\partial c_i} = 0 \quad i = 1, 2, \dots, 9 \quad (21)$$

It can be shown that equation (21) can be written as (Austrell, 1997):

$$\mathbf{A}^T \mathbf{A} \mathbf{c} = \mathbf{A}^T \mathbf{b} \quad (22)$$

The equation system has now been rewritten as an ordinary linear system of equations that can be solved with standard methods. To conclude, to obtain the hyperelastic material parameters in the Yeoh model (equation (13)) by this method, matrix \mathbf{A} and \mathbf{b} have to be set up and equation (22) has to be solved. This gives the best fit of the material parameters in terms of minimizing the sum of the squares of the relative error in each data point.

2.1.3 Modelling dynamic behaviour

The theory presented in subsection 2.1.2 is only concerned with the elastic properties of rubber. These properties are the governing the static behaviour of rubber materials. For the dynamic behaviour, other properties such as damping, creep and stress relaxation will be of importance. For dynamic analysis of rubber, the elastic models are not sufficient.

The dynamic behaviour of rubber is dependent of several properties, such as, frequency/time, temperature, static pre-load and amplitude (Austrell, 1997). The damping behaviour can be modelled using a viscoelastic model taking into account the frequency/time dependency (Austrell, 1997). For carbon-black-filled rubbers there will also be frictional part originating in the rubber-carbon and carbon-carbon interfaces that can be modelled with a rate-independent frictional element, giving a viscoplastic model in combination with the viscoelastic model (Austrell, 1997).

Öhrn (2015) used a viscoplastic in combination with a viscoelastic model for large strains based on the Yeoh hyperelastic model and overlaid small viscoelastic fluctuations to model dynamic behaviour of torque rods. This project will focus on the static behaviour of rubber, wherefore the dynamical models for rubber will not be investigated further.

2.2 Finite element analysis of torque rods

The finite element method (FEM) is used to solve, for example, partial differential equations of solid and structural analysis. The basic idea is to find the distribution of some field variable, for example, displacement. The FEM can find a solution to this distribution numerically, something that is often difficult to do analytically (Liu & Quek, 2014). This is done by dividing the model of the structure into a number of small pieces of simple geometry called *elements*. The elements are built up of *nodes*. Physical and mathematical principles can then be applied to each element. The elements are tied together in the nodes to make it possible to describe the distribution of the field in the whole structure. The process eliminates spatial derivative. This leads to, for static and steady state problems, a set of algebraic equations that can easily be solved to yield the field variable. The method converges with respect to the number of elements. The number of elements is often large to get a sufficiently accurate model, which means that the number of equations is large wherefore computers are used for solving the equation system.

The procedure of using the FEM is in most cases (Liu & Quek, 2014):

1. *Modelling (Pre-processing)*: This step includes modelling of the geometry using Computer Aided Design (CAD) software, meshing the model, which is the process of dividing it into elements and applying material properties and boundary, initial and loading conditions.
2. *Solving*: This step is where the equation system is solved, which is a very computer-hardware demanding process.
3. *Results visualization (Post-processing)*: This is the final step where the results are visualized in form of, for example, contours and deformations of the model.

There are many different computer software for using the FEM. In this project HyperMesh with *Abaqus* was used for modelling, *OptiStruct* and *Abaqus* for solving and *Abaqus/Viewer* and *Abaqus/CAE* for results visualization.

An important feature in this project that some pre-processing software support, including HyperMesh, is *Morphing*. HyperMesh has a built in tool called *HyperMorph*, which enables three different approaches for morphing. In this project, the Domains and Handles Concept was used. It means that the model is divided into domains with handles that are used to control the shape of the domains. The domains in turn controls the position of the nodes of the elements inside the domain. This can be used to alter the shape of a geometry, which can be used in, for example, shape optimization. Morphing is central for the optimization method developed in this project.

2.3 Structural optimization

“Structural optimization is the subject of making an assemblage of materials sustain loads in the best way” (Christensen & Klarbring, 2009). For this to make sense, the “best way” has to be specified. For a torque rod, sustaining loads in the best way primarily means sustaining the reaction forces from the powertrain according to its stiffness requirements. Thus, every optimization needs to have an objective. The objective is usually specified in an objective function, f_{obj} . An objective function is a function used to classify a certain design; it returns a number that indicates how good the design is (Christensen & Klarbring, 2009). In most cases f_{obj} is chosen so that a small value indicates a good design, and the optimization will therefore be a minimization problem. A structural optimization problem also need to have design

variables, **dv**, and state variables, **sv** (Christensen & Klarbring, 2009). A design variable describes a certain design and can be changed during an optimization. It can, for example, represent the geometry; either directly as a dimension or indirectly by describing a certain shape of an object, or the material of a design. A state variable describes the response of a structure for a certain design, for example, in terms of displacement or force. A structural optimization problem can then be written as (Christensen & Klarbring, 2009):

$$\begin{aligned} &\text{minimize } f_{\text{obj}}(\mathbf{dv}, \mathbf{sv}) \\ &\text{subject to } \text{behavioral constraints on } \mathbf{sv} \\ &\quad \text{design constraints on } \mathbf{dv} \end{aligned}$$

For structural optimization where the design variables represent some sort of geometrical feature, the optimization can be divided into three different classes (Christensen & Klarbring, 2009):

- *Sizing optimization*: Here the design variables represent some sort of structural thickness, such as, cross-sectional areas of truss members or the thickness of a sheet.
- *Shape optimization*: Here the design variables represent the form or contour of the geometry. The connectivity of the structure is not changed, that is, new boundaries are not formed.
- *Topology optimization*: Here the design variables represent a density-like variable that can take the values 0 or 1. This means that the topology of the structure can change. This is the most general class of structural optimization.

It shall be noted that shape optimization requires a more detailed input than topology optimization. Shape optimization require some sort of concept geometry as input where the form and boundaries of the structure are set. Topology optimization only require a design space from which the form of the structure will evolve.

Structural optimization is in almost all cases performed using computer tools like FE analysis (FEA) as described above to calculate the responses of the structure. There are also dedicated computer tools for carrying out the optimization problem. In this project, *HyperStudy* was used as optimization software with Abaqus as FEA software.

HyperStudy has a number of different methods to solve optimization problems. The following methods were applicable in this project:

- *Adaptive Response Surface Method (ARSM)*: This method is the default method in HyperStudy, but for large number of design variables the GRSM (see below) is suggested. This method works by building response surfaces and adaptively updating them for each new design. It then finds the optimum for the current surface and compare it with the exact simulation. If they are not close, the response surface is updated until one of the convergence criteria are met.
- *Global Response Surface Method (GRSM)*: This method is also a response surface based approach, similar to the ARSM, but with global search capability by also doing a global sampling for each iteration. It is therefore more capable of finding a global optima and more suitable for large number of design variables.

- *Sequential Quadratic Programming (SQP)*: This is a gradient-based iterative method. A drawback with this method is that it is likely that this method finds the local optima.
- *Method of Feasible Directions (MFD)*: This is one of the earliest methods for solving constrained optimization problems. It is a gradient-based method, which works by moving from one feasible design to an improved feasible design.

2.4 Theory summary

To conclude the theory section, an illustrative picture is presented in Figure 2.4. The three theory parts presented in this section form the basis for the optimization method developed in this project. To enable structural optimization, and more specifically shape optimization, of torque rods, FE models with accurate material models are needed. This is most critical for the rubber parts since rubber is more complicated to model than, for example, aluminium. Theories for modelling rubber, presented in Subsection 2.1, are therefore the foundation in this project. As mentioned, an FE-model is then needed to enable structural optimization, wherefore the FEM was presented in Subsection 2.2. Finally, structural optimization was presented in Subsection 2.3, which is the part that is desired to implement at Volvo Cars using the optimization method.

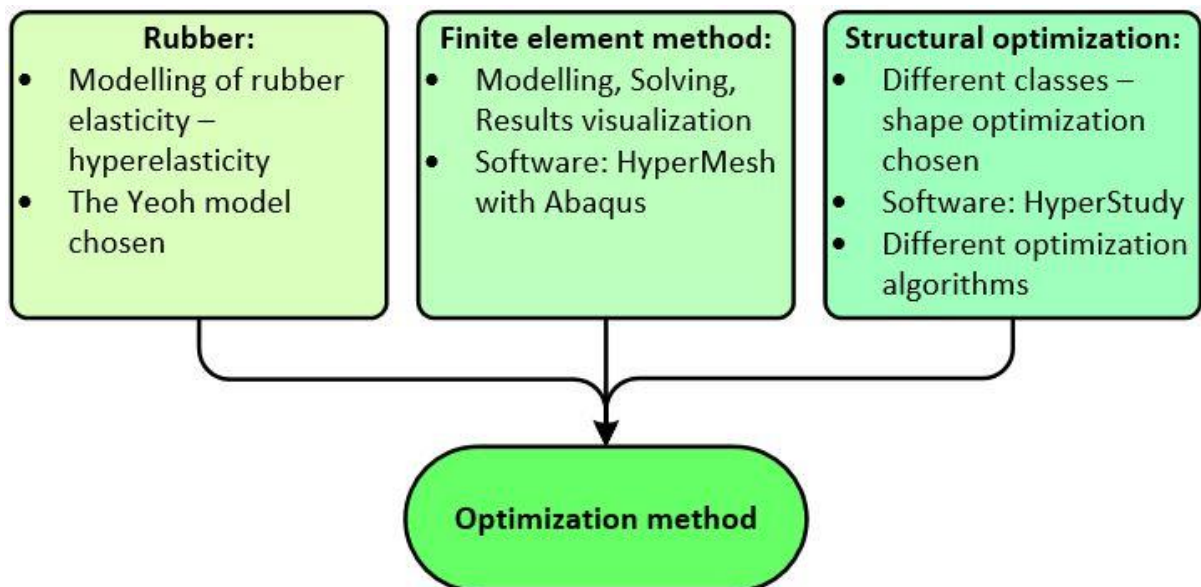


Figure 2.4: Theory from three main areas are used to form the optimization method proposed in this report.

3 Project methodology

This section describes the methodology used to carry out this project, not to be confused with the optimization method that is the deliverable of this project. The project methodology was designed around the research questions to ensure that they would be answered properly. The project was divided into five phases, each with a number of activities. The methodology is illustrated in Figure 3.1. As this project is a method development project, there is not always a clear distinction between the methodology used in the steps of this project and the optimization method developed. Therefore, this section only gives an overview of the steps carried out; the details are covered in the Results section.

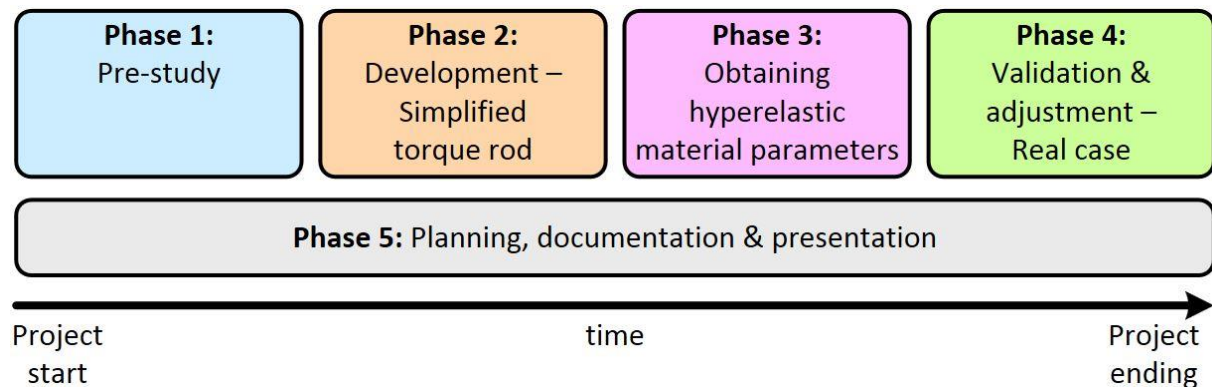
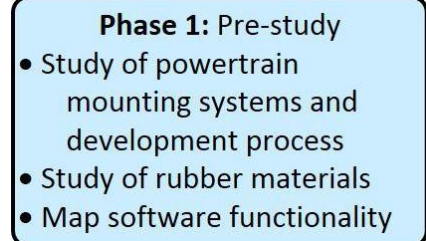


Figure 3.1: Overview of the different phases that the project methodology is composed of.

3.1 Phase 1: Pre-study

The project began with a pre-study with the purpose of both breaking down the problem into research questions, and building knowledge as a base for answering these questions. Answers on Research question 1 and to some extent research question 4 were based on the knowledge gained in this phase, which is presented in the Background and Theory sections. The other research questions were answered in the following phases, which build on the knowledge from this phase.



The first activity of the pre-study was a study of powertrain mounting systems used at Volvo Cars, with extra focus on torque rods. The current development process and requirements of torque rods were also studied. Modelling and analysis techniques for rubber materials were then studied. As mentioned earlier, the Master's thesis (Öhrn, 2015) done at the Powertrain Mounts group before this project was a starting point for this project.

Another important activity of the pre-study was to map the functionality of the software so that it could be used in an efficient way. Focus of the pre-study was on studying the two applications HyperMesh and HyperStudy included in the HyperWorks platform.² HyperMesh is an FE pre-processor that was studied through a number of tutorials, HyperStudy is an analysis software including optimization capabilities that was studied through example studies and demonstrations from Altair.

² HyperWorks, Altair, Troy, United States, <http://www.altairhyperworks.com/>

The pre-study was completed when the knowledge level was considered sufficient for starting development of the optimization method, that is, a base knowledge on powertrain mounts and rubber materials, and sufficient software knowledge for performing basic FEA were gained.

3.2 Phase 2: Method development – simplified torque rod

Phase 2 meant development and design of the optimization method and, thus, answering Research question 2. The methodology for developing the optimization method was organized in two phases; the development phase covered in this phase and the validation phase covered in Phase 4. An iterative approach was used in this phase when it comes to building an FE

Phase 2: Development

- Design simplified torque rod
- Set up FE model
- Optimization
- Data management & visualization

model and preparing it for shape optimization. Research question 4 was also largely answered based on the knowledge gained in this phase, but also on the knowledge from Phase 4.

For this phase, a simplified torque rod was chosen as the subject to develop the method around. The reason for developing the optimization method around a simplified torque rod was that it would enable quick and easy geometry updates if necessary and that it would be more straightforward and faster to perform FEA on compared to a full-feature component with more detailed geometry. There is a risk that unknown difficulties will arise when the method later is applied to a full-feature component, but the advantages with development around a simplified geometry are expected to outweigh the disadvantages.

The first activity after designing the simplified torque rod was to carry out an initial static analysis to verify the model and calculate the nominal stiffness. For this, a model was built up in HyperMesh and pre-processed. Altair's own FE solver software OptiStruct was used for the analysis. There were some issues using OptiStruct with hyperelastic material and large displacement non-linear FEA, wherefore after some iterative testing a decision was made to use Abaqus as solver software instead, see Subsection 0 for more information on the FE solver software issues.

The FE model was then prepared for optimization by creating shapes through morphing which were used as design variables. A fictitious static stiffness requirement was created and the simplified torque rod was then optimized to this requirement. As different settings for the optimization were tried out, the need for convenient data management and visualization became clear. For this, two *MATLAB* scripts were written; a pre-optimization and a post-optimization.³ These scripts were used for setting up the optimization and for visualizing the results of the optimization. The optimization settings investigated included optimization method, inclusion of different rubber materials as a design variable and different setting for initial sampling. Last in the development phase, a dynamic analysis of the torque rod was done to investigate the possibility of including dynamic stiffness requirements in the optimization.

³ MATLAB, MathWorks, Natick, United States, <http://se.mathworks.com/products/matlab/>

3.3 Phase 3: Obtaining hyperelastic material parameters

The third phase was design for answering Research question 3, that is, investigating the possibility of extracting material parameters to be used in the Yeoh hyperelastic material model. This was done in two activities; a tensile test and a data analysis and calculation phase. The tensile test was done at Chalmers with the Department of Applied Mechanics tensile test machine, a Bent Tram UCT 50kN.⁴

The test set-up is shown in Figure 3.2. The rubber test specimens were water jet cut at Chalmers from in production Volvo Cars torque rods, including the V40 LLTB. The focus was on this particular torque rod since this was the subject of the next phase, but other Volvo Cars torque rods have longer main rubber elements that would give longer test specimens. This was considered important since the test specimens from the V40 LLTB were very short, thus, a comparison with longer test specimens were sought. The test specimens were cut as rectangular blocks; see Figure 3.3 for a picture of the specimens. As can be seen in the figure, two different thicknesses of the V40 LLTB specimens were cut out. This was because the first round of obtaining hyperelastic material parameters did not show accurate results compared to the material parameters used in Öhrn's (2015) work for the V40 LLTB. It was therefore decided to do another round with thinner specimens.

Phase 3: Material parameters

- Cut test specimens
- Perform tensile test
- Obtain material parameters
- Optimize material parameters



Figure 3.2: The tensile test machine used in this project with a test specimen clamped in place for testing.

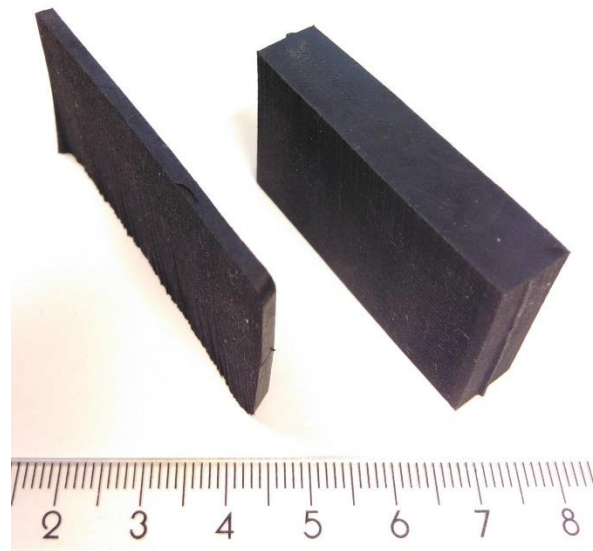


Figure 3.3: The two test specimens used in the tensile test: the thin specimen (left) and the thick specimen (right). The main unit of the scale included is cm.

⁴ Bent Tram UCT 50kN, Bent Tram A/S, Aalborg, Denmark, http://www.benttram.com/Machine_UCT50kN.html

The test procedure started with measuring the dimensions of the specimen, which was then clamped to the tensile test machine. It was clamped as firm as possible, and due to the clamping mechanism the clamping resulted in a slight compression of the specimen. The upper movable clamp where therefore raised carefully until the specimen was considered neutral, that is, not under tension or compression. The distance between the upper and lower clamp were measured, and the tensile test were then started. The tensile test machine plotted the force and displacement for the upper clamp. For the thick specimens the test was automatically aborted when the specimen started to slide in the clamp, which resulted in a fast decrease in force. The thin specimens were possible to clamp more firmly in relation to the force needed to reach a certain stretch value, which meant that they did not start to slide as quick as the thick specimens did. The test was therefore aborted manually when the force-displacement curve changed direction and started to flatten, which meant that sliding occurred. The results were saved in text files, which were then loaded into a MATLAB script for analysis, calculation and visualization of the material parameters. Validation simulations were then done by doing static FEA of the V40 LLTB with the different calculated material parameters.

Because of the inaccurate results of the fitted hyperelastic models for the tensile test data (see Subsection 4.1.9), the idea of optimizing the material parameters to model a certain component accurately emerged. The optimization method was therefore applied also in this phase, and the material parameters used to model the V40 LLTB were optimized to accurately model the component.

3.4 Phase 4: Method validation and adjustment – Real case

In this phase, the optimization method was applied to a real case, the V40 LLTB, for validation and adjustment of the method and, thus, validating the answer on Research question 2. An already existing FE model of the torque rod was used in this phase; the FE mesh was kept the same but the boundary conditions were updated to the same set-up used for the simplified torque rod and the model was prepared for shape optimization. The torque rod was then optimized to its static stiffness requirement with the goal of getting closer to the requirement than the already manufactured component. This phase was also iterative and improvements to the optimization method were done continuously.

Phase 4: Validation & adjustment

- Pre-processing
- Optimization
- Verification & adjustments

3.5 Phase 5: Planning, documentation and presentation

Phase 5 was ongoing throughout the whole project, but most of the work in this phase was done in the end of the project. The first activity of this phase was project planning, which was done first in the project and documented in a planning report and a time plan. After that, a number of short activities in form of status review presentations were carried out. The last activity included writing this report and preparing the final presentation. An important task was also to write the step-by-step optimization guide for Volvo Cars.

Phase 5: Planning, documentation & presentation

- Planning
- Status reviews
- Report & presentation

4 Results

In this section, the results of the project are presented. As the Background and Theory parts of this report present the findings of the first phase of the project, this section presents the findings from phase 2, 3 and 4 as well as answers to the research questions. The structure of the section follows the three phases it presents, starting with the development phase, then the material parameter phase, leading to a presentation of the optimization method followed by the validation and adjustment phase. The section concludes with an evaluation of the optimization method and the proposed product development process.

4.1 Method development – simplified torque rod

As mentioned earlier, a simplified torque rod was used for the development phase of the optimization method. It is simplified in a geometrical sense compared to Volvo Cars' production torque rods. This means that most of the radii were removed, and the MRE were made as rectangular blocks instead of having the angled short sides. The simplified torque rod was designed in the CAD software Catia V5, and the geometry was exported as a STEP-file for importation in HyperMesh. The CAD model of the simplified torque rod is seen in Figure 4.1.

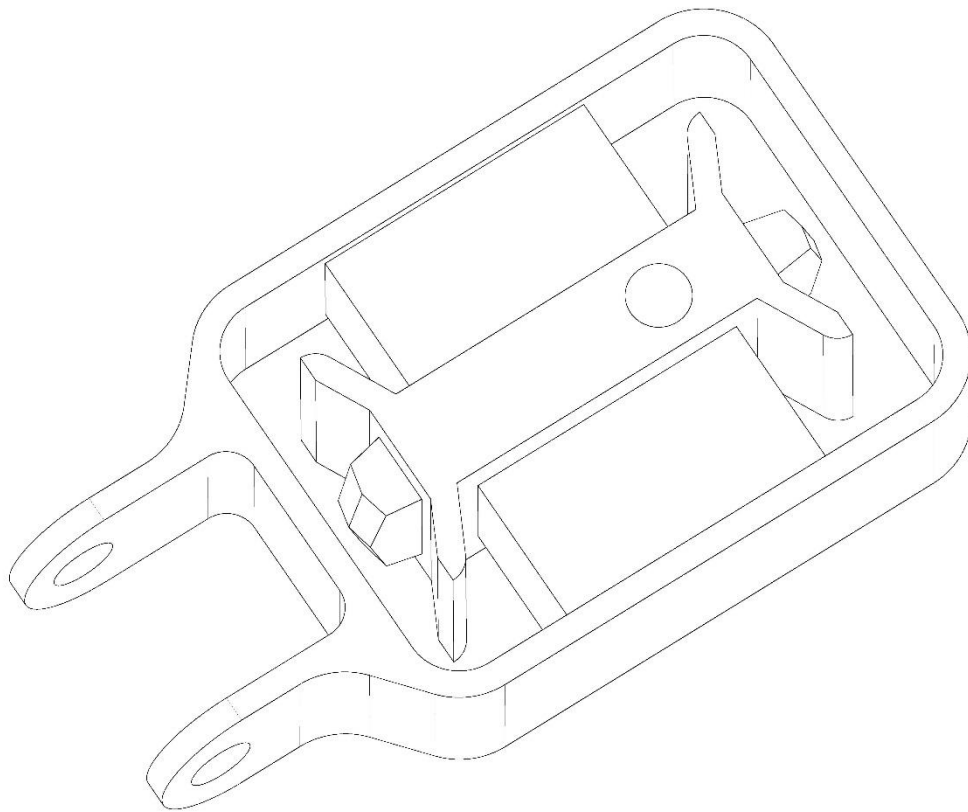


Figure 4.1: CAD mod of the simplified torque rod. Note the simple geometry of the different parts.

4.1.1 Pre-processing

The geometry was imported into HyperMesh, and because it is symmetric in two planes, it was split into four symmetrical pieces. The analysis was then done using only one fourth of the geometry, which reduces the number of elements and, thus, the computation time. Once the geometry was split, it was cleaned up from unwanted surface lines, and then meshed with mostly hexahedral elements. Thanks to the simplified geometry, it was possible to get a good quality mesh with hexahedral elements. The aluminium parts were modelled with the Abaqus element types C3D8 and C3D6. For Hyperelastic and almost incompressible materials such as rubber, hybrid elements are recommended (Dassault Systèmes, 2014). The rubber parts were therefore modelled with C3D8H elements. Each part of the geometry was meshed individually, and the rubber to aluminium bonding areas were connected with fixed surface-to-surface connections. The mesh was kept quite coarse, since the purpose with the simplified torque was not to get accurate results but to develop the method. An element size of around 2 mm for most of the parts and a bit finer for the bump stops and insert arms was used; see Figure 4.2 for a picture of the mesh.

Material properties and material models were applied; the Yeoh hyperelastic model with the hyperelastic material parameters for a 65 IRHD rubber used in Öhrn (2015) was used, and an elastic model was used for the aluminium. Boundary conditions were created; the frame was fixed in all degrees of freedom with rigid connections between a fixed node and the nodes in the attachment hole of the frame, and symmetry conditions were applied to the split surfaces. It was chosen to do the analysis based on an applied force and not on an applied displacement, wherefore a force was applied to the insert connection hole with rigid elements connecting the loading node with the surface nodes of the hole. There are benefits and disadvantages with both ways, which are discussed in the Discussion section. For the initial analysis, only one loading direction was analysed but for the optimization method both directions, that is, tension and compression should be analysed. This could be done in a single Abaqus analysis, but it was not found out how to restart the analysis from zero for the other direction. This meant that the analysis would include the unloading sequence when changing direction, which would give an unnecessary long analysis time. The analysis was therefore split in two; one for each direction with its own input file. The only difference between the two analyses is, thus, the loading direction and load magnitude.

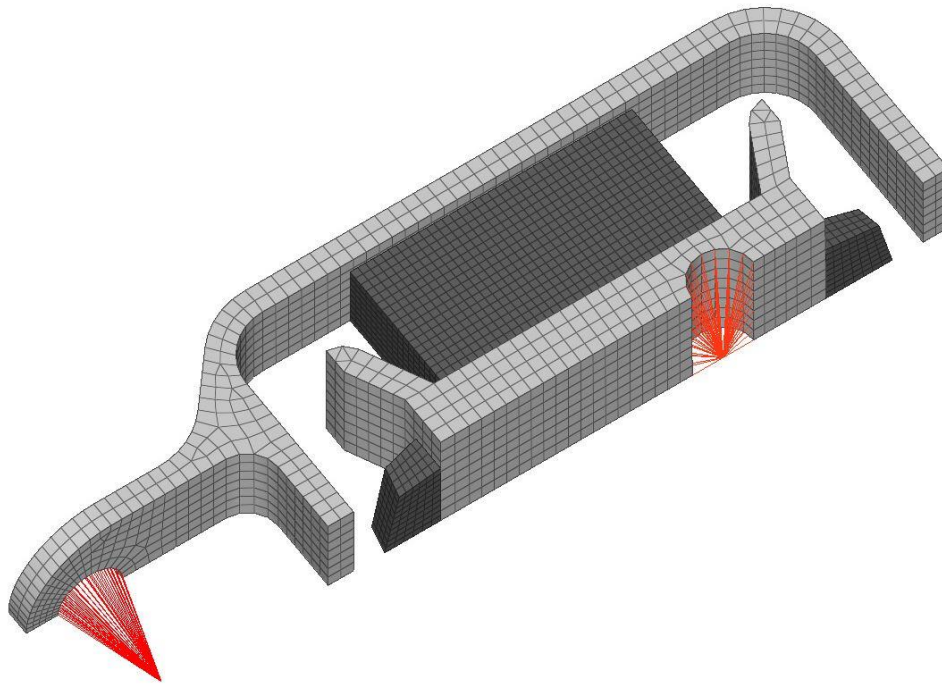


Figure 4.2: FE model of one quarter of the simplified torque rod. The red parts are rigid elements coupled to the attachment points of the torque rod for application of load and fixation constraint. Note the quite coarse mesh and that it is only a quarter model of the complete geometry.

4.1.2 Initial analysis

For the initial static analysis, a force of 3,5 kN in the negative x -direction was applied to the quarter model, which is equivalent to $4 \times 3,5 = 14$ kN for the complete component. As mentioned in Subsection 2.2, FEA of torque rods means that it is a non-linear analysis with large displacements. OptiStruct was therefore set up for this, but the analysis did not converge. The analysis was re-run but without the option for large displacements. This analysis did converge, but probably not with accurate results. The Altair support team was involved trying to solve the problem, and did manage to reach convergence but with the friction coefficient for the contact between rubber and aluminium decreased to 0.2 to reach convergence. It was never clarified why OptiStruct could not handle large displacements for the non-linear analysis with the prescribed frictional coefficient of 0.4 used at the Powertrain Mounts group for this type of contact. Because of the trouble with OptiStruct, it was decided to use Abaqus as FE solver instead. Another important reason for changing to Abaqus is that Abaqus is the most used FE solver at the Powertrain Mounts group at Volvo Cars, and having good knowledge of the software is very important for an efficient and accurate analysis. Running HyperMesh with Abaqus instead of OptiStruct meant some re-learning of the user interface and some re-building of the model. The analysis was then run again with good results, and the deformed mesh from the Abaqus simulation is shown in Figure 4.3.

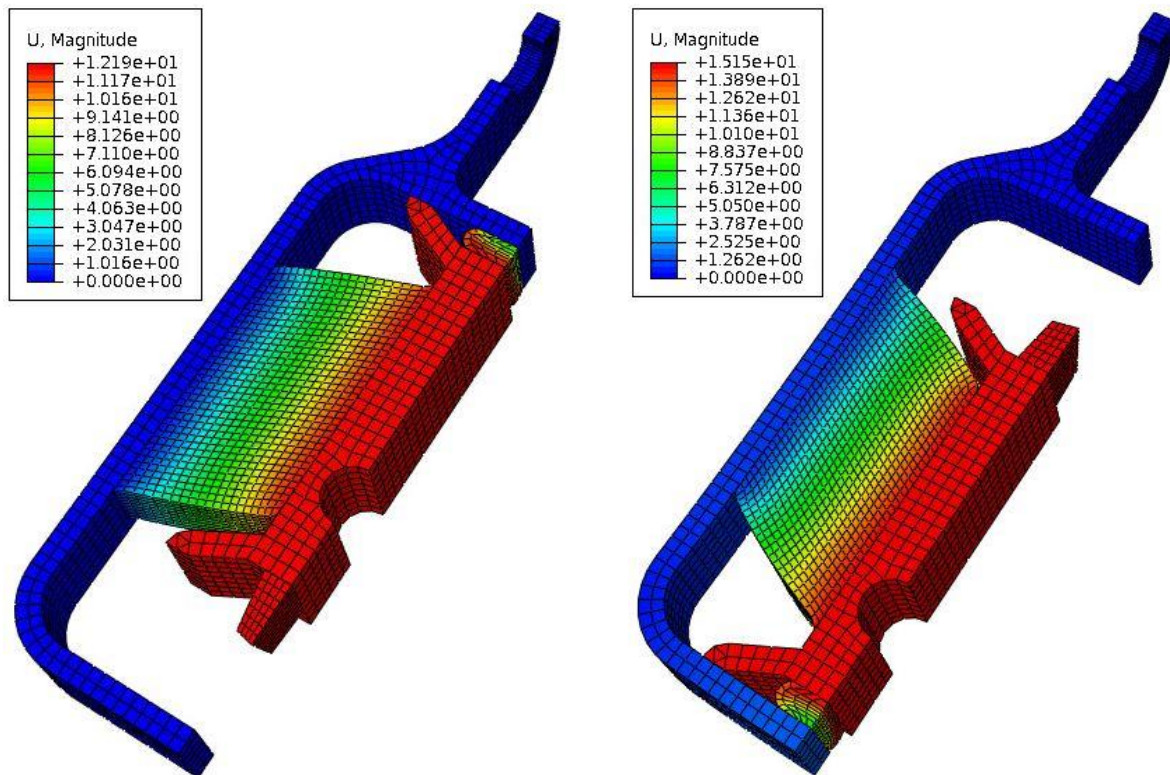


Figure 4.3: Results from the initial analysis of the simplified torque rod; deformed mesh for the positive loading direction (left) and for the negative loading direction (right). The scale indicates displacement magnitude in mm.

4.1.3 Morphing

As the initial static analysis using Abaqus as solver showed good results, the model was prepared for morphing. The standard settings in HyperMesh for dividing the model into 3D domains gave good results because of the simple geometry of the model; see Figure 4.4 for a picture of the domains and handles. The morphing was done as efficiently as possible, that is; it was desirable to have as few design variables as possible for keeping the optimization time down but at the same time make the morphing affect the geometry as much as possible to give a large feasible region of different degrees of stiffness. The MRE was morphed with two different shapes; length and thickness. For the length shape, a symmetry was made so that the length of the MRE were symmetrically altered in each direction from the centre of the MRE. The bump stops were morphed with shapes altering the height, width and thickness, and the top plane angle that was a combination of two shapes. The insert arms were morphed with two different shapes each, altering the distance to the frame and the thickness of the arms. Finally, the frame was morphed with three shapes altering the width of the frame at the front, side and back. When performing the morphing, the shapes were created so that they made the component stiffer, that is, making the dimensions larger and moving the insert arms towards the frame.

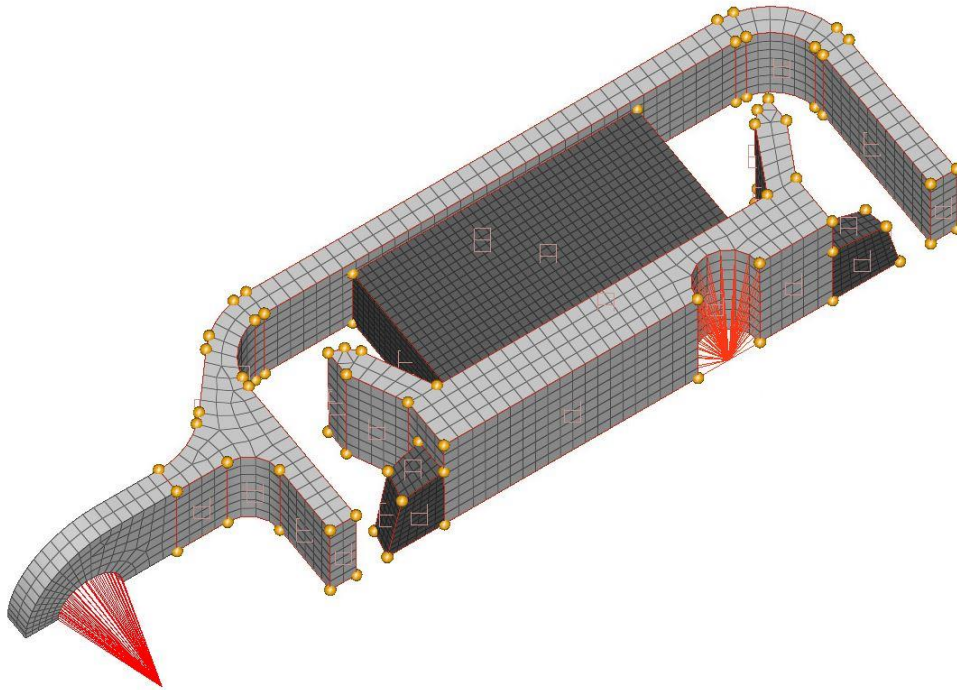


Figure 4.4: The FE model of the simplified torque rod divided into domains for morphing. The yellow points are handles connected to the different domains that are moved when morphing.

This means that a total number of 17 shapes were created, and then saved as design variables. This was done using the standard settings in HyperMesh, which means that the design variables have a range from -1 to $+1$ with 0 as default value. Having the same range for all the design variables does not mean that they have the same geometrical range; it means that the geometrical movements of the shapes are scaled to -1 to $+1$. If a shape has the maximum geometrical movement of 1.5 mm, setting the corresponding design variable to $+1$ would mean that the shape alters the geometry with 1.5 mm. Since all shapes were made so that they made the geometry stiffer in in the positive range, the geometry would have maximum stiffness for the upper bound (*ub*) of the design variables ($+1$), minimum stiffness for the lower bound (*lb*) of the design variables (-1) and nominal (original) stiffness for the design variables at the 0 value. The design variables were then exported as node data in a format compatible with Abaqus input-files. For a list of the design variables, see Table A.1 in Appendix A.

4.1.4 Requirement and objective function

The stiffness requirement for the simplified torque rod was designed from the nominal stiffness by offsetting the displacements for certain force levels. An objective function, quantifying the difference between the calculated and the required stiffness, was needed. A number of different functions were evaluated; the simplest would probably be to sum the difference in displacement for the required and calculated stiffness curves at a number of predefined force levels. Another possibility would be to sum the squares of the differences; this kind of function is used as the objective function in both Kim and Kim's (1997) and Li et al.'s optimization methods. Having the differences squared means that a large difference in a certain point would have a larger impact on the objective function compared to not having the differences squared. This seems good for this purpose since it is important that the stiffness requirement is evenly met for the whole range of the torque rod. Using the Chi-square term as in Kaya's (2014) optimization method, which divides each squared difference with the corresponding target value, was ruled out since the impact of a difference at a certain level would decrease for increasing target values. The function with just the differences squared were therefore chosen, and the objective function could be written as:

$$f_{\text{obj}}(\mathbf{d}_{\text{calc}}) = \sum_{i=1}^n (d_{\text{req},i} - d_{\text{calc},i})^2 \quad (23)$$

where n is the number of predefined force levels, $d_{\text{req},i}$ are the required displacement values and $d_{\text{calc},i}$ are the calculated displacement values for a certain torque rod design at these force levels. The calculated displacements \mathbf{d}_{calc} are the state variables in the optimization problem. Volvo Cars' torque rod requirements are usually expressed as certain force values for a number equally spaced displacement values. This means that the stiffness curve-data points will have very small force steps for low displacement values and large force steps for high displacement values since the curve because of the varying slope (stiffness) of the curve. Having many data points for the low displacement values is unnecessary since this part is linear and is equally well described with fewer data points. An algorithm that picks a more appropriate number of data points were therefore developed, see Figure 4.5.

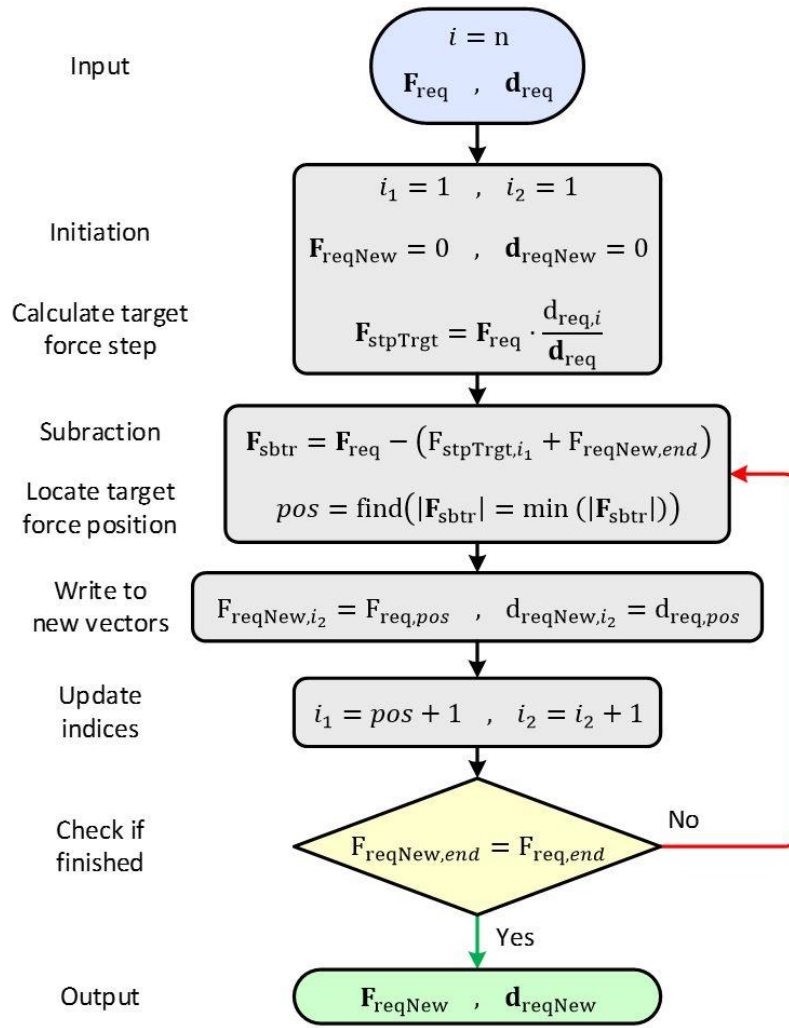


Figure 4.5: The data point-picking algorithm. n is set to a number between 1 and the maximum number of data points, but usually not higher than 5. \mathbf{F}_{req} and \mathbf{d}_{req} are vectors with the requirement forces and displacements, $\mathbf{F}_{\text{reqNew}}$ and $\mathbf{d}_{\text{reqNew}}$ are vectors with the updated forces and displacements.

The basic idea of the data point-picking algorithm is that it picks data points from the original data set that are spaced according to certain force steps. These steps are calculated so that the algorithm will increase the force steps for low forces and decrease the force steps for high forces. This means that data points close to the origin will be skipped and data points near the ends of the stiffness curves will be included. The algorithm was designed to work with positive forces and displacements only, wherefore the negative part of the stiffness curve is made positive before it is processed by the algorithm by taking the absolute value of the forces and displacements. The data points are then made negative again after processed in the algorithm. Reducing the number of data points has two important benefits: It reduces the amount of data to be managed when setting up the optimization and the amount of output data from the FEA, and it makes the influence of the data points on the objective function be more equal for low and high force values. Another advantage of the algorithm is that it picks existing data points, so there is no need of interpolation between the requirement data points. Since the requirement data set for the simplified torque rod was created for this project, it did not have unnecessary many data points, wherefore the parameter n in the algorithm in Figure 4.5 was set to 1, meaning that all data points were chosen. This can be seen in Figure 4.6.

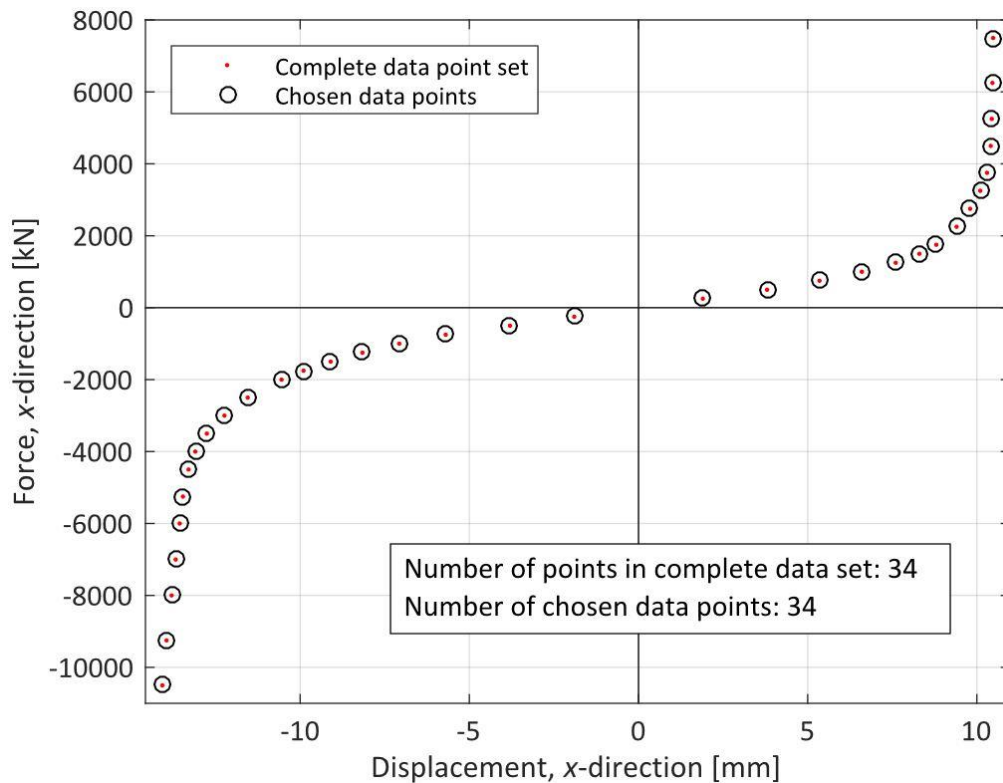


Figure 4.6: Chosen data points to be used in the objective function for the optimization of the simplified torque rod. Note that the parameter n in the data point-picking algorithm was set to 1, which meant that all data points were chosen.

The data point-picking algorithm was implemented in the pre-optimization script written in MATLAB. It imports the requirement forces and displacements from an excel document. Besides this algorithm, the pre-optimization script has a number of different features to facilitate the use of the optimization method. It saves the requirement forces and displacements in text files, which are used in the post-optimization script. It prints the objective function with the data points picked by the data point-picking algorithm in the format that it should be entered in HyperStudy and saves it in a text file. It also prints the time points that should be inserted in the Abaqus input files in the prescribed format and saves them in text files. The time points decide at what time increment the requested output should be written from Abaqus. For the optimization method, the maximum time increment was set to be equal to the maximum force applied in each loading direction, and the time points were therefore chosen as the requirement forces with the first force level in each loading direction as initial time increment.

4.1.5 Optimization set-up and system bounds check

For the optimization in HyperStudy, Abaqus had to be registered as solver since it is not a built in solver. For this, a Python script was used that was available from HyperWorks. The script acts like a link between HyperWorks and Abaqus. It sends information to Abaqus about what job to run based on a request from HyperStudy. The two input files were imported and parameterized, that is, the node data was changed to the shape node data with the design variables. The Yeoh hyperelastic material parameters were also parameterized, which means that the rubber material was a design variable. Three different sets of hyperelastic material parameters modelling different rubber materials with different hardness were included in the input files; a 50 IRHD, a 65 IRHD and a 78 IRHD. The 65 IRHD rubber has been used earlier at the Powertrain Mounts group and is known to model the V40 LLTB well. When the parameterization was completed, the design variables were imported to HyperStudy from the input files. If necessary, the upper and lower bounds could be adjusted at this stage. For example, some shapes altering the bump stops made the geometry too thin at the lower bound, and was, thus, adjusted from -1 to -0.5 to halve the movement of the shape in the negative range.

The fact that two input files were used for the same geometry but for different loading directions meant that the design variables were doubled. Since it is the same geometry that is optimized for both loading directions, the design variables were linked so that each design variable had the same value for both the positive and negative loading direction for each run. When two design variables are linked, one of them is controlling the value of the other. Thus, linking the design variables has to be done with great care; for example, it is important that the design variables for the drive bump stop has its controlling design variable from the input file corresponding to the loading direction that makes the drive bump stop meet the frame. For those design variables that affects both loading direction such as the side thickness of the frame, it does not matter from which input file the controlling design variable is from, but it is recommended to choose the one the input file with the loading direction that is most affected by the design variable. Linking the design variables for the two input files means that it does not matter which results file that is used after the optimization is done; the two FE meshes are representing exactly the same optimized geometry.

The first approach performed in HyperStudy was a system bounds check (SBC). A SBC runs the analysis with the design variables at initial value (0), at the *lb* (-1 or -0.5) and at the *ub* ($+1$). A SBC therefore gives the nominal stiffness and the feasible region by giving the minimum and maximum stiffness. Another MATLAB script, the post-optimization script, was written to visualize the results from an optimization. This script also visualizes the result from the SBC by plotting the stiffness curves and the feasible region in a force-displacement plot. For the simplified torque rod, three different SBCs were run since three different rubber material models were used. The result from the SBC is visualized in Figure 4.7. As can be seen in Figure 4.7, using three different rubber materials enlarges the feasible region. This is true mainly for the range of the torque rod where the MRE and the bump stops shapes the stiffness curve (small and medium displacements), but for large displacements where the insert arms meet the frame, the effect is negligible. A conclusion drawn from this is that for small and medium displacements, the stiffness curve can be adjusted with the rubber hardness, but to adjust the whole range including large displacements geometrical changes have to be done.

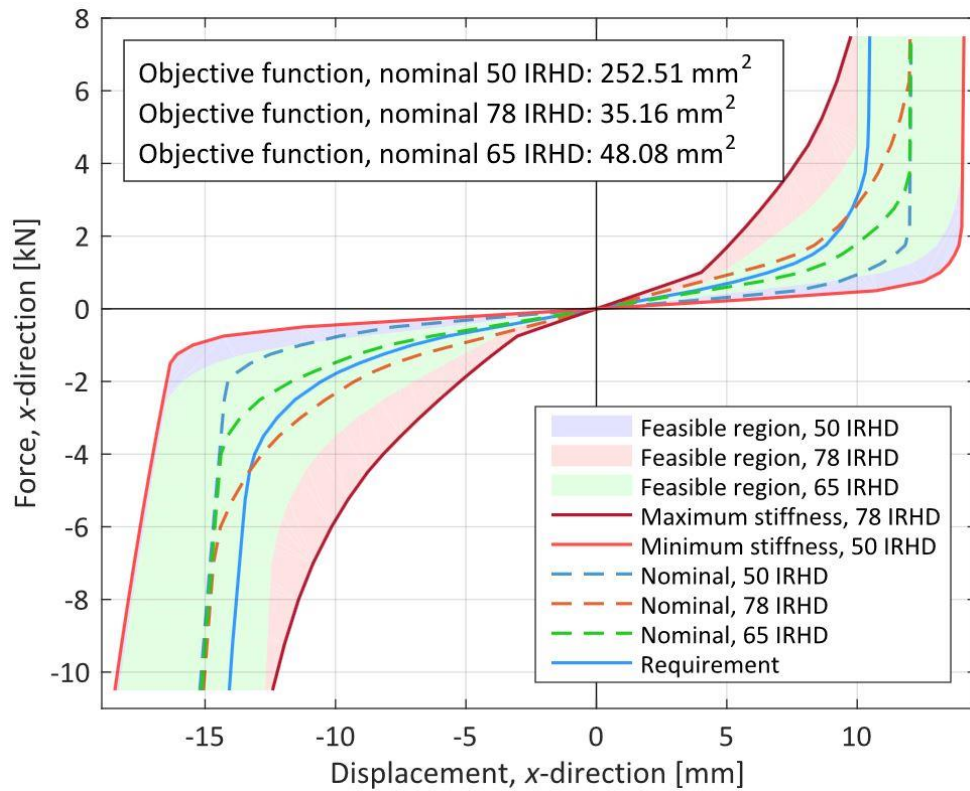


Figure 4.7: Force-displacement plot of the SBC for the simplified torque rod with three different rubber material models. Note that the feasible regions for each of the three models are overlapping; the feasible region for the 65 IRHD model (light green) was placed in front in the plot.

When the SBC was done, responses could be created in HyperStudy. Responses are values that are monitored and used in the optimization. In this project, the responses consist of the displacement values for the different force levels for which Abaqus writes output data. The displacement values were read from the output database (ODB-file) that was the chosen result output type from the Abaqus analyses. An additional response was also created; the objective response, in which the expression for the objective function generated in the pre-optimization script, was inserted.

4.1.6 Design of experiments

A design of experiments (DOE) was run to show the effect of each design variable on the responses. Because of the large number of design variables, a Latin Hypercube design was chosen for the DOE to cover the whole continuous range of the shape design variables with few runs. Since the material parameter-design variable was a discrete variable with three different steps, it could not be included in the DOE. This was not considered a problem because the purpose of the DOE was primarily to see the effects of the shape design variables on the objective function. The effect of the different degrees of hardness of the rubber material is more evident and can be seen in the SBC (see Figure 4.7). When deciding how many runs to do in the DOE, the fractional factorial design in HyperStudy was used as an indicator, which has an auto option that recommended 30 runs for this number of design variables. It was therefore chosen to do 30 runs for the Latin Hypercube as well. The DOE showed differences in how much they affected the objective function, but it was decided to keep all design variables for the optimization. It could also be seen, as expected, that some design variables have large effect on small displacements but not on large, and some design variables have large effect on large displacements but not on small. This holds for, for example, the design variables for the MRE with large effect on small displacements and the design variables for the bump stops with large effect on large displacements.

There is a new feature in HyperStudy version 14.0 that allows including runs made in a DOE and/or SBC in an optimization (Altair, 2016). This is a very beneficial feature since it means that no runs are made in vain; the data from initial approaches can be used as input in optimizations. It is suitable to use the data from a DOE in an optimization since the optimization methods in HyperStudy starts with some random sampling. This step can therefore be skipped and the optimization approach can start optimizing immediately.

4.1.7 Optimization

The objective with the optimization was to make the stiffness curve of the simplified torque rod come as close as possible to the requirement stiffness curve. This was done by minimizing the objective function, and the optimization can be formulated as:

$$\begin{aligned} &\text{minimize } f_{\text{obj}}(\mathbf{d}_{\text{calc}}) \\ &\text{subject to } \mathbf{lb} \leq \mathbf{dv} \leq \mathbf{ub} \end{aligned} \tag{24}$$

where \mathbf{dv} are the design variables, \mathbf{lb} are the lower bounds for the design variables and \mathbf{ub} are the upper bounds for the design variables. The state variables, the calculated displacements \mathbf{d}_{calc} , are a function of the design variables; $\mathbf{d}_{\text{calc}} = f(\mathbf{dv})$.

For the optimization of the simplified torque rod, a number of different HyperStudy optimization methods were tested. The GRSM should be the best choice for this task because the large number of design variables. To verify that, all methods that were possible to use for this task, including the GRSM, were tested. The result from this test is shown in Table 4.1.

Table 4.1: Comparison of different HyperStudy optimization methods and set-ups. Optimization number 2 gave the best result, which can be seen in the last row where as low value as possible is wanted.

Optimization no.	1	2	3	4	5	6	7
Optimization algorithm	GRSM	GRSM	ARSM	MFD	SQP	GRSM	GRSM
Material parameter-des. var. incl. in opt?	Yes	No	No	No	No	No	No
Initial sampling points from	9 fr. SBC, 20 fr. opt.	DOE	DOE	DOE	DOE	Opt.	Opt.
Maximum no. of evaluations allowed	50	50	38	25	25	82	82
Convergence before maximum iteration?	Yes	Yes	Yes	Yes	No	Yes	Yes
No. of initial sample points	29	32	32	32	32	32	19
Objective function optimum [mm ²]	9.73	2.26	8.52	8.94	4.32	2.39	3.82
Optimum reached on run no.	50	63	68	72	372	63	48
Obj. function opt. × opt. run no. [mm ²]	486	142	580	644	1606	150	183

The first thing to note from the results in Table 4.1 is that the material parameter-design variable was only included in one of the optimizations. As can be seen in optimization number 1 and 2, a comparison between the GRSM with and without the material parameter-design variable done. The comparison shows that the optimization is not able to get as good result with the material parameter-design variable included as without it. Because the material parameter-design variable is a discrete variable and affects such large part of the stiffness curve it seems that it is difficult for the optimization method to converge with the most suitable material. When the material parameter-design variable is changed, almost all the shape design variables are badly adjusted and need to be changed. This problem does not occur for the shape design variables since they are continuous and only affect a limited part of the stiffness curve each. It was therefore chosen to not include the material parameter-design variable in the optimization. The proposed method is instead to only include the material parameter-design variable in the SBC and then choose the most suitable rubber material for the optimization. This is of course only necessary to do when designing completely new components where the most suitable rubber material is unknown.

In optimization number 3-5 the other HyperStudy optimization methods were tested. None of them were able to give better results in terms of accuracy or efficiency than the GRSM. In optimization number 6 it was tested if there were any difference in letting the optimization algorithm doing the initial sampling instead of in a DOE as in optimization number 2. The results show only a very small difference that is assumed negligible. Doing the initial sampling in a DOE does though have some advantages in form of the results from the DOE such as linear

effects of the design variables on the objective function. In optimization number 7 it was tested if it would be possible to decrease the number of initial sampling points with maintained result. The result shows that it was not possible to reach as low value for the objective function as with the larger number of sampling points. It seems, as a certain size of the initial sampling is needed to reach a low value of the objective function.

To make it easy to compare the different optimizations performed, values that are the products of the objective function optima and their corresponding run number can be seen in the last row, where a low value is good. It can be seen that the GRSM with initial sampling points from the DOE is the most suitable method to use for this application. The other methods show the expected weaknesses in form of lack in accuracy or efficiency. It was therefore decided to use the GRSM in the optimization method.

4.1.8 Post-processing

To visualize the result from the optimization, the post optimization script was run again. When the optimization is completed, it adds the optimized stiffness curve to the force-displacement plot with the results from the SBC. The resulting plot of the optimization of the simplified torque rod is shown in Figure 4.8. The objective function was lowered from 48.08 mm^2 to 2.26 mm^2 . Ideally, the optimal design would lower the objective function to 0, but as can be seen in Figure 4.8 the optimized stiffness curve has two spots where the stiffness changes more rapidly. This is a consequence of the simplified geometry of the simplified torque rod; at these spots, the insert arms meet the frame and since the simplified torque rod does not have rubber around the insert arms, which is usually the case, the component gets a rapid stiffness change. The optimization result can therefore be considered as good as possible with this simple geometry and for the geometry relatively difficult requirement to meet.

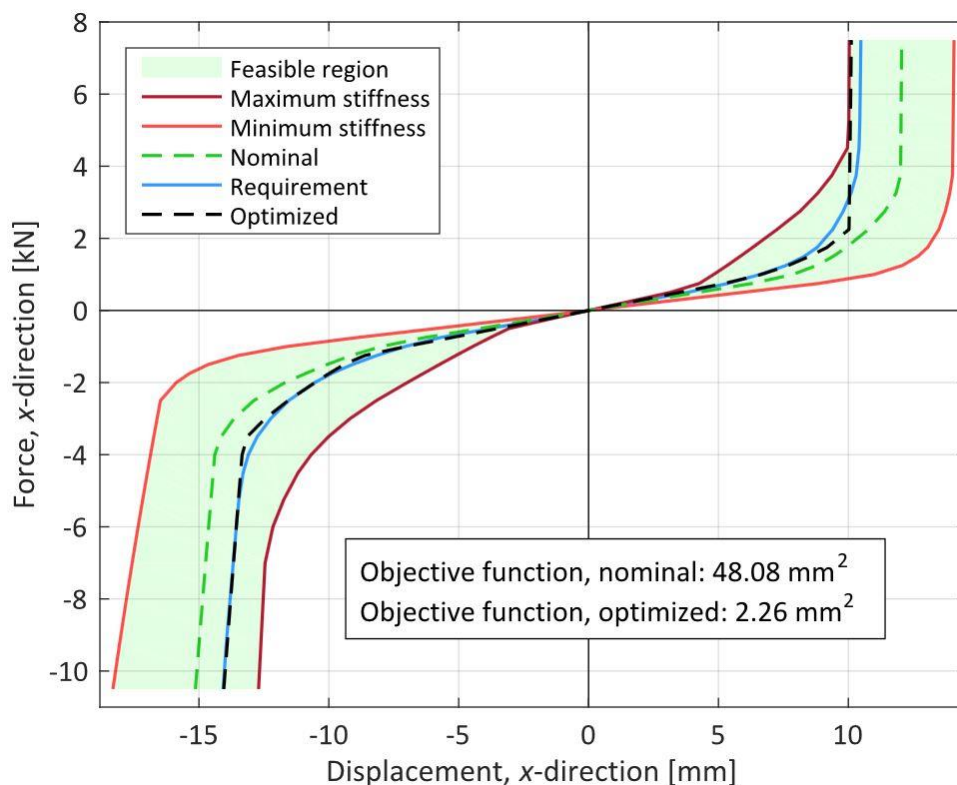


Figure 4.8: Force-displacement plot for the optimization of the simplified torque rod.

In Figure 4.9, a view from HyperStudy is pictured, showing how the value of the objective function changed during the optimization. In Figure 4.10, a corresponding plot for the design variables is pictured. As can be seen, there is a large difference in how much the different shapes are changed for the optimum design; some design variables are close to the boundaries, some are close to the nominal value (0) and some are in between these points.

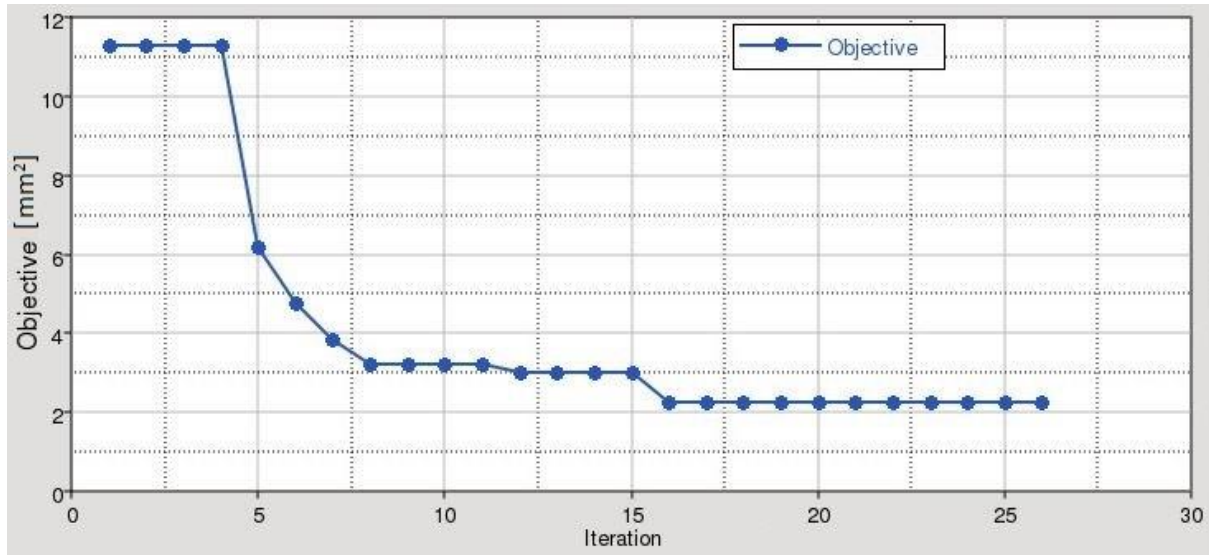


Figure 4.9: View from HyperStudy showing the value of the objective function for each iteration during the optimization of the simplified torque rod. The reason for that the value of the objective function starts at a lower value in this plot than the objective function value for the nominal design is that the optimization starts from the best design from the initial sampling, which had a value of the objective function of approximately 11 mm².

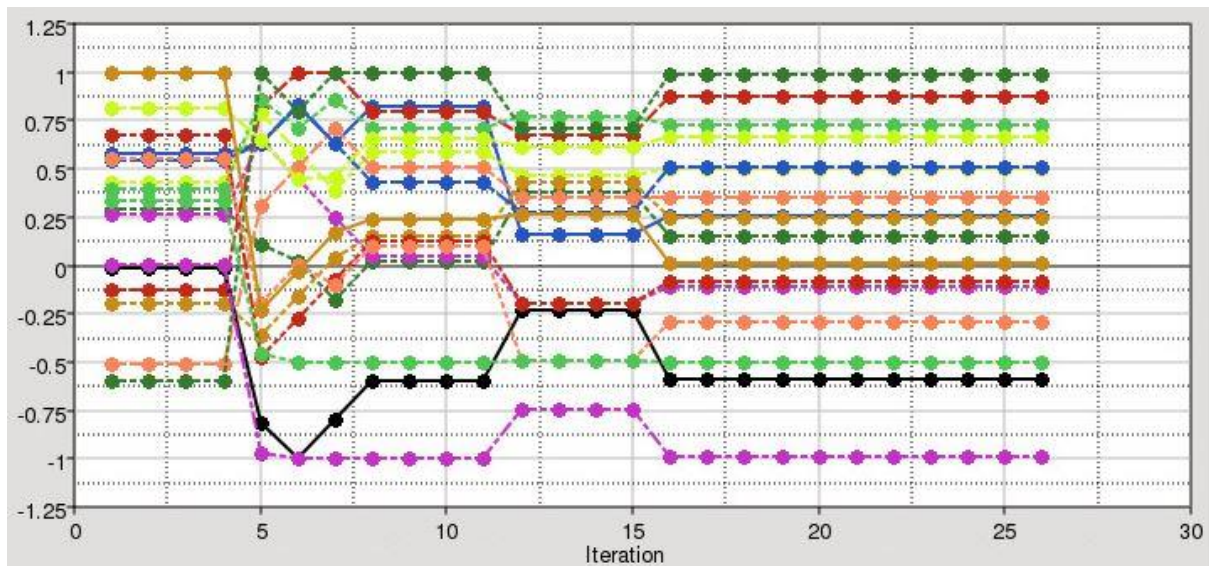


Figure 4.10: View from HyperStudy showing the values of the design variables for each iteration during the optimization of the simplified torque rod. As described in Figure 4.9, the optimization starts from the best design from the initial sampling. For a legend to the plot, see Table A.1 in Appendix A.

4.1.9 Dynamic analysis

A dynamic analysis was performed to evaluate the possibility of including dynamic stiffness requirements in the optimization method. An analysis using the same analysis set-up as Öhrn (2015) was performed. The simplified torque rod was subjected to a sinusoidal displacement of ± 0.1 mm for one period. The analysis converged but as expected, it took longer time than the static analysis. An optimization of a torque rod takes many FE-simulations, and if dynamic simulations were to be included it would more than double the optimization time. It was therefore not feasible to include dynamic simulations with the current analysis set-up in the optimization method.

4.2 Obtaining hyperelastic material parameters

In this subsection, the results from the material parameter-obtaining phase are presented.

4.2.1 Tensile test result

The results from the tensile tests are presented in stress-stretch plots in Figure 4.11 and Figure 4.12. The plots include the test data and the fitted curve for that data. Before obtaining the material parameters, the data was processed in a MATLAB script in the following way: For each test, the first run was omitted for obtaining of the material parameters. This run was used as mechanical conditioning of the specimen. For the thin specimen, three more runs stood out from the rest and were therefore omitted. The last data points for each of the remaining runs were then removed. This was done since these data points represented the part of the curve where the specimens started to slide in the clamps, and were therefore not representative of the rubber behaviour.

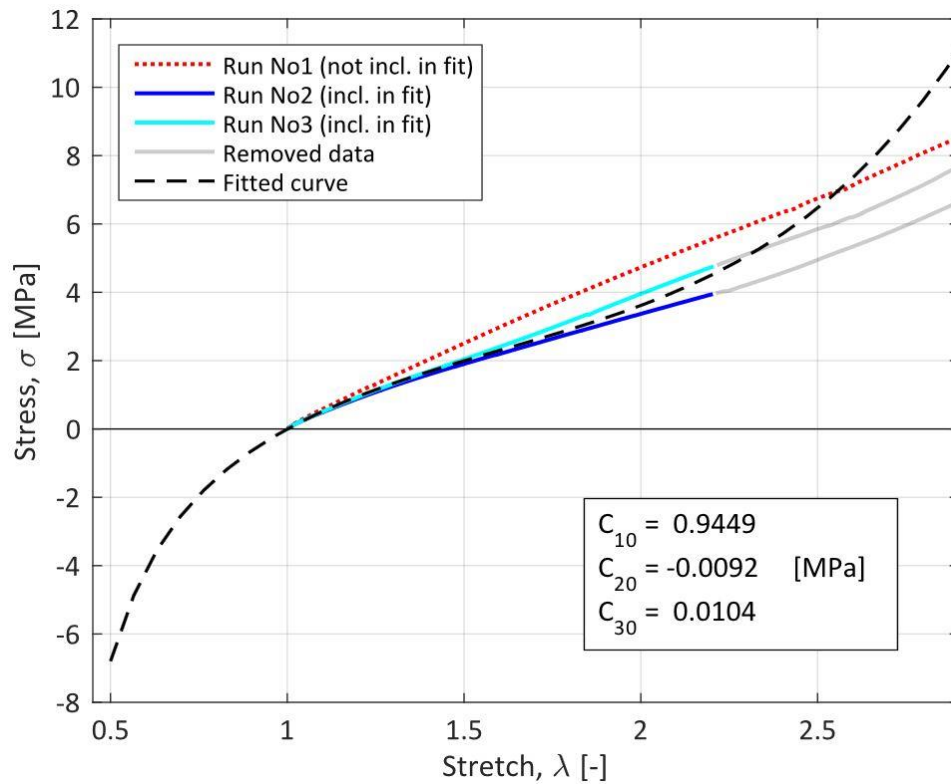


Figure 4.11: Stress-stretch plot for the result of the tensile test of the thick test specimen.

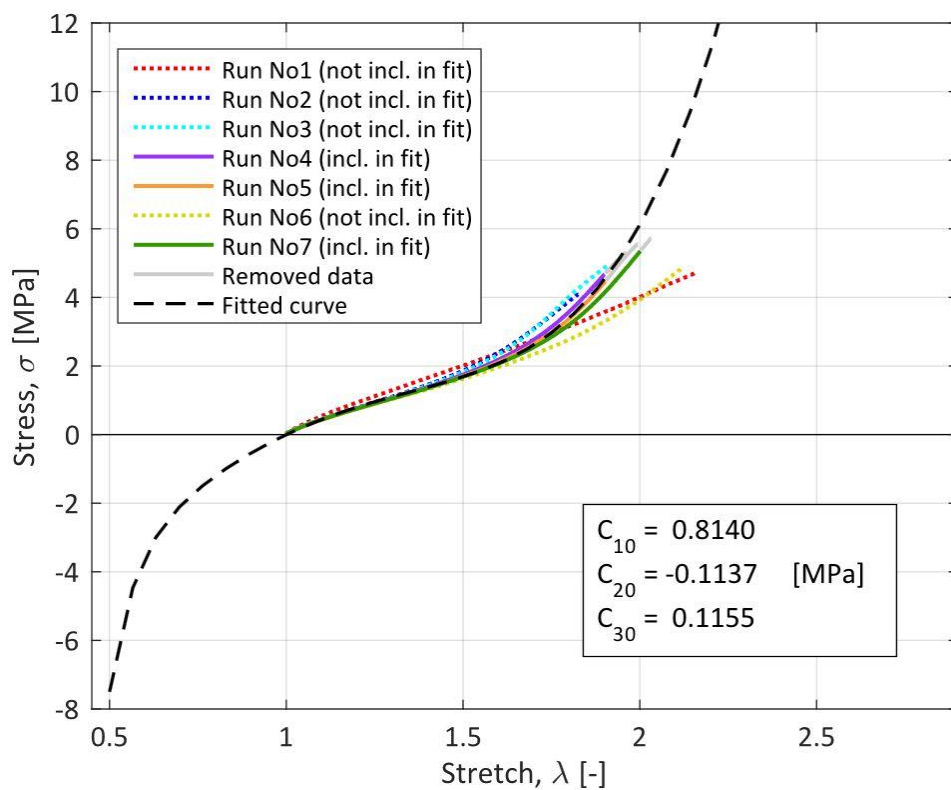


Figure 4.12: Stress-stretch plot for the result of the tensile test of the thin test specimen.

4.2.2 Obtaining the material parameters

The hyperelastic material parameters were then obtained for each of the kept runs, and an average value for each parameter for each test was calculated. The material parameters were obtained using the method described in Subsection 2.1.2.1. The corresponding stress-stretch curve based on the averaged material parameters can be seen in Figure 4.11 and Figure 4.12 respectively. The models were also plotted in the same plot together with the stress-stretch curve for the 65 IRHD rubber material parameters from Austrell (1997) previously used for modelling the V40 LLTB at the Powertrain Mounts group. This plot is presented in Figure 4.13. As can be seen, there is a clear difference between the three models. The fitted curve for the thin specimen seems to be closer to the 65 IRHD model for low stretch values, and the fitted curve for the thick specimen seems to be closer to the 65 IRHD model for high stretch values.

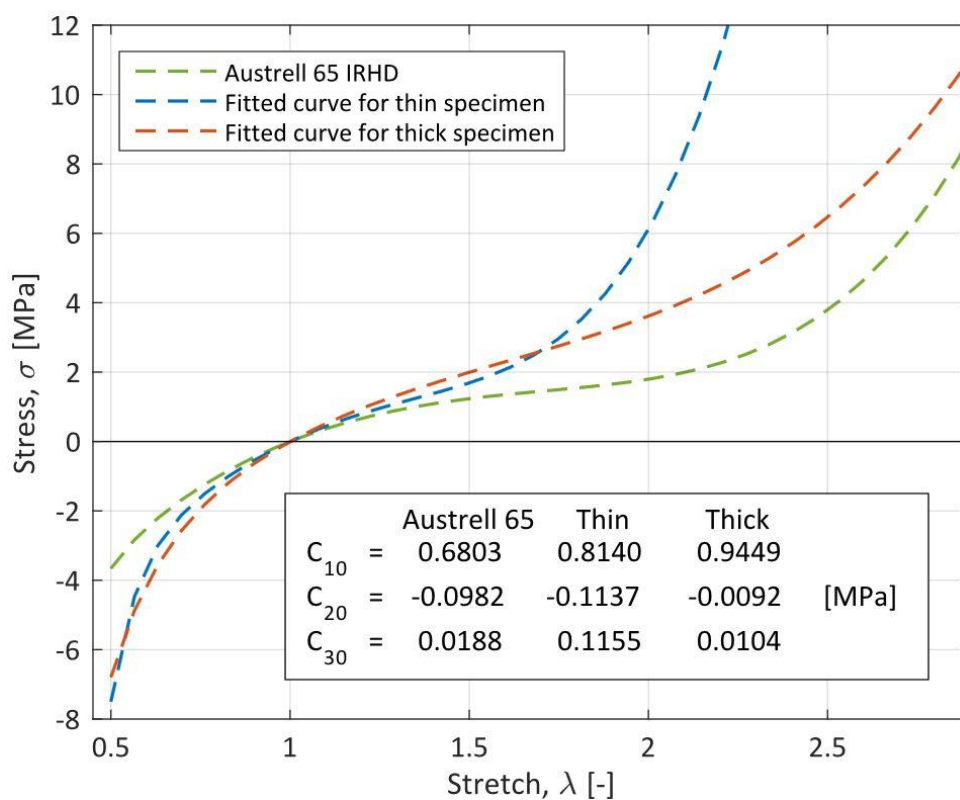


Figure 4.13: Stress-stretch plot for comparison of the obtained models from the tensile tests and the Austrell 65 IRHD rubber.

4.2.3 Model validation

To find out which of the models that most accurately modelled the V40 LLTB rubber, FE analyses of the V40 LLTB with the different models were carried out. The result from those analyses are presented in a force-displacement plot in Figure 4.14. The corresponding objective function values were also calculated. As can be seen, the 65 IRHD model models the component considerably better with respect to the measurement data than the models obtained from the tensile tests, which are too inaccurate to use.

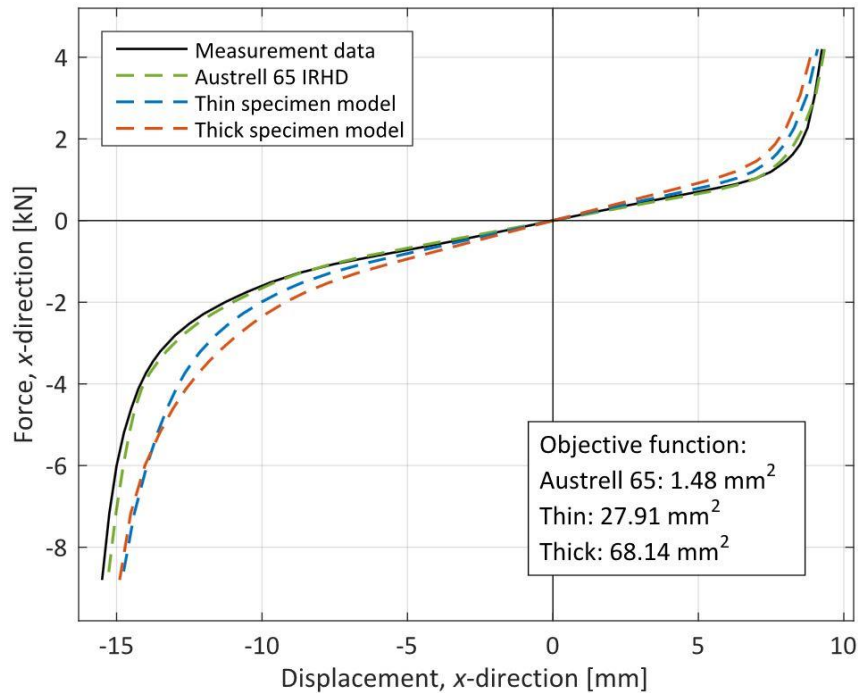


Figure 4.14: Force-displacement plot for the validation analyses of the three different material models.

4.2.4 Material parameter optimization

As mentioned earlier the idea of applying the optimization method to the hyperelastic material parameters emerged. For optimizing the material parameters, the same method used for optimizing the geometry was applied, but with different input. Instead of using the shapes as design variables, the three hyperelastic parameters in the Yeoh model were used as design variables. Instead of using the requirement stiffness curve in the objective function, measurement data was used. This means that the material parameters can only be optimized in this way if there is measurement data for the component with the rubber that is to be modelled. For most of the powertrain mounts in production at Volvo Cars, the Powertrain Mounts group has this measurement data in form of force-displacement data. This application of the optimization method can therefore be suitable if it is desirable to model the rubber of an existing component.

It was chosen to optimize the hyperelastic material parameters for the 65 IRHD model, since this (as shown above) was the model that most accurately modelled the V40 LLTB rubber. The possibility of obtaining an even more accurate model through material parameter optimization should therefore be large. For the optimization, the material parameters were allowed to vary $\pm 20\%$ from their original value. 50 evaluations were run with the GRSM. The result of the material parameter optimization for the V40 LLTB is shown in a force-displacement plot in Figure 4.15. As can be seen, it was possible to obtain a more accurate model; the objective function was reduced from 1.48 mm^2 to 1.41 mm^2 . It can also be seen that the feasible region does not fully cover the measurement data, which means that the range of $\pm 20\%$ was a bit too small. This does not seem to be the reason for that the optimization did not result in a lower value of the objective function, as the optimized stiffness curve does not lie on the edges of the feasible region.

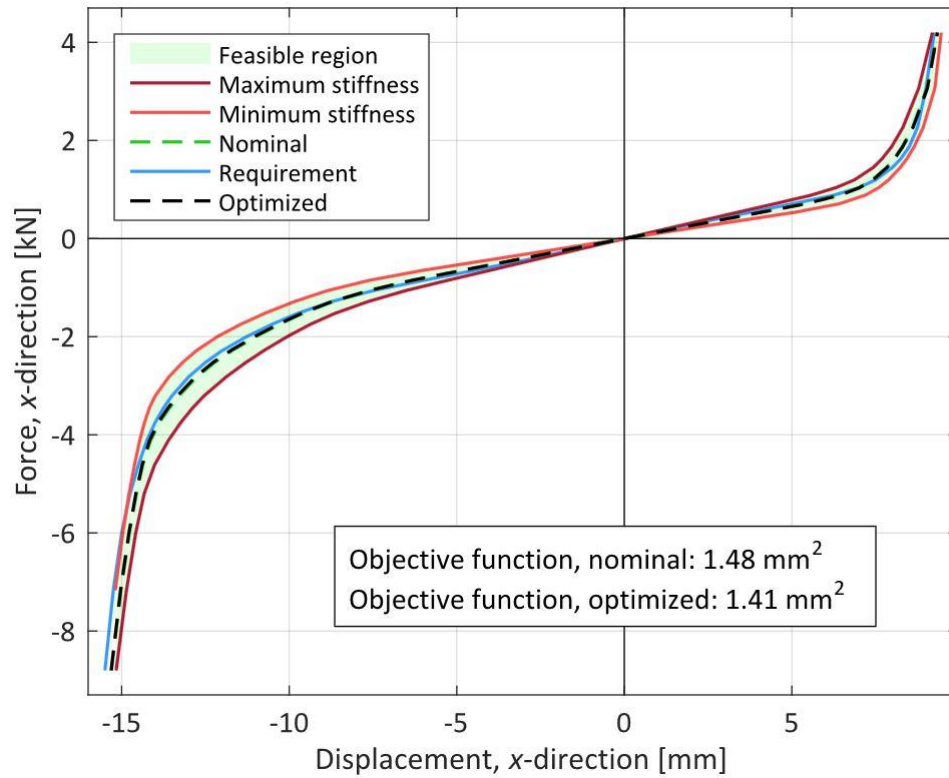


Figure 4.15: Force displacement plot for the optimization of the 65 IRHD material parameters.

To investigate if it would be possible to obtain an equally accurate model by material parameter optimization of the models from the tensile tests, the parameters obtained from the thin test specimen were also optimized. As the material parameters for this optimization were further away from the optimum, the ranges for the parameters needed to be larger to allow the feasible region to cover the measurement data. The material parameters were therefore allowed to vary $\pm 90\%$ from their original value. This range was chosen so that the parameters could assume the values of the optimized 65 IRHD parameters with good margin. Two rounds of 50 evaluations each were run with the GRSM. The resulting force-displacement plot is shown in Figure 4.16. The first round resulted in a reduction of the objective function from 27.91 mm^2 to 3.54 mm^2 , and the second round reduced the objective function further to 2.86 mm^2 .

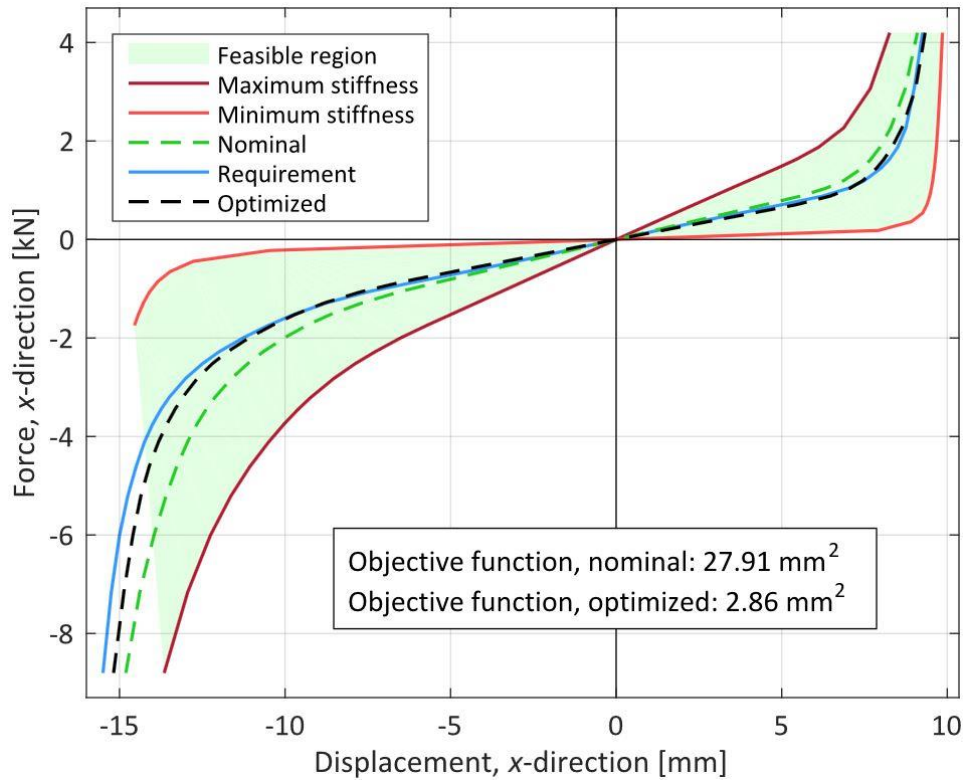


Figure 4.16: Force-displacement plot for the optimization of the material parameters from the thin specimen. The reason for that the feasible region is not covering the whole operational range is that the analysis for the minimum stiffness did not converge for large displacements in the negative x -direction.

4.2.5 Summary

In this subsection, the results from the material parameter obtaining-phase are presented. This is done in Table 4.2, where the three hyperelastic material parameters of the Yeoh model and the value of the objective function for the V40 LLTB are presented.

Table 4.2: Summary of the different obtained and optimized hyperelastic material parameters.

	C_{10} [MPa]	C_{20} [MPa]	C_{30} [MPa]	Obj. func. [mm ²]
Austrell 65 IRHD	0.6803	-0.0982	0.0188	1,48
Thin specimen model	0.8140	-0.1137	0.1155	27,91
Thick specimen model	0.9449	-0.0092	0.0104	68,14
Optimized 65 IRHD	0.6752	-0.0999	0.0187	1,41
Optimized thin model	0.6712	-0.1284	0.0537	2,86

As can be seen in Table 4.2, the optimized 65 IRHD material parameters have the lowest objective function value and are, thus, the ones that best describe the behaviour of the V40 LLTB. These parameters were therefore used in the validation and adjustment phase. It can also be seen that the material parameters obtained directly from the test specimens are not able to model the V40 LLTB behaviour accurately, but when optimized a relatively accurate model can be obtained.

4.3 Presentation of the optimization method

In this subsection, the optimization method will be summarized and clearly presented in its entirety. This is done in three levels:

- Top level: Compact flowchart
- Middle level: Detailed flowchart
- Base level: Step-by-step guide

The top level gives a comprehensible presentation and an overview of the method. The middle level gives more details by describing the sub-steps in each main step. Finally, the Base level describes all the steps and sub-steps in detail in a step-by-step guide targeted for the end user of the optimization method.

4.3.1 Top level: Compact flowchart

In Figure 4.17, the method is presented in a compact flowchart, covering all its main steps. The method is organized in nine main steps and one supplementary step. When using the optimization method for optimizing material parameters as described in subsection 4.2.4, some steps of the method are skipped and the content of some steps are changed. For a compact flowchart of the material parameter-optimization version of the method, see Appendix B.

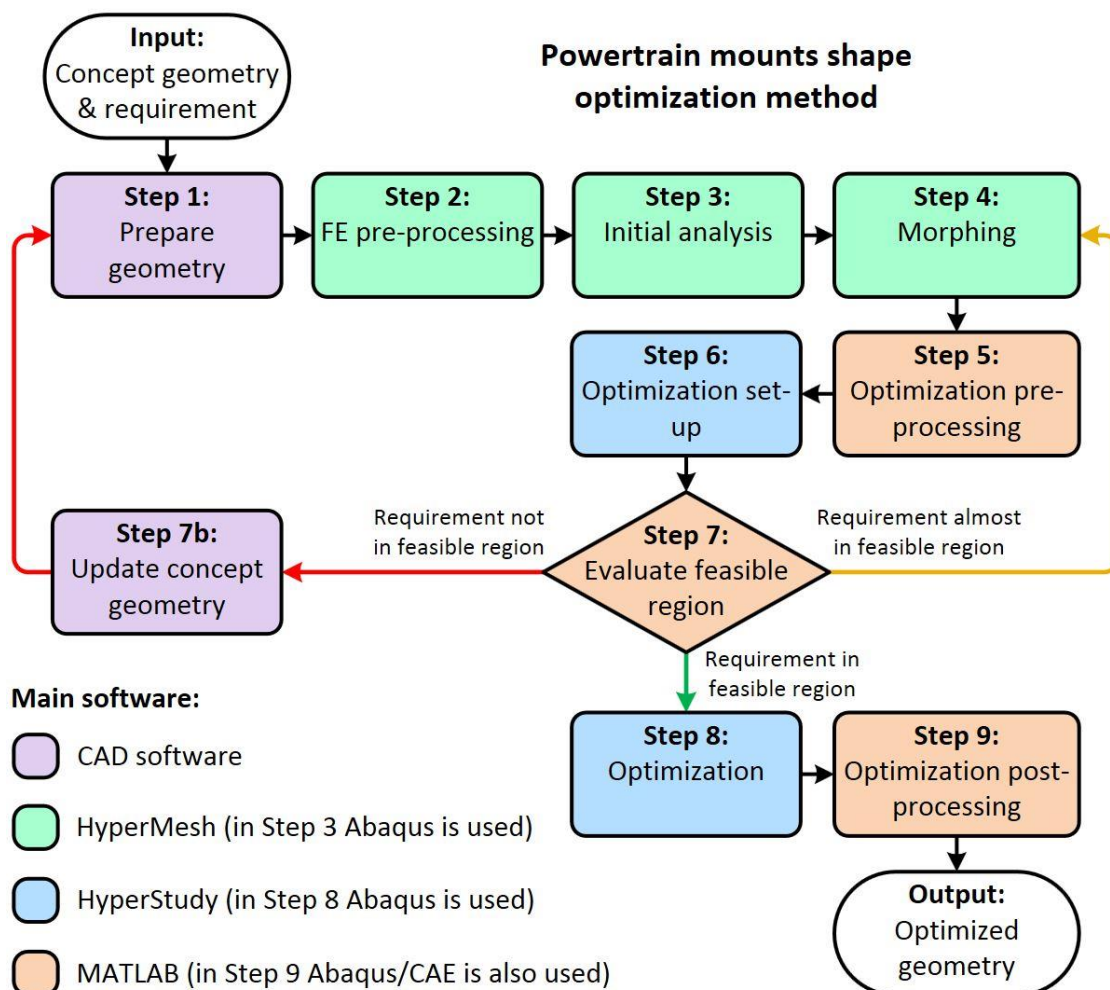


Figure 4.17: Compact flowchart of the optimization method developed in this project.

4.3.2 Middle level: Detailed flowchart

This level uses the same layout as the top level, but with each main step broken down into sub-steps. The detailed flowchart is presented in Appendix C. For the detailed flowchart of the material parameter-optimization version of the method, see Appendix D.

4.3.3 Base level: Step-by-step guide

This level is targeted to the end user of the optimization method in form of a detailed guide to be used by Volvo Cars when using the method. It is based on the detailed flowchart, with each sub-step broken down into detailed step-by-step instructions. It is not included in this report, but an extract of the guide can be seen in Appendix E.

4.3.4 Using the optimization method

There are of course many different ways of using the proposed optimization method. In this subsection, proposals on how to implement the optimization method in three different scenarios are presented, thus, answering Research question 4. The answer to this question was also based on the validation phase described in the next subsection, but it was chosen to present the answer here. The first scenario is new product development, such as a build-to-print project. The second scenario is optimization of material parameters to model an existing torque rod. The third scenario is to optimize a design proposal from a supplier.

4.3.4.1 New product development

In this subsection, a suggestion of a process for the primary application of the optimization method, that is, in new product development such as Build-to-Print projects, is presented.

To enable a large feasible region, which increase the chance of having the requirement stiffness curve within that region, it is recommended to start with a simplified concept geometry similar to the simplified torque rod used in this concept. The simplified geometry will enable large geometry changes when morphing and, thus, a large feasible region. When designing the concept geometry, it is recommended to use an existing mount with a similar stiffness requirement as design basis. The closer the concept geometry is to the final geometry, the more efficient and accurate the optimization will be.

As shown in the Subsection 4.1, it is not recommended to include the rubber material parameter-design variable when optimizing the shape of the geometry. It is instead recommended to start optimizing only the rubber material to find an appropriate material. This can be done in two ways. The first way is to do it as it was done for the simplified torque rod in this project, that is, by including a material library with predefined material parameters and find the most suitable materials among those. The second way is to start with a suitable material model with given material parameters and optimize the material parameters themselves the way it was done in the material parameter-obtaining phase in this project. The advantage with the first way is that the material library can be chosen so that it only contains models for rubber compounds that a certain supplier is known to be able to deliver. The advantage with the second way is that the material model is optimized for this certain geometry, but it is not given that a supplier is able to deliver a rubber compound with those properties. If the rubber compound that would give those properties is not feasible, the obvious action would be to choose the most similar available rubber compound to the rubber compound suggested by the material parameter optimization.

The first way is more focused on optimizing the shape of the geometry for the most suitable of a number of available rubber compounds, and the second way is more focused on optimizing the material for a given geometry. A third way would be to combine the second way with the next step, that is, optimizing the shape of the concept geometry, and optimized the material parameters and the shape of the geometry simultaneously. This has not been tested in this project though.

After the material model is chosen, the shape of the concept geometry is optimized to adjust the main dimensions of the mount. The CAD model should then be updated according to the optimization, and the model should be made more complete in terms of geometrical features such as rounded edges. The full-feature geometry can then be optimized a second time to fine tune the shape of the mount, which will then be used as basis for the final design made in a CAD software. An overview of the development process is shown in Figure 4.18.

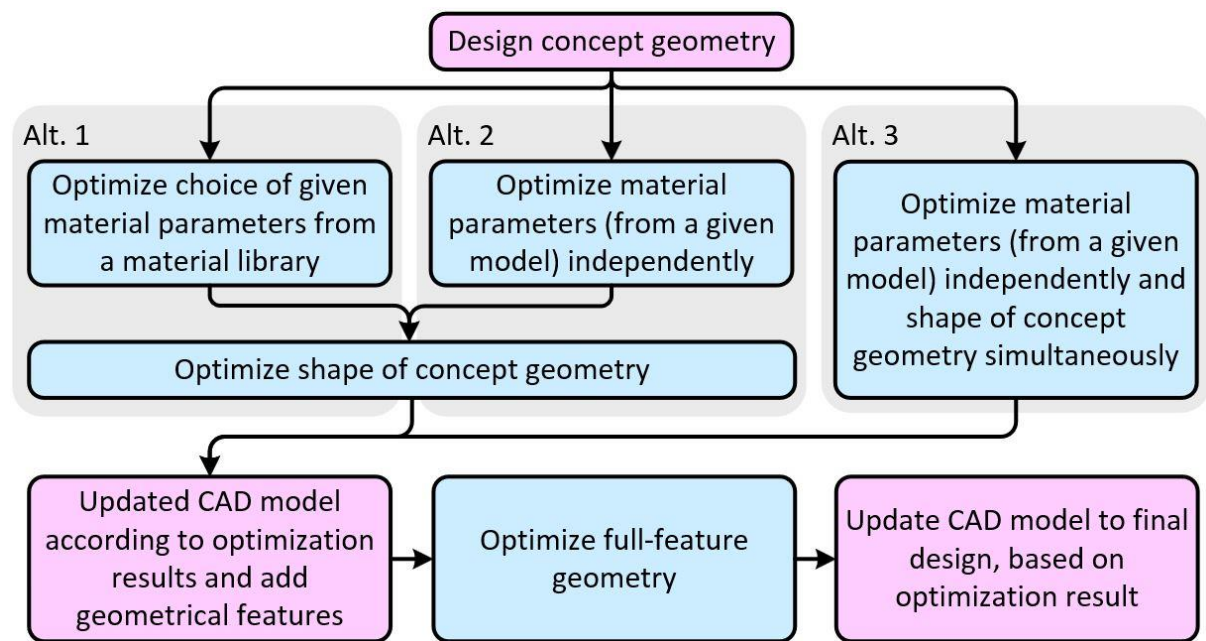


Figure 4.18: Overview of suggested process for implementation of the optimization method in a new product development process.

4.3.4.2 Analysis of existing components

As described in Subsection 4.2.4, the optimization method can be used for optimization of material parameters. This can be useful if analysis of an existing component needs to be done. If there exist measurement data for the component, the hyperelastic material parameters can then be optimized using the material parameter-optimization version of the method, see Appendix B. This can give a more accurate model of the component compared to using an existing set of material parameters. It could also be useful to create a library of hyperelastic material parameters based on the rubber of existing components with known rubber hardness.

4.3.4.3 Optimization of design proposal

The optimization method can also be used in the current development method to validate design proposals from a supplier in a similar way as will be described in Subsection 4.4. This can be useful to evaluate a design proposal in terms of how good it meets static stiffness requirements. It can also be used as a tool to give proposals for design changes if it is difficult to meet specification in the development of a certain component.

4.4 Method validation and adjustment – Real case

The geometry of the V40 LLTB torque rod used in this phase has a lot more features in form of more complex geometry and rounded edges. The CAD model of the V40 LLTB is shown in Figure 4.19. Since an already existing FE-model created at the Powertrain Mounts group was used in this phase, this phase began with FE pre-processing.

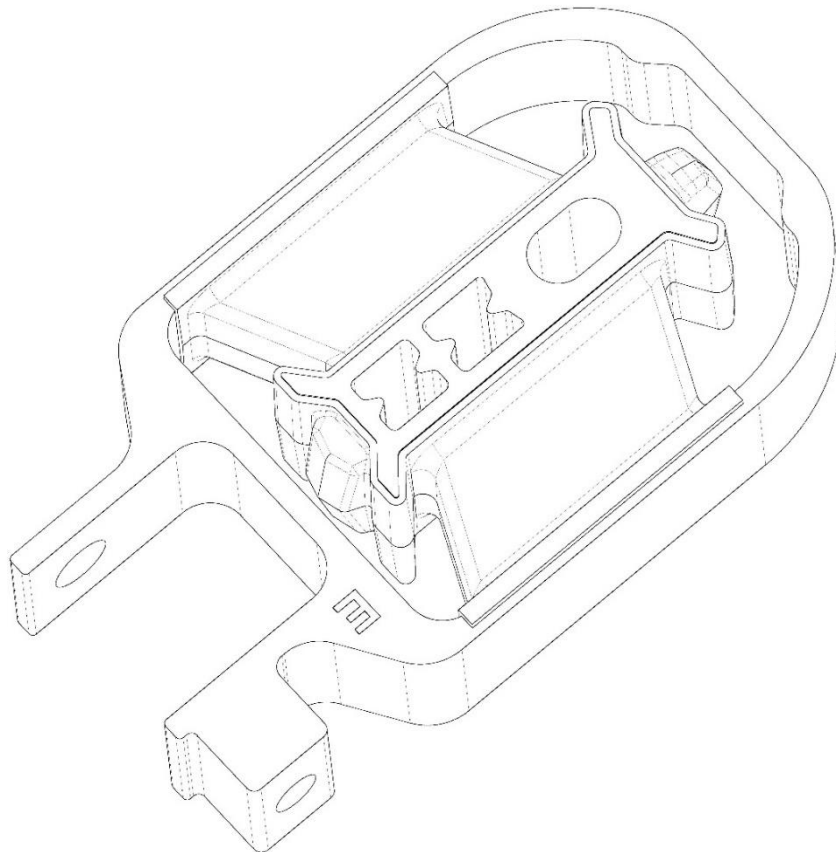


Figure 4.19: CAD model of the V40 LLTB. Note the more complex geometry with rounded edges etc.

4.4.1 Pre-processing and initial analysis

The mesh was already convergence-tested by the Powertrain Mounts-group, and could therefore be kept as it was. See Figure 4.20 for a picture of the FE model. As for the rest, the model was pre-processed in the same way as the simplified torque rod, but with the exception that the optimized 65 IRHD hyperelastic material parameters (see Subsection 4.2.4) were used. The initial analysis converged and the model was, thus, working properly. See Figure 4.21 for pictures of the result from the initial analysis FE-simulation.

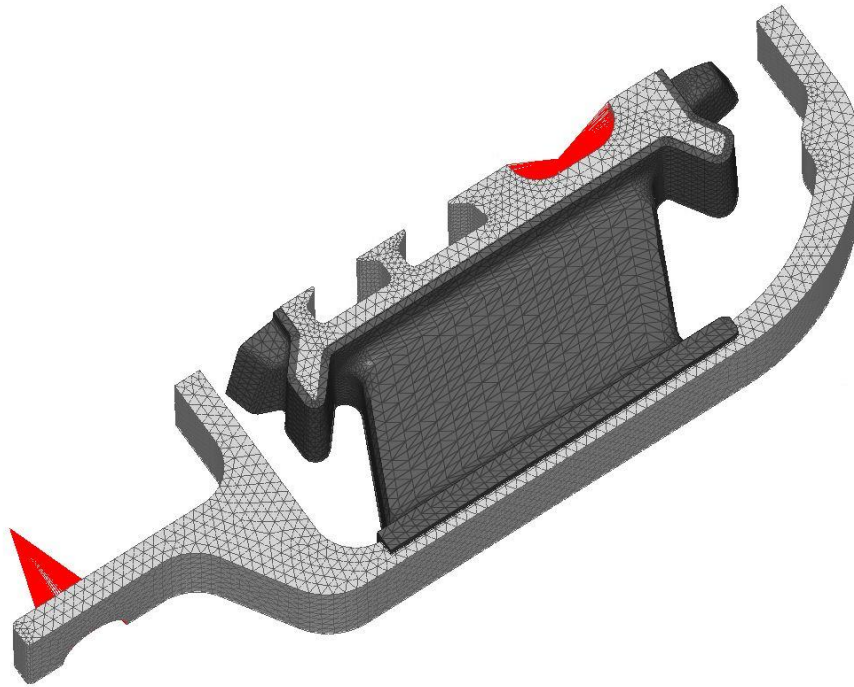


Figure 4.20: FE model of one quarter of the V40 LLTB. The red parts are rigid elements coupled to the attachment points of the torque rod for application of load and fixation constraint. The V40 LLTB model had tetra elements and a finer mesh than the simplified torque rod.

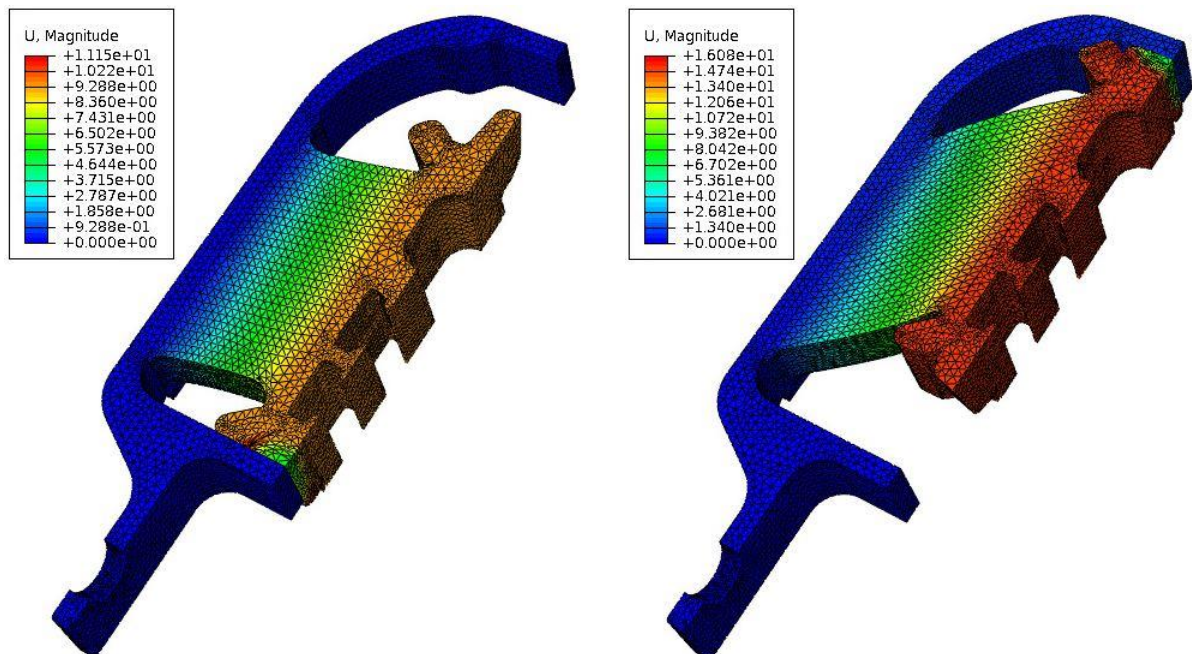


Figure 4.21: Results from the initial analysis of the V40 LLTB; deformed mesh for the positive loading direction (left) and for the negative loading direction (right). The scale indicates displacement magnitude in mm.

4.4.2 Morphing

The morphing of the V40 LLTB model was more difficult than for the simplified torque rod. This was of course expected because of the more complicated geometry, but it was also made more difficult because the original geometry that the mesh was created from was not available in the HyperMesh model. The reason for this is that the existing FE model was not made in HyperMesh and was, thus, imported as a solver deck into HyperMesh that does not include geometry. This made the morphing, or especially dividing the model into domains, more difficult since HyperMesh could not use the geometry as support for creating the domains. This resulted in that the domains did not always follow the edges of the geometry but other paths on the mesh. Having domains that does not follow the geometry edges makes the morphing more difficult since it makes it harder to morph a certain feature of the geometry without affecting the surrounding geometry. This was solved by letting HyperMesh create rough domains capturing most of the correct geometry edges and the rest of the edges were then made into domains manually. The manual work was facilitated by importing the original geometry into HyperMesh and using it as map to find the geometry edges in the mesh. This did, thus, not mean that HyperMesh could use the geometry to generate the proper domains automatically as it normally can, since the mesh was not coupled to the geometry as it is when the mesh is created from the geometry in HyperMesh.

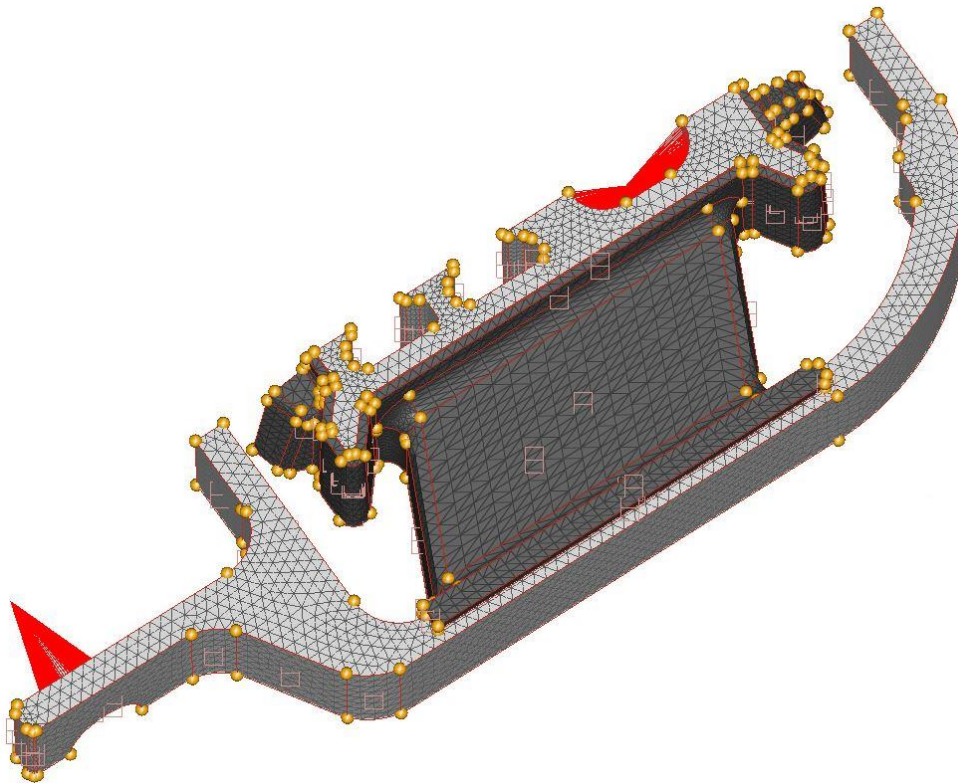


Figure 4.22: The FE model of the V40 LLTB divided into domains for morphing. The yellow points are handles connected to the different domains that are moved when morphing.

The manual morphing gave a good result with a well-divided model; see Figure 4.22 for a picture of the domains. The morphing was done with the same approach as used for the simplified torque rod. In total 18 different shapes were created and saved as design variables. The shapes did not have as large change of the geometry as the shapes for the simplified torque rod because it was not possible to morph the more complex geometry of the V40 LLTB as much. This was not considered a problem since the geometry for this torque rod was much closer to its requirement than the simplified one and would, thus, not need to change very much to meet its requirement fully. For a list of the design variables, see Table A.2 in Appendix A.

4.4.3 Requirement and objective function

As the V40 LLTB is a finished product already on the market, it already has its requirement static stiffness curve and it already has been designed to meet it. It is therefore not a very realistic case to optimize this component, but it was considered a good case for testing the performance of the optimization method. It is very difficult, if not impossible, to design a torque rod that completely meet its static stiffness requirement. The static stiffness curve of the V40 LLTB does fully lie within the acceptable margins of its requirement, but there is room for getting even closer to the requirement curve. The objective with this phase is, thus, to try to optimize the static stiffness of the V40 LLTB even closer to its requirement.

The pre-optimization script was run, and for the V40 LLTB static stiffness requirement data it was chosen to reduce the number of data points substantially. It was also decided to not include the two last data points in each direction to lower the analysis time and reduce the risk of convergence errors. The data point-picking algorithm was set to use the fifth and sixth data point in the positive and negative direction respectively as the target force step. The number of data points was reduced from 62 to 28 and the resulting data set can be seen in Figure 4.23. The objective function was created in the same way as for the simplified torque rod.

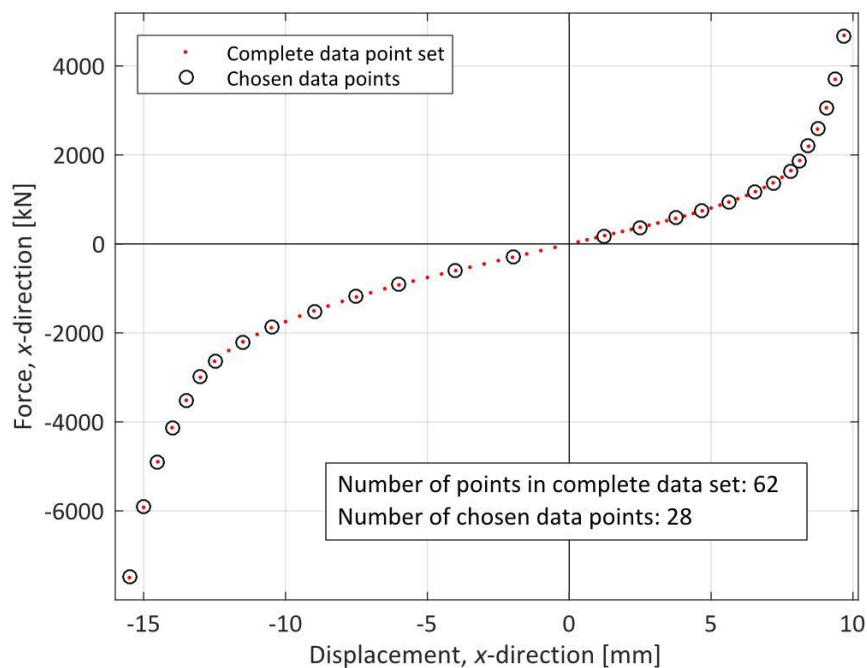


Figure 4.23: Chosen data points to be used in the objective function for the optimization of the V40 LLTB. The parameter n in the data point-picking algorithm was set to 4 for the positive direction and 5 for the negative direction, reducing the number of data points from 62 to 28.

4.4.4 Optimization set-up and system bounds check

The optimization set-up was done in the same way as for the simplified torque rod. A system bounds check was made, which showed that the requirement stiffness was within the feasible region for almost every part of the curve; it was outside the maximum stiffness at the end of the linear part of the positive part of the curve. This can be seen if studying Figure 4.24 carefully. The recommended action to take in such cases according to the optimization method is to redo the morphing. This was not done since the FE model was not considered capable of taking larger geometry changes when morphing. This meant that the requirement was not fully feasible, but there was still room for optimizing the geometry.

4.4.5 Design of experiments

A DOE with a Latin hypercube design with 32 sample points was done, to give a good set of initial sample points for the optimization and to study the effects of the design variables. The effects corresponded well to anticipations; not every design variable had large effect on the objective function, but every design variable affected the stiffness curve at some part of its operational range. All the design variables were, thus, kept for the optimization.

4.4.6 Optimization and post-processing

Two optimization rounds with 50 evaluations each using the GRSM were run. The objective function was lowered from 5.96 mm^2 to 1.58 mm^2 in the first round and further lowered to 1.42 mm^2 in the second round. The result of the optimization is shown in Figure 4.24. For a view from HyperStudy of how the objective function changed for each iteration, see Figure 4.25. For corresponding images of how the design variables changed, see Figure 4.26 for the first round and Figure 4.27 for the second round. In Figure 4.28 the optimization result is shown in terms of geometry changes.

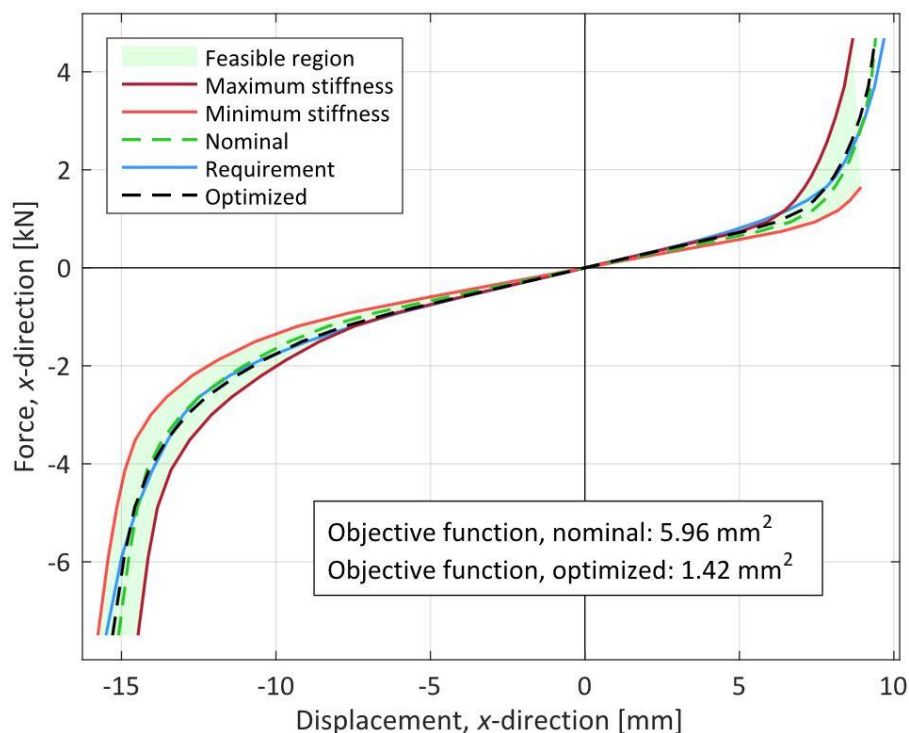


Figure 4.24: Force-displacement plot for the optimization of the V40 LLTB. The reason for that the feasible region is not covering the whole operational range is that the analysis for the minimum stiffness did not converge for large displacements in the positive x-direction.

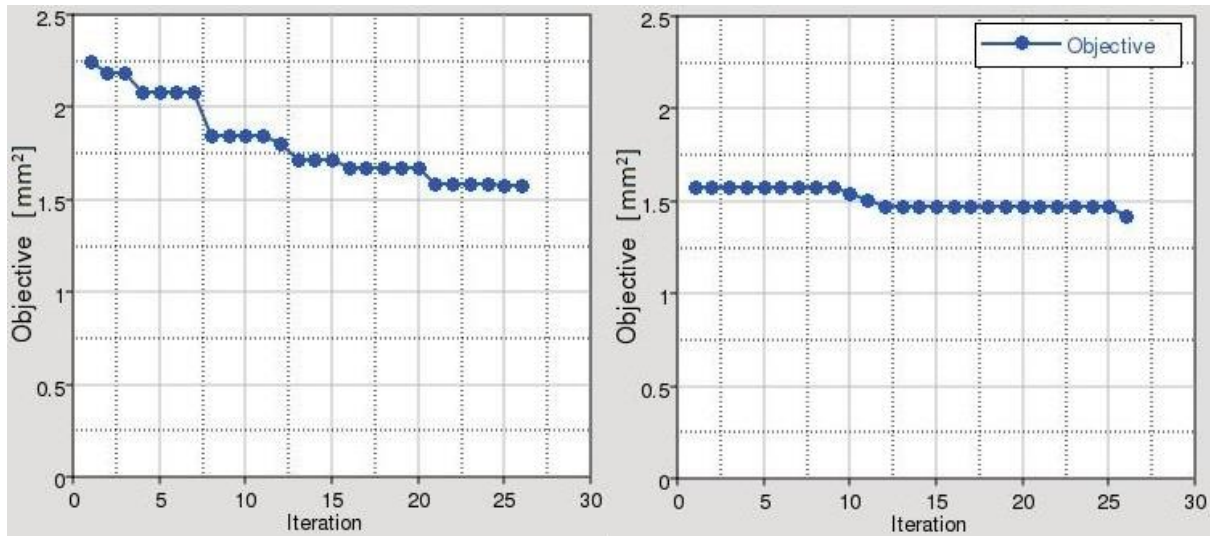


Figure 4.25: View from HyperStudy showing the value of the objective function for each iteration during the first optimization round (left) and the second optimization round (right) of the V40 LLTB. The reason for that the value of the objective function for the first round starts at a lower in the first round value in this plot than the objective function value for the nominal design is that the optimization starts from the best design from the initial sampling, which had a value of the objective function of approximately 2.25 mm².

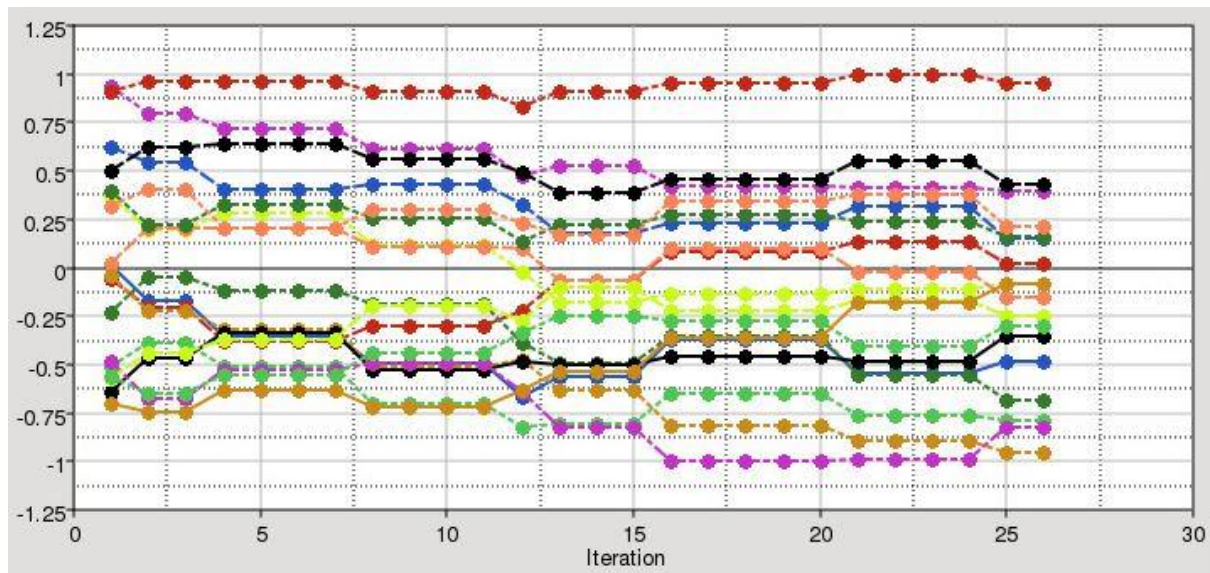


Figure 4.26: View from HyperStudy showing the values of the design variables for each iteration during the first optimization round of the V40 LLTB. As described in Figure 4.25, the optimization starts from the best design from the initial sampling. For a legend to the plot, see Table A.2 in Appendix A.

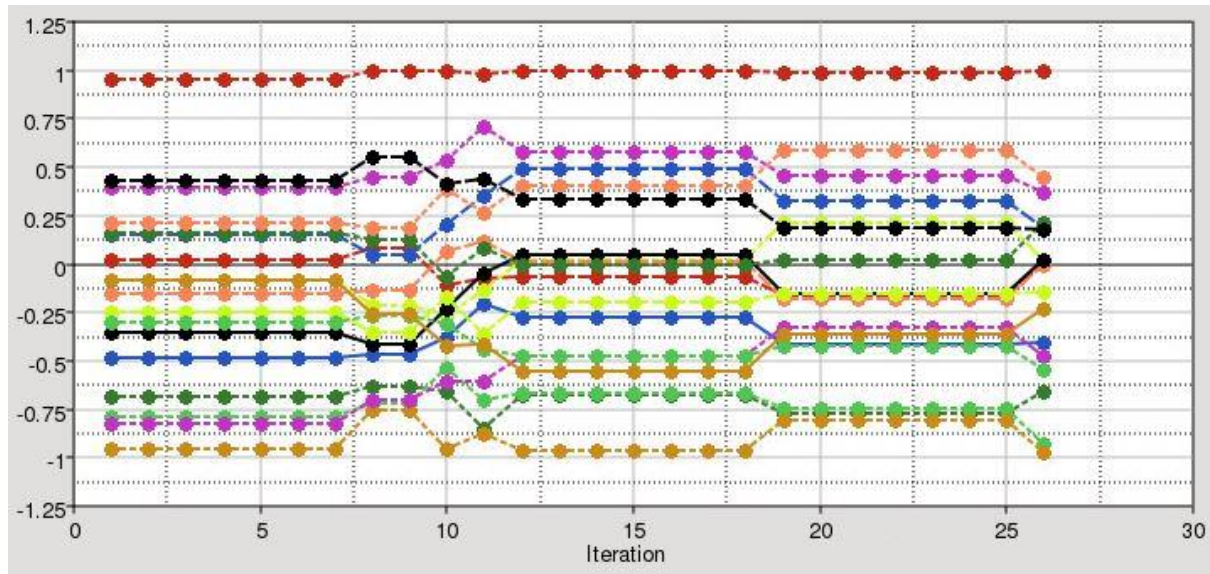


Figure 4.27: View from HyperStudy showing the values of the design variables for each iteration during the second optimization round of the V40 LLTB. For a legend to the plot, see Table A.2 in Appendix A.

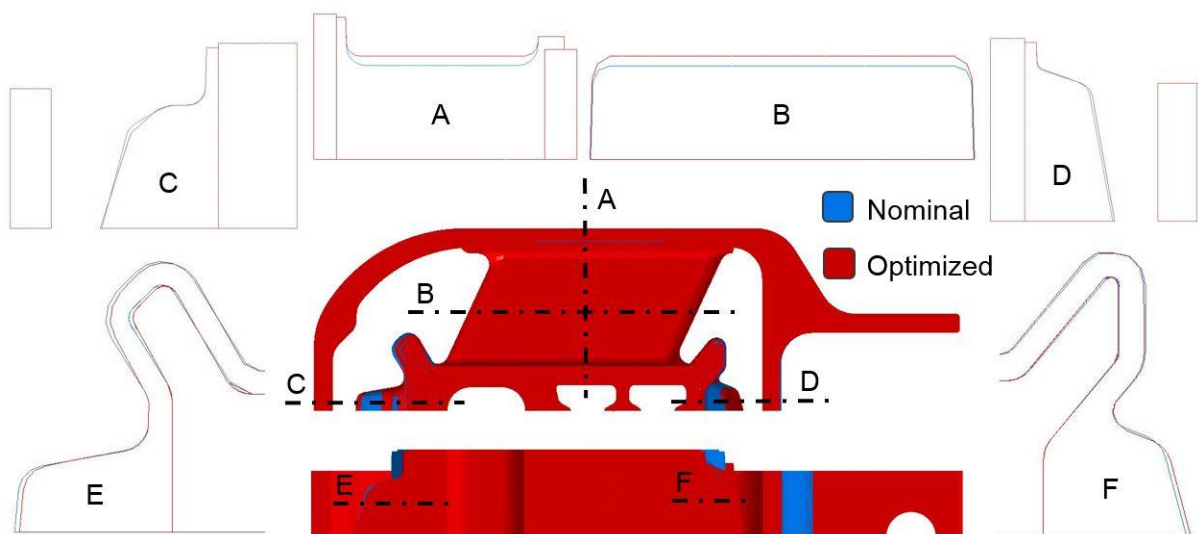


Figure 4.28: The result from the optimization of the V40 LLTB shown in terms of geometry changes. The two main views are the geometry from the STL-file that is the output of the optimization method. For the frame and insert, the red colour makes it look like every surface of them are optimized. This is not the case; the red surface is the one that happened to be shown when there is no difference between the nominal and optimized geometry. A number of section views (A-F) are also included to show the geometry changes.

5 Discussion

In this section, the project will be discussed. It is divided in two subsections, where the first treats the project methodology and how the project was carried out, and the second treats the results of the project.

5.1 Project discussion

The project methodology is considered to have suited the project well. The choice of developing the optimization method using a simplified torque rod was favourable since it made the iterative development process faster and easier. For example, the morphing was made very simple in comparison of morphing the real torque rod (the V40 LLTB), which can though be seen as a disadvantage since the much more difficult morphing of the real torque rod was a bit unexpected. Overall the simplified torque rod was very useful.

It would have been interesting to apply the optimization method in a real development of a new component for validation. For this to add additional value than the optimization of the simplified torque rod, a prototype would have to be manufactured to validate the optimized geometry. This would not have been possible to do in this project in terms of time and other resources. As mentioned earlier, optimizing the geometry of an existing product is not the best way of evaluating the method as only minor changes in geometry are expected, but was found to be the best way for this project.

Something that could have been improved regarding the project methodology is that it could have been more detailed. The project was very iterative and the path of the project determined as the project was carried out. It would have been good to have a clearer plan of what to be investigated and what to be delivered. This is of course a challenge for every project, but the fact that the student carrying out this project did not have much experience in powertrain mounting systems or modelling and analysing rubber components made it extra difficult to make a detailed plan for the project.

5.2 Results discussion

The results will be discussed in the same order as they were presented in the results section, that is, beginning with the results from the development phase followed by the material parameter-obtaining phase, the presentation of the optimization method and the validation and adjustment phase. In the end, some general topics not connected to any particular phase will be discussed.

5.2.1 Development phase

The most important result of this phase is of course the proposed optimization method, but it will be discussed in Subsection 5.2.3. In this subsection, the partial results on the way to the development method will be presented, that is, the results of optimizing the simplified torque rod.

The first important result is that the optimization method was able to optimize the simplified geometry to a low value of the objective function from a simple and not thoroughly thought out concept geometry, that is, with a high value of the objective function. It was not given that that would be possible, but it was a satisfying result. It was a consequence of partly that it was possible to use the morphing tool so well, which gave a large feasible region and partly because the chosen optimization algorithm worked well. This imply that the concept geometry does not

have to be very close to the final geometry; in other words, there is room for ample inaccuracy when designing the concept geometry, which lowers the demands on the concept geometry.

The main result of this project is a shape optimization method, which is nothing new considering the basic function. What is new is how the tools are applied in this certain application. An important part in this is the MATLAB scripts written in the development phase. To begin with, the pre-optimization script includes many convenient tools for setting up the optimization. The most interesting feature in this script is probably the data point-picking algorithm, which is completely new and tailored algorithm for this application. The post-optimization script also includes very convenient features to visualize the result of an optimization. Currently, no feature for plotting, for example, force versus displacement, which is used as a response, is available directly in HyperStudy. This motivate the need of the post-optimization script, which in an easy way can make such plots based on the optimization result.

Another important result from the development phase is how the two different loading directions was handled by using one model for each direction and linking the design variables in HyperStudy. This meant that the unloading simulation sequence when changing loading direction was avoided. The linking ensured that the geometry changes were not split up in the two models, so that all changes were made in both models which facilitates the use of the optimized model as design basis.

5.2.2 Material parameter-obtaining phase

This phase showed that it was not possible obtain sufficiently accurate hyperelastic material parameters directly from tensile tests in the way they were carried out in this project. There are probably several different reasons for this. An important source of error are probably the test specimens. Ideally, longer specimens and more even surfaces of the specimens is desired. Longer specimens were not possible to obtain from the existing components. Having a short length of the specimen makes the displacement measurement more sensitive, which means higher demands on accuracy. For this project, it also meant that an extensometer could not be used as no one small enough was available. This meant that the displacement was measured by the tensile test machine between the two attachment clamps, which is not as accurate as using an extensometer. It was also difficult to measure the original length between the attachment clamps accurately. The surface quality of the thick specimen was good, but for the thin specimen it was not possible to obtain a good surface quality. This shows that water jet cutting of rubber has potential of cutting with good surface quality, but it is difficult to cut thin strips because of that the rubber material is soft and easily collapses. The tensile test machine used in this project was also not ideal for this application; it was designed for much higher loads. A smaller and more suitable machine would have been desirable for such small specimens.

An unexpected result from this phase was though that the optimization method developed can be used to optimize the material parameters to better model a certain rubber with of a certain geometry. This can be useful for Volvo Cars if it is desired to model component for which it exist measurement data but not any hyperelastic material parameters for the rubber, which is the case for most of Volvo Cars' mounts. It can be questioned why it was not possible to optimize the material parameters to model the V40 LLTB even more. The reason for this could be that there are limitations in how well the Yeoh model can describe the rubber, and that there can be errors in the measurement data so that it is not entirely accurate. It is also possible that the material model for the aluminium parts is not entirely accurate.

5.2.3 Presentation of the optimization method

The optimization method is the main result of this project. It is well documented in three different levels, on one hand to give a good overview of it and on the other hand to provide a detailed guide on how to use it. It can also be used in two different versions; the primary is for shape optimization and the secondary is for material parameter optimization. The method has been designed to be user friendly and fast to use, as the purpose of this project includes development of an efficient method. However, there are things to improve in this area. For example, the MATLAB scripts ought to be made into standalone applications with a user-friendly interface.

Three different scenarios have been identified where the optimization method can be used. For the main scenario where the method is intended to be used in a new product development process, it was not given clear answer on how to incorporate material optimization with the shape optimization. Three possible ways are though suggested, and as this project's main focus was shape optimization it is considered adequate to not have solved that part completely. It shall be noted that for the third way of incorporating material parameter and shape optimization (see Subsection 4.3.4.1), there is probably a need for additional constraints as that becomes a very open optimization problem.

No evaluation of the proposed new development process performance has been done, but it can be considered to have large potential of lowering the development lead-time and cost. The main argument for this is that by doing development in-house the communication between everyone involved in the development process will be much easier and faster, which would lower the development lead-time. In addition, it would be cheaper to do development in-house instead of buying this service from an external supplier. There are of course disadvantages with in-house development as well; it requires more labour, expert knowledge and experience from specialized suppliers cannot be used and it might be necessary to find new suppliers that agree to manufacture a build-to-print component, as this makes the supplier's development service unnecessary.

5.2.4 Validation and adjustment phase

This phase, in combination with the optimization of the simplified torque rod, showed that the performance of the optimization method is sufficient. This phase showed that the optimization method is able to fine-tune a design very accurately to reach a low value of the objective function, whereas the development phase showed that the method is also capable of starting with a concept geometry very different from the final geometry. The optimization of the V40 LLTB model made the geometry come much closer to its requirement; despite the fact that the feasible region did not completely cover the requirement stiffness curve (see Subsection 4.4.3). It should though be remembered that the optimization method in its current form only optimizes the static stiffness of a component. Of course, there are other requirements that are not optimized or even observed such as fatigue resistance in form of stress requirements. It should though be noted that the morphing of the V40 LLTB was made as careful as possible to preserve geometrical features such as radii and to only change the main dimensions in as large extent as possible. The real case also showed that it is much more difficult and time consuming to morph a model without the original geometry still in the HyperMesh model (see Subsection 1.1.1).

5.3 General topics

To conclude this section, some general topics will be discussed. To begin with, an important question is the use of constraints in the optimization method. In its current form the only constraints used are the limits for the shapes or design variables. This means that if the morphing is done in a way that does not create a geometry that is not implementable in terms of, for example, too high stress levels, there is no actual need for additional constraints. However, this can be difficult to control, so it would probably be useful with some sort of constraint for stress levels in the structure. It should be remembered though, that the component might not be optimized for maximum loads, as it can be difficult to get the analysis to converge for high loads, and there can be awkward stress concentrations in sharp edges of the geometry. Stress constraint needs, thus, to be implemented with care. For example, it might be good to not include every element in the structure but only some critical zones because of the risk with stress concentrations. Other constraints such as manufacturing constraints in terms of for example draft angles are more difficult to implement; the recommendation for this is to make the morphing in a way so that the geometry will always be manufacturable.

Another topic for discussion is how the optimization should be set up. First, it can be discussed if it is best to set up the FE model based on force (as in this project) or on displacement. Having it set up based on force has the disadvantage of that a certain design always will be subjected to a certain displacement, even though it is too stiff to converge for that displacement. Having it set up based on displacement has on the other hand the opposite disadvantage; a certain design will always be subjected to a certain force, even though it is too flexible to converge for that force. This is not a big issue since it would probably only be a problem for the extreme designs near the boundaries of the feasible region, and HyperStudy has the feature of ignoring a failed analysis due to convergence errors.

It will though affect the objective function; force-based analysis means that the objective function is based on the displacements as in this project, which in turn means that the stiffness curve can be said to be optimized in the horizontal direction of the force-displacement plot. For displacement-based analysis, the objective function would be based on the force levels and the stiffness curve can be said to be optimized in the vertical direction. If the stiffness curve would have the slope of 1 for the whole range, this would have no significant meaning. However, this is not the case. For a flat stiffness curve, it would have made sense to optimize it in the vertical direction and for a steep stiffness curve, it would have made sense to optimize it in the horizontal direction. The actual stiffness curves of torque rods are for low displacements relatively flat, but for high displacement steep. By the reasoning that the linear part of a torque rod's stiffness curve should be quite easy to optimize as it is mostly dependent of the shape of only the MRE, it was chosen to optimize the stiffness curve in the horizontal direction of the force-displacement plot since the steep part of the stiffness curve was considered more difficult to optimize as it is affected by the shape of the MRE, the bump stop, the insert arms and the frame. It was, thus, chosen to use force-based models resulting in displacement-based objective functions (horizontal direction of the force-displacement plot). Studying the force-displacements plots in this report, this reasoning seems reasonable since most of the optimized stiffness curves seem to meet the linear part of the requirement stiffness curve better than the progressive parts for large displacements.

Continuing the discussion above, it would have been interesting to investigate the possibility of optimizing low degrees of stiffness with respect to force level (vertically) and high degrees of stiffness with respect to displacement (horizontally). However, as mentioned above, the low degrees of stiffness seem to be well optimized and the optimization is already set up with respect to displacement. Another idea would be to first optimize the shape of the MRE to get the linear part of the stiffness curve correct and then optimize the rest of the torque rod to get the progressive parts correct.

6 Conclusion

In this section, the research questions are first answered and then the major findings of the report are highlighted and put into context by reflecting on the purpose of the project. Other conclusions drawn are also presented.

6.1 Research question answers

The first research question was about what kind of output the optimization method should deliver. It has been showed in this project that for the application that this method is to be used in, that is, a Build-to-Print project, it has to deliver an optimized mount geometry that can be used as a design basis for the final design of the mount. It was also asked in what phase and what role that are the receivers of this output. The phase, in a product development project, would be the detailed design phase and the role would be a design engineer. It was therefore important that the optimization method delivered an optimized geometry in a format that would be useful for a design engineer in the tools that the design engineer uses, which is some sort of CAD software. This was met by delivering the optimized geometry in a STL-format that can be opened in CAD software. During the project, another use of the method was also identified, which is the material parameter-optimization application. In this case, the method delivers optimized material parameters and the receiver to this output is a CAE engineer.

The second research question was the most extensive and the core of this project, and was about hoe the method should be designed to deliver what is asked for in the first research question in an efficient way. The first sub-question asked how shape optimization should be implemented to meet the demands of the project. The answer to this is that it can be implemented using morphing, which was shown to be an effective tool for shape optimization. It is a flexible tool that can be applied to any geometry. The second sub-question asked how the method workflow should look like and what steps should be included. The answer to this is given in Subsection 4.3 where an easily comprehensible flowchart of the method is presented. The main steps include FE pre-processing, morphing, optimization pre-processing and set-up, evaluation of feasible region, optimization and optimization post-processing. The third sub-question asked what kind of input is needed to perform these tasks. The answer to this is that a concept geometry is needed that is of a fairly good representation of the final geometry. A static stiffness requirement in the form of force-displacement data points is also needed as input.

Research question number three was a slight detour from the main subject of this project, and asked if it is possible to obtain material data from powertrain mounts rubber parts to properly model rubber material. The answer to this is that tensile tests can be used as an easy experiment to obtain hyperelastic material parameters for modelling rubber using the Yeoh hyperelastic model, however, with the limited size and difficulties with obtaining good test specimens from existing powertrain mounts, it was not possible to obtain material parameters directly from the tensile test that sufficiently accurate modelled the rubber behaviour. However, as mentioned above, it was found that the optimization method can be used for optimizing the obtained material parameters. This gives the possibility of obtaining a quite accurate material model based on data from tensile tests.

The fourth and last research question asked how the optimization method should be implemented in the product development process at Volvo Cars. For this, three scenarios, presented in Subsection 4.3.4, were suggested. The first and primary scenario is in new product

development like a Build-to-Print project. The optimization method is here used to first make a rough optimization of the main dimensions of the geometry, and then for a fine-tuning optimization of the final dimensions. The second scenario is for use in analysis of existing components by optimizing the hyperelastic material parameters used to model the rubber parts to sufficiently accurately model the component. The third scenario is for use of the optimization method to give suggestions on changes of design proposals if there are difficulties to meet static stiffness specification. It was also asked who the end user of the optimization method is. The answer to this is most probably a CAE engineer. The method has therefore been designed to be easily understandable and usable for a CAE engineer.

6.2 General conclusions

The purpose of the project was to develop an efficient powertrain mounts development method, which by structural optimization finds the optimal mount geometry to meet stiffness requirements. The purpose has largely been fulfilled; a method using shape optimization (a class of structural optimization) has been developed to optimize the mount geometries to meet static stiffness requirements. The parts that are not fully fulfilled is that the method only considers one type of stiffness requirements, that is, static stiffness requirements. Dynamic stiffness is also a very important property of powertrain mounts. However, it is more difficult to design a mount for a certain dynamic stiffness than for a certain static stiffness, and even in today's development process the mount geometry is designed largely to meet the static stiffness requirement. This method therefore solves the main design challenges in powertrain mounts design. The efficiency of the method has also not been quantified, but it is very likely that the method has the potential of being an important piece in reducing development lead-times.

Other conclusions to draw is that this is very wide and complex subject. Volvo Cars are not ready for Build-to-Print projects just because this method is available. This is just one piece and many other pieces are needed, and the proposed optimization method needs to be further developed (recommendations on future work is presented in the next section). However, the method is ready to be used to give suggestions on approximate mount geometries, but as described earlier manufacturing aspects and other constraints are probably needed to be included in the method. An application where the method is immediately applicable is though for material parameter optimization for existing components.

To conclude the optimization method has great potential in being a useful tool in new product development and modelling of rubber components at Volvo Cars.

7 Future work

In this section, recommendations for future action are presented. It is divided in two parts, where the first part describes actions for the next step, that is, relatively small actions that can be implemented in a near future, and the second part describes possible future research areas.

7.1 Recommendations for next step

The first recommended step to take next is to include additional constraints in the optimization method. It is, for example, recommended to implement stress constraints to avoid that the morphing gives a structure with stresses above prescribed limits. For manufacturing constraints, it is probably possible to include constraints for, for example, draft angles, but it could also be wise to develop detailed guidelines for how the morphing should be done so that it will not result in structures that are not manufacturable.

The second recommended step is to make the optimization method a bit more automated and user friendly by creating standalone and intuitive applications for the MATLAB scripts. It would also be good to fine-tune the GRSM optimization method in HyperStudy; it has a number of different settings that has not been worked with in this project.

For the obtaining of material parameters from existing powertrain mounts, it is recommended to investigate if a modified hardness test described by Austrell (1997) could be more suitable than a tensile test for this application. One of the main difficulties with the tensile test is that it is difficult to obtain good test specimens from existing products, something that might not be the problem for a modified hardness test.

It is also recommended to investigate in more detail how this method can be implemented in new product development processes. A plan for Build-to-Print projects for powertrain mounts including the optimization method needs to be developed.

7.2 Suggestions on future research areas

The first recommendation for future research areas is to investigate the possibility of including dynamic stiffness requirements in the optimization method. This should preferably be a next step activity, but it is considered to demand more investigation than what is needed from the next step activities. The main difficulty with including dynamic stiffness requirements is probably that it requires much longer simulation time than the static analyses. It is not feasible to do optimization if each evaluation of the FE model takes too long time. It is also more difficult to model the dynamic behaviour of rubber accurately wherefore it is probably necessary to build more knowledge in that area.

The second recommendation for future research is to build more knowledge in rubber material testing and modelling. It is recommended to map both the needs of Volvo Cars in terms of what material properties that are needed to obtain, and to map other available methods of performing the testing. The Yeoh model seems to work well for modelling powertrain mounts, but as mentioned above dynamic modelling needs to be further investigated.

When the method is considered ready for use in a real development project, it is recommended to investigate how it should be adapted so that it can be used for other powertrain mounts than torque rods. It is also recommended to investigate if the method can be used for other components than powertrain mounts. There are many rubber components in a car, such as bushings and vibration dampers that might be suitable for shape optimization.

The optimization method could also lead to another way of setting requirements on components by the introduction of an objective function. If some sort of standard for how the objective function should be designed and how data points should be chosen, it might be possible to set requirements on, for example, static stiffness in terms of a value of the objective function that must be met.

A difficulty with rubber components is that it is not possible to make rapid prototypes, as the rubber needs to be moulded and bonded to the metal parts. It would be of great use to develop a method for making quick prototypes for verifying results from optimizations. This could be very useful in new product development projects where the FE model could be verified by comparing it to measurement data from a prototype. The hyperelastic material parameters could then be optimized with the measurement data as requirement stiffness to ensure the required accuracy of the model. Having a sufficiently accurate model is very important for getting good results from the shape optimization that also applies to a physical component. A suggestion is to investigate if it would be possible to use some sort of standard parts with rubber bonded to aluminium that could be water jet cut to according to the optimized geometry and then assembled into, for example, a torque rod using conventional joining techniques.

A drawback with shape optimization is that it needs some initial or concept geometry to start from. To avoid this, it might be possible to use topology optimization for design of the concept geometry. However, topology optimization generally results in complex geometries that are not immediately manufacturable in rubber. Special care is needed when formulating constraints for generalisation. This is a field recommended for investigation further ahead. It has great potential; a method that would take a design space with two attachment points and a stiffness curve as input and deliver an optimized topology describing how metal and rubber should be distributed as output would be of great use. The optimized topology could then be fine-tuned using the shape optimization method proposed in this project.

References

- Altair. (2016, July 5). *HyperStudy 14.0 New Features*. Retrieved from Altair HyperWorks: http://www.altairhyperworks.com/training/new_feature_videos/14/content/hyperstudy.htm
- Austrell, P.-E. (1997). *Modeling of Elasticity and Damping for Filled Elastomers*. Lund: Structural Mechanics, Lund University.
- Boyce, M. C., & Arruda, E. M. (2000). Constitutive Models of Rubber Elasticity: A Review. *Rubber Chemistry and Technology*, 73(3), 504 - 523.
- Christensen, P. W., & Klarbring, A. (2009). *An Introduction to Structural Optimization*. Dordrecht: Springer.
- Dassault Systèmes. (2014, January 28). Abaqus 6.14 Online Documentation. Retrieved July 5, 2016
- Freakley, P. K., & Payne, A. R. (1978). *Theory and Practice of Engineering with Rubber*. Essex: Applied Science Publishers Ltd.
- Holzappel, G. A. (2000). *Nonlinear Solid Mechanics: A Continuum Approach for Engineering*. Chichester: John Wiley & Sons.
- Kaya, N. (2014). Shape Optimization of Rubber Bushing Using Differential Evolution Algorithm. *The Scientific World Journal*.
- Kim, J. J., & Kim, H. Y. (1997). Shape design of an engine mount by a method of parameter optimization. *Computers & Structures*, 725-731.
- Lee, W.-S., & Youn, S.-K. (2004). Topology optimization of rubber isolators considering static and dynamic behaviours. *Structural and Multidisciplinary Optimization*, 284-294.
- Li, Q., Zhao, J., Zhao, B., & Zhu, X. (2009). Parameter Optimization of Rubber Mounts Based on Finite Element Analysis and Genetic Neural Network. *Journal of Macromolecular Science, Part A: Pure and Applied Chemistry*, 186-192.
- Lindley, P. B. (1974). *Engineering Design with Natural Rubber*. Hertford: The Malaysian Rubber Producers' Research Association.
- Liu, G. R., & Quek, S. S. (2014). *The Finite Element Method: A Practical Course* (2 ed.). Oxford: Butterworth-Heinemann.
- Mooney, M. (1940). A Theory of Large Elastic Deformation. *Journal of Applied Physics*, 11, 582-592.
- Park, C.-H., Shim, H.-J., Choi, D.-H., Kim, J.-K., & Lee, S.-M. (2012). Shape optimization of rubber isolators in automotive cooling modules for the maximization of vibration isolation and fatigue life. *International Journal of Automotive Technology*, 61-75.
- Rivlin, R. S. (1956). Large Elastic Deformations. In F. R. Eirich, *Rheology: Theory and Applications* (Vol. 1, pp. 351-385). New York: Academic Press.

- TrellebeorgVibracoustic (Ed.). (2015). *Automotive Vibration Control Technology: Fundamentals, Materials, Construction, Simulation, and Applications* (1 ed.). Würzburg: Vogel Business Media.
- Treloar, L. R. (1975). *The Physics of Rubber Elasticity* (3rd ed.). Oxford: Clarendon Press.
- Volvo Cars. (2016, July 1). *This is Volvo Cars*. Retrieved from Volvo Cars Web site: <http://www.volvocars.com/intl/about/our-company/this-is-volvo-cars>
- Yeoh, O. H. (1990). Characterization of Elastic Properties of Carbon-black-filled Rubber Vulcanizates. *Rubber Chemistry and Technology*, 63, 792-805.
- Yeoh, O. H., & Fleming, P. D. (1997). A New Attempt to Reconcile the Statistical and Phenomenological Theories of Rubber Elasticity. *Journal of Polymer Science: Part B: Polymer Physics*, 35, 1919–1931.
- Öhrn, R. (2015). *Prediction of static and dynamic behavior of powertrain suspension rubber components*. Linköping: Linköping University. (Master's Thesis at the Division of Solid Mechanics, Department of Management and Engineering).

Appendix

A Design variables

Table A.1: Design variables for the simplified torque rod optimization.



































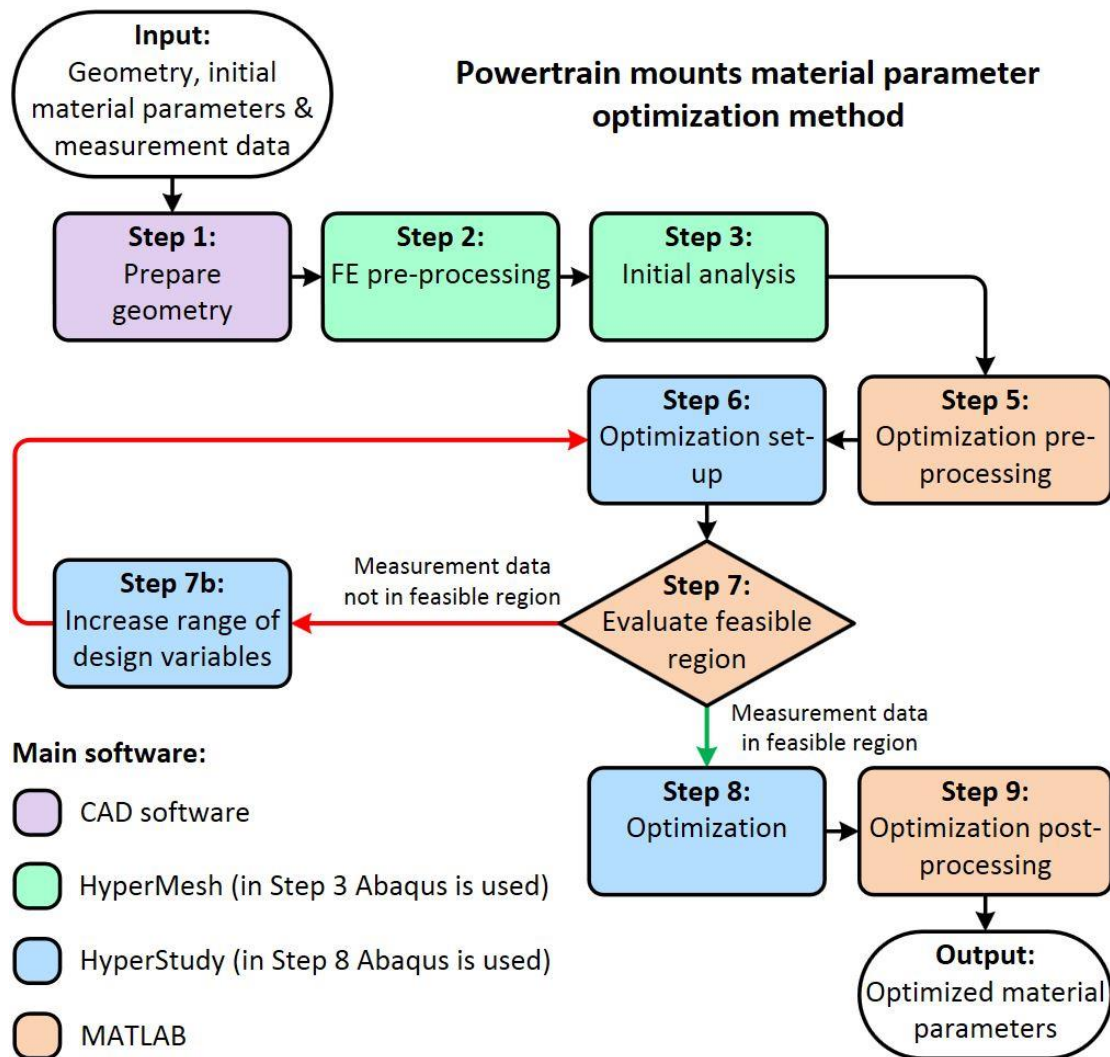
Name	Lower bound	Initial value	Upper bound	Optimized value
 MRE length	-1	0	1	 0.256
 MRE thickness	-1	0	1	 0.878
 Front frame thickness	-1	0	1	 0.153
 Side frame thickness	-1	0	1	 -0.110
 Front insert arms Xpos	-1	0	1	 0.501
 Front insert arms thickness	-1	0	1	 0.353
 Front bump stop width	-1	0	1	 0.730
 Front bump stop depth	-1	0	1	 0.250
 Front bump stop height	-1	0	1	 -0.590
 Front bump stop top plane angle	-1	0	1	 0.509
 Back frame thickness	-1	0	1	 -0.087
 Back insert arms Xpos	-1	0	1	 0.990
 Back insert arms thickness	-1	0	1	 -0.991
 Back bump stop height	-1	0	1	 0.666
 Back bump stop depth	-1	0	1	 -0.289
 Back bump stop width	-1	0	0.5	 -0.498
 Back bump stop top plane angle	-1	0	1	 0.017

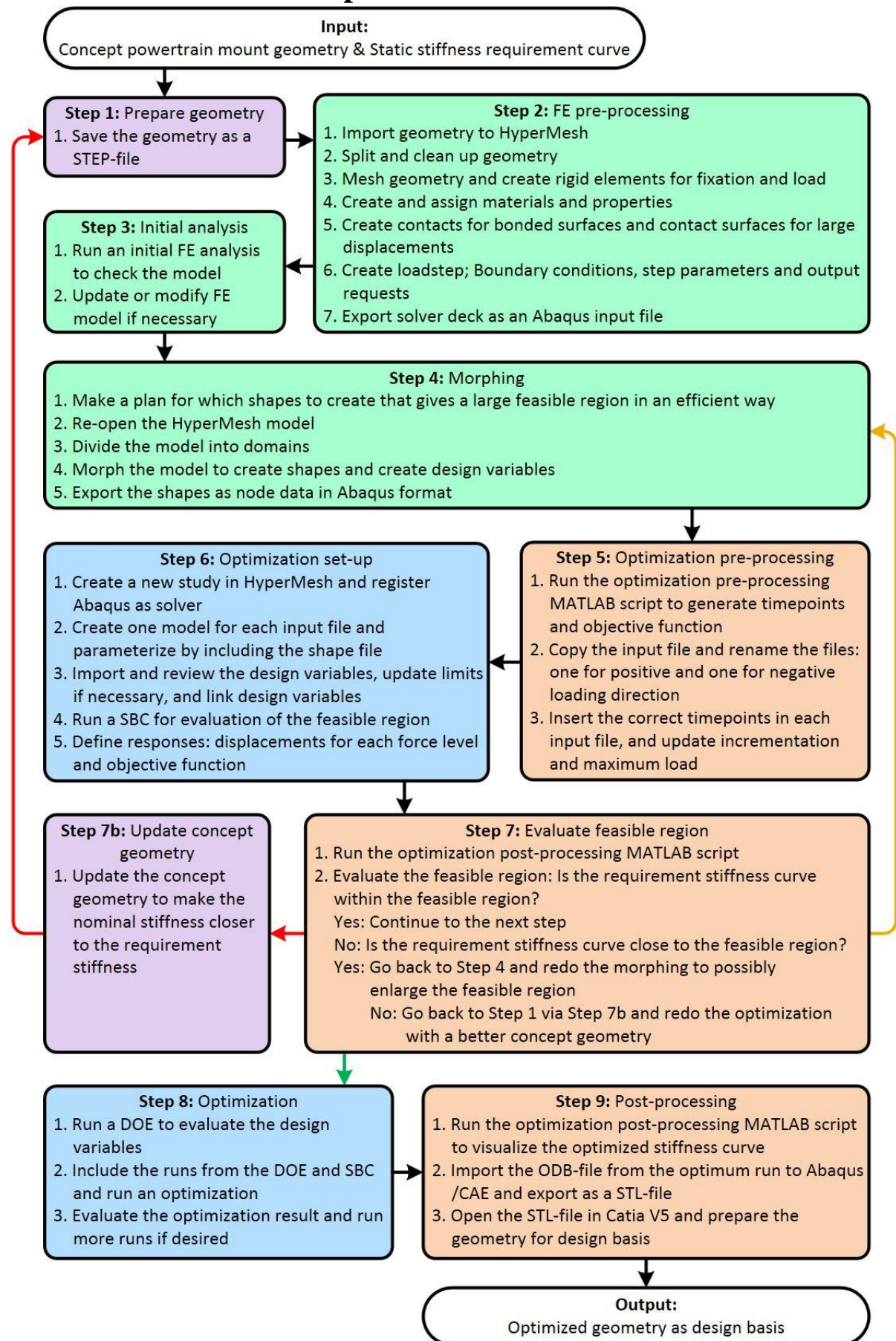
Table A.2: Design variables for the V40 LLTB optimization.

Name	Lower bound	Initial value	Upper bound	Optimized value
 Front insert arms thickness	-1	0	1	 -0.407
 Front frame thickness	-1	0	1	 0.003
 Front insert arms Xpos	-1	0	1	 -0.655
 Front bump stop height	-1	0	1	 0.371
 Front bump stop width	-1	0	1	 0.019
 Front bump stop depth	-1	0	1	 -0.002
 Front bump stop top plane angle	-1	0	1	 -0.928
 Front bump stop side plane angle	-1	0	1	 -0.971
 Side frame thickness	-1	0	1	 0.018
 MRE length	-1	0	1	 0.190
 MRE thickness	-1	0	1	 0.995
 Back insert arms thickness	-1	0	1	 0.213
 Back frame thickness	-1	0	1	 -0.474
 Back insert arms Xpos	-1	0	1	 -0.146
 Back bump stop height	-1	0	1	 0.452
 Back bump stop width	-1	0	0.5	 -0.547
 Back bump stop depth	-1	0	1	 -0.232
 Back bump stop top plane angle	-0.5	0	1	 0.176

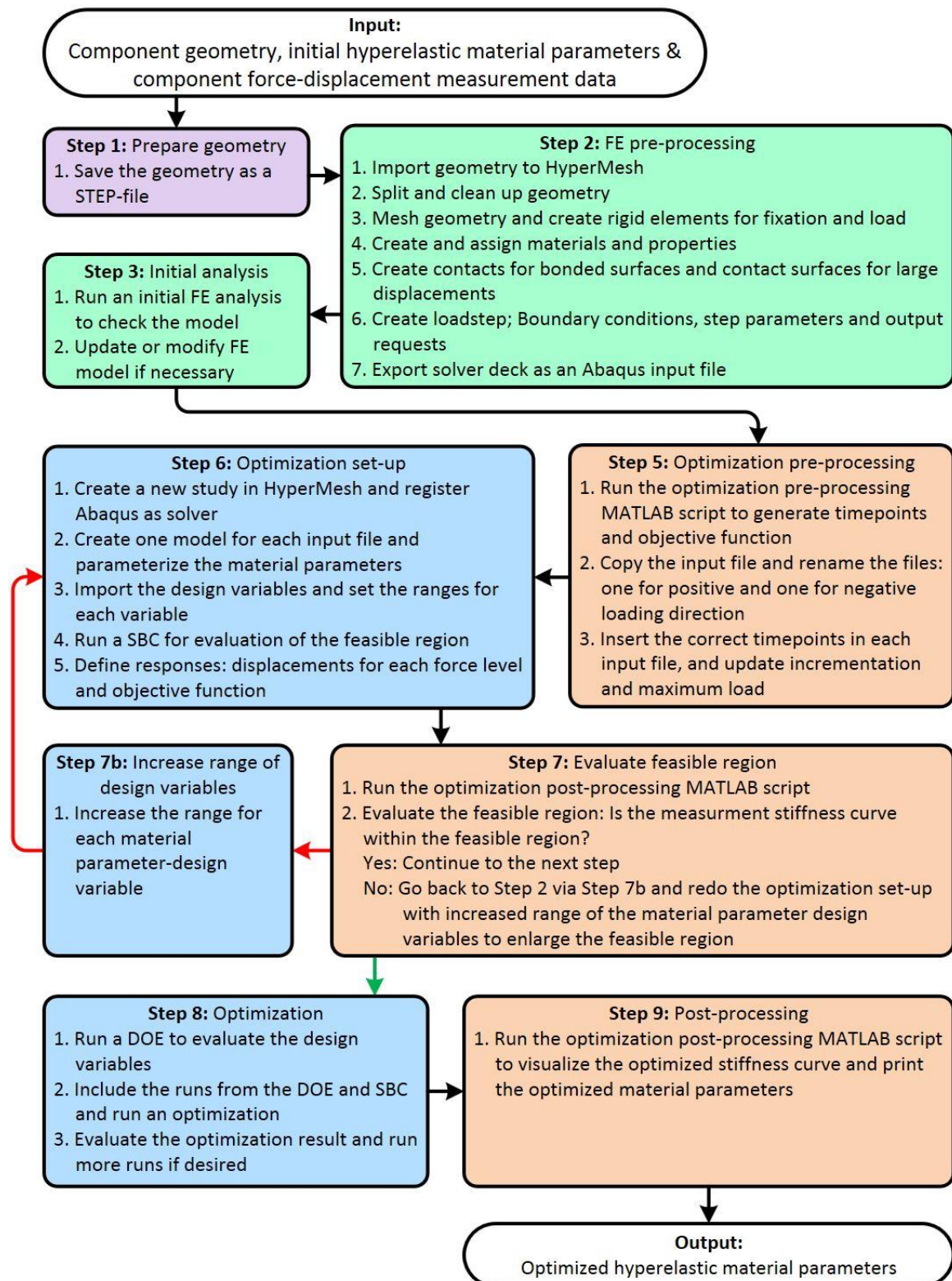
B Compact flowchart: Material parameter-optimization



C Detailed flowchart: Optimization method



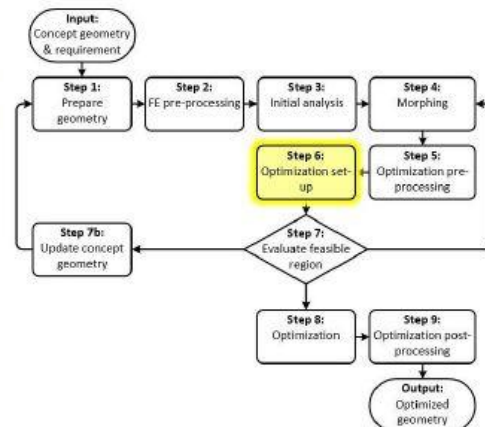
D Detailed flowchart: Material parameter-optimization



E Extract from step-by-step guide

Step 6: Optimization set-up

The purpose of this step is to set up HyperStudy for the optimization and to run the SBC for the evaluation of the feasible region.



Sub-step 1: Create a new study in HyperMesh and register Abaqus as solver

- 6.1.1 Copy and paste the ***Abaqus_solverScript.py*** file into the optimization folder.
(Note: open the file in a text editor to change if running local or on the cluster and how many cpus that are used.)
- 6.1.2 Open HyperStudy (Syntax when starting the program from a terminal using ThinLinc: ***hst -Ver 14.0***).
- 6.1.3 Click **Edit > Register Solver Script...** and then click **Add Solver Script**.
- 6.1.4 Enter **Abaqus** for **Label** and **Varname** (Type should be **Generic**) and click **OK**.
- 6.1.5 Copy the **Path** of script number **5 (Python)** and past it into the **Abaqus Path**.
- 6.1.6 Click the icon to the right in the **Argument** box for the **Abaqus** script, go to the optimization folder and select the ***Abaqus_solverScript.py*** file, and then click **Open**.
- 6.1.7 Click **Close** (Note: Not saving means that you have to register Abaqus every time you start HyperStudy. It is probably possible to use the save function to avoid this.).
- 6.1.8 Click **New Study** and select the optimization folder as the **Location** by clicking the folder icon, select the folder and then click **OK** twice.

Sub-step 2: Create one model for each input file and parameterize by including the shape file

- 6.2.1 Click **Define models** and then click **Add model**.
- 6.2.2 Enter **Pos** as **Label** and **pos** as **Varname** (Type should be Parameterized File) and then click **Apply**.
- 6.2.3 Enter **Neg** as **Label** and **neg** as **Varname** and the click **OK**.
- 6.2.4 Click the **ABC (...)** icon for the **Pos** model, select the **_pos** input file.
- 6.2.5 In the dialog, click **Yes** to parameterize the file.
- 6.2.6 Right-click on the text and click **Select Nodes > *NODE**.
- 6.2.7 Right-click on the selected text and click **Include Shape**.
- 6.2.8 Select the **.abaqus.node.tpl** file.